Control and optimization with dimensionality constraints

A THESIS
SUBMITTED TO THE FACULTY OF THE GRADUATE SCHOOL
OF THE UNIVERSITY OF MINNESOTA
BY

Mir Shahrouz Takyar

IN PARTIAL FULFILLMENT OF THE REQUIREMENTS
FOR THE DEGREE OF
DOCTOR OF PHILOSOPHY

Prof. Tryphon T. Georgiou, Adviser

October 2008

Acknowledgments

My deepest gratitude and appreciation go to my advisor, Professor Tryphon Georgiou, for his continuous academic support as well as financial assistance over the past five years. I am greatly honored to work with him. His passion for science, great insights, and incredible knowledge made him a role model in research and an exemplary mentor. I am indebted to him for the freedom he gave me in my research, the constructive feedbacks he provided me with, and of course his patience! I hope to run a Marathon with him someday! Tryphon, thank you so much for everything!

I wish to express my most sincere appreciation to Professor Gary Balas, the chairman of my dissertation committee. I enjoyed the System Identification and Robust Control classes thought by him and I was fortunate to complete my master degree in Aerospace Engineering and Mechanics under his supervision. I am also most grateful to Professor Tom Luo for his time and effort to serve on my examining committee. His class on Convex Optimization was one of the most valuable experiences during my years in Minnesota.

Many thanks go to Professor Mihailo Jovanovic whose presence in the department amazingly energizes the control group. He has been a great teacher during the lectures on Distributed Systems and Adaptive Control, a good friend at the office with his priceless advices, and a pleasant company at the Sally's bar. Mihailo, I will never forget your help and support! I would also like to extend my deep gratitude to Professor Stergios Roumeliotis, from the Department of Computer Science and Engineering, who kindly accepted to serve on my examining committee. He has always been there; anytime I needed his help.

I wish to acknowledge Professor M. Massoumnia, my former advisor in Sharif University of Technology, who had significant influence in my education. He is the one who introduced me to Controls and System Theory. It was during his lectures on Linear Systems where I was impressed and struck by the beauty of science for the very first time.

It has been a privilege to get to know Professor Demoz Gebre-Egziabher from the Department of Aerospace Engineering and Mechanics. I would like to thank him for the time he spent with me during my studies in that department and of course for his positive attitude.

My warmest thanks go to my dear friend and officemate Ali Nasiri Amini for the wonderful times we had at the office on the fourth floor. Ali was the greatest help to me with my move to Minnesota and I will be forever grateful for his friendship. My invaluable friend Johan Karlsson from Royal Institute of Technology in Sweden has always been an inspiring coworker with fresh ideas. The quality times we spent on research and sports during his visits to Minneapolis are unforgettable and I could not wish for a better company.

The interactions with my officemate Xianhua Jiang and our joint research on speech synthesis have been very enjoyable. I have also had so many memorable days and nights with my other officemates: Jim, Rashad, Fu, Binh, Gerald, and Makan. I thank them all for fruitful technical discussions as well as fun times at the office on the fifth floor!

All the administrative staff at the Department of Electrical Engineering are gratefully acknowledged, especially Ms. Linda Jagerson who was my first line of contact with milestone events in the course of my study. I would also like to thank the committee members at the University of Minnesota Graduate School who awarded me the doctoral dissertation fellowship.

My stay in Minnesota has been a unique experience in many aspects of my life. What made this experience magnificent was the support that I received from good old friends from Iran and my roommates and many wonderful friends in Minnesota. Without them my graduate school years would have been tough! I will definitely miss our study hours and other gatherings in Coffeehouses Espresso 22 and Starbucks. It would be an overwhelming task to name all these friends here. But in my heart, I always remember them one by one, and their comradeship.

Finally, I am eternally beholden to my parents Shahrokh and Touba, my brother Shahram, and my sister Shohreh. Words cannot express how much they helped me pursue my studies with their endless encouragement, unconditional love, and untold sacrifices!

To my brother ***Shahram***

... And to

Rumi (the 13th Century brilliant Persian mystic):

The chess master says nothing,

other than moving the silent chess piece.

That I am part of the ploys of this game

makes me amazingly happy.

Abstract

The purpose of this thesis is to develop synthesis tools for control design with dimensionality constraints. In particular, given a model for a physical process, the goal is to characterize all possible controllers of a certain dimension which satisfy given performance criteria.

In classical feedback design, the complexity of controller adversely affects robustness of the regulatory mechanisms of the feedback and adds to the fragility of the system. The complexity is often due to the difficulty in imposing performance specifications in a natural mathematical context. Typically, this is done using "weight functions" which encapsulate the specifications, and then introducing those in a suitable optimization problem. A contribution of this work is to address a certain type of optimization problem and the choice of weight functions. More precisely, we develop a new design approach which leads to a controller achieving both requirements, the performance specifications and low complexity, at the same time.

Further, this thesis generalizes the previous methods for multivariable systems by developing analogous theory and techniques. The main contribution in multivariable analytic interpolation is to characterize a family of minimal McMillan degree solutions by a choice of spectral-zero dynamics. In addition to application of this theory for model-matching in control design, we show how to use the same techniques for maximum power transfer in circuit theory, and for spectral estimation in signal analysis.

Also in this thesis we give new results on implementation of controllers with some very specific elements. One such, which is hard to simulate on a digital computer, is what could be described as "half capacitor". It implements a "fractional integration" and can be used to a great advantage in classical feedback design, providing gain but without introducing time-lag.

Contents

List of Figures

Chapter 1

Introduction

From airplanes to disc drives, biological cells, and financial markets, feedback is an integral component of underlying dynamical processes. Man-made devices, very much like homeostatic mechanisms in biology, rely on feedback to provide regulation.

Over the last 30 years, control design techniques rely more heavily on numerical optimization tools which apply to processes with increasingly larger number of parameters. For instance, nowadays, modern automotive technology provides performance cars with hundreds of feedback loops, often interconnected, for regulating exhaust, braking, handling, and suspension. Unfortunately, the benefits of feedback are often diminished by the complexity of the control loops themselves. The complexity of controllers is often responsible for fragility, sensitivity, and delays due to increased computational demands.

Robust control evolved to address the issues of complexity. In the 1980's and 1990's great strides were made in quantifying robustness and performance of regulatory mechanisms. However, complexity was not addressed in a systematic manner. R.E. Kalman to G. Zames, founders of the field, repeatedly drew attention to the fundamental issue of dimensionality and complexity of feedback. This issue still remains at the forefront of control systems.

1.1 Goals and objectives

One goal of this thesis is to advance an on-going program for developing synthesis tools in controller design with complexity constraints. More specifically, given a model for a physical process we would like to characterize all possible choices for a controller of a given dimension which satisfies given performance specifications. Complexity is often a relative term. Computational complexity and reliance on digital processing, points to the size of a system of equations that need to be solved as being the critical parameter. This in turn suggests that the dimensionality of controllers for ordinary electro-mechanical systems must be kept as small as possible.

Early works in this area by T. Georgiou, C. Byrnes, A. Lindquist, A. Megretski and their coworkers (e.g., [13–15, 17, 33, 34]) have laid out the foundation for addressing such issues, but only for single-input/single-output (SISO) dynamical systems. The main objective of this thesis is to enhance this program by developing, in the context of linear dynamical systems, analogous theory and techniques that are capable of handling multi-input/multi-output (MIMO) models. Control which takes into account many inputs and decides on many outputs is referred to as multivariable.

The second related theme in this thesis, which addresses certain "distributed parameter" elements, is pertinent in that it will make such elements available for classical feedback design. Complexity of these elements often depends on the choice of implementation. Time-delays are simple and natural in transmission lines but horrendously complicated when they affect fast systems whose dynamics are dictated by ordinary differential equations. Often a part of the control loop may be realized using actual physical components as opposed to virtual computational and digital ones. It is important to understand how fragility depends on implementation and the presence of hard to model, but nevertheless tame, physical distributed parameter systems.

In this thesis, we plan to re-evaluate how the use of certain physical components such as time-delays and, in particular, a fractional integrator affects what we consider as "complex" in feedback design. The mathematical dimension of such elements is infinite, yet their physical behavior is tame and quite beneficial when properly used. There is a vast literature on distributed parameter models and fractional calculus, motivated by physics of diffusive processes, turbulence, and other distributed processes, e.g., [18, 25, 26]. The originality of the work in this thesis is the study of such models and processes as feedback design tools.

1.2 Design and methodology

This thesis primarily focuses on the complexity of feedback control design. The underlying mathematical problem has a long history [33, 47]. Although the initial goal has been to devise tools for controller design with complexity constraints, these tools have a dual use; they can be utilized in modeling, system identification, and signal analysis, where measurements specify constraints on the signal model. Throughout this thesis, we will be considering theoretical aspects and a variety of practical techniques in these topics, outlined as follows.

1.2.1 Robust control

In classical feedback design, the complexity of controller adversely affects robustness of the regulatory mechanisms of the feedback. The complexity of controllers is often due to the difficulty in imposing performance specifications in a natural mathematical context. Typically, this is done using "weight functions" which encapsulate the specifications, and then introducing those in a suitable optimization problem.

In Chapter 2, we will present a systematic approach to weight selection in loop-shaping for SISO systems. This is to achieve the required performance specifications under dimensionality constraints. These weight functions themselves will be obtained as the solutions of another well-defined optimization problem.

1.2.2 Multivariable design: control, signal analysis, and circuit theory

In Chapter 3 and 4, we will study the analytic interpolation problem in the multivariable setting. More specifically, we will characterize the generically minimal-degree solutions to the underlying mathematical problem of matricial interpolation with a dimensionality constraint. We will also develop the numerical implementation of the problem and address certain technical non-generic situations as well.

One can build on the results in Chapter 3 and tackle the problem of weight selection in multivariable loop-shaping. The challenge herein is to cast the weight selection as a tractable optimization problem. Another relevant application is in high resolution signal analysis of multivariable processes, and namely, the reconstruction of matricial power spectral densities from second-order statistics. We will discuss this subject in detail using a couple of illustrating examples.

Multivariable interpolation problem is also pertinent to circuit theory, and in particular, to the classical broadband matching problem. This is defined as follows: given a load system (an antenna), we wish to drive it with a power source (a transmitter) having unit internal impedance. The source can be connected to the load system through an intermediate matching circuit and the problem is to find the matching circuit which delivers the maximal power to the load system. This has already been studied for more than a few decades in e.g., [27, 44, 70]. At the end of Chapter 3, we will have a fresh look at this problem by taking into account complexity constraints. Incorporating complexity constraints in broadband matching directly affects the number of required (passive) components, and hence, has an impact on robustness as well as economic considerations in a specific circuit design.

1.2.3 Fractional-order systems

In Chapter 5, we will investigate the implementation of controllers with some very specific, physically appealing, elements. One such, which is hard to simulate on a digital computer, is what could be described as "half-capacitor", i.e., half integrator. The fractional integration can be used to a great advantage in classical feedback design, providing gain without introducing time-lag (usually associated with usual integration).

Further, the possible implementations using lumped elements will be discussed based on the mathematical theory of continued fractions. We will also conduct similar analysis for more general systems with more complicated frequency characteristics– in particular, a sinusoidal tracking element which introduces less time-lag compared to the traditional design. These distributed parameter models may eventually be realized using micro-electro-mechanical systems (MEMS) or integrated circuits. Indeed, the ultimate goal would be to fabricate a physical device with the precise characteristics of a fractional element.

In addition to applications in control design, analysis of different biological processes such as speech, music, and electrocardiogram (ECG) signals reveals that they have characteristics close to distributed parameter models [62]. Such areas of application underscore the need for further improvements in the relevant tools. We close this introduction with a reminder that the identification of MIMO distributed parameter systems using optimization techniques is yet another wide open area of research.

Chapter 2

Weight selection in scalar interpolation with a degree constraint

In this chapter, we present an approach for feedback design which is based on recent developments in analytic interpolation with a degree constraint. Performance is cast as an interpolation problem with bounded analytic functions. Minimizers of a certain weighted-entropy functional provide interpolants having degree less than the number of constraints. The choice of weight parameterizes all such bounded-degree solutions. However, the relationship between the weights and the shape of corresponding transfer functions is not direct. Thus, in this chapter we present two formalisms that guide weight selection.

2.1 Introduction

Modern robust control design focuses on shaping the frequency response of closed-loop transfer functions. Performance is cast as a weighted optimization problem where weights relate to desired frequency responses [53, 72]. A drawback of standard H_∞-based methodologies is that they result in a degree inflation for controller and the feedback system beyond what is necessary for achieving performance.

This chapter is about a new formalism based on recent developments in analytic interpolation with a degree constraint [13, 14, 41, 42]. Here, interpolants are obtained as minimizers of a weighted entropy-like functional and the choice of weight affects the shape of the optimal closed-loop operator (interpolant). Although this approach allows some handle on the degree of interpolants, the relation between the weighting function and the shape of the corresponding interpolant is not direct.

Here, building on earlier studies by Nagamune, Blomqvist, and others (see e.g. [8, 48, 54–57]), we present two alternative approaches to address this issue. Both cases begin with an optimization problem which is not convex. The first one is based on a suitable relaxation into a computationally attractive convex problem (Section 2.3), while the second approach explores a solution of the optimization problem in a quasi-convex framework (Section 2.4). We deal with sensitivity shaping of single-input/single-output systems and demonstrate the efficacy of the new methodology with illustrative examples in Section 2.5. We then end this chapter with a more efficient formulation of the problem in Section 2.6, followed by concluding remarks (Section 2.7).

2.2 Extrema of weighted entropy functionals

Given a nominal scalar plant model $P(z)$, in discrete-time, internal stability of the closed-loop system with a suitable control $C(z)$ can be expressed via interpolation conditions on the sensitivity function $S(z) = (1 + P(z)C(z))^{-1}$ (see [68]). The conditions are as follows: first $S(z)$ must be analytic in the complement of the open unit disk $\mathbb{D}^c$, and then

$$S(z_i) = \begin{cases} 0 & \text{when } z_i \text{ is a pole of } P \text{ in } \mathbb{D}^c \\ 1 & \text{when } z_i \text{ is a root of } P \text{ in } \mathbb{D}^c \end{cases}, \tag{2.1}$$

for $i = 0, 1 \ldots, n$, i.e., the number of interpolation conditions is assumed to be $n + 1$. Multiple poles and zeros induce interpolation on the derivatives of S, however, for simplicity of notation we assume these to be simple.

Feedback control synthesis was formulated by Zames [72] as an H_∞-minimization problem. In this, performance specifications were translated into a desired shape for e.g. the sensitivity function $S(z)$, and then an admissible sensitivity function

was sought which abides by the constraints (2.1). Herein, we begin with an overall acceptable level $\|S\|_\infty < \gamma$ and a desired shape $|S_d|$ for the sensitivity gain $|S|$. These stem from the interest in noise attenuation and disturbance reduction for the closed-loop system. Then, we search for a low-degree function S, analytic in $\mathbb{D}^c$, which satisfies (2.1) and whose shape approximates $|S_d(e^{j\theta})|$. This is sought as a maximizer of a weighted entropy functional [13, 14]

$$\int_{-\pi}^{\pi} \Psi(e^{j\theta}) \log(\gamma^2 - |S(e^{j\theta})|^2) d\theta, \tag{2.2}$$

where the weight-function Ψ depends on S_d. Indeed, if Ψ is a positive function with poles at the interpolation points and their conjugates, i.e., $\Psi(e^{j\theta}) =: |\sigma(e^{j\theta})|^2$ with $\sigma(z) \in \mathcal{K}$ and

$$\mathcal{K} := \{\frac{\rho(z)}{\tau(z)} : \quad \tau(z) = \prod_{i=0}^{n}(1 - \overline{z}_i z), \quad \rho(z) \text{ is a polynomial of degree at most } n\}.$$

then there exists an interpolant (i.e., a sensitivity function $S(e^{j\theta})$) of degree less than or equal to n which maximizes (2.2) subject to (2.1) (see [14]). Further, all interpolants of degree $\leq n$ are maximizers of (2.2) for a suitable weight. Hence, provided the interpolation problem is solvable, the desired shape of the sensitivity function can be obtained with a "suitable" choice of Ψ. In view of this, our approach amounts to first selecting a "suitable" weight and then obtaining a maximizer of (2.2) subject to (2.1). We begin by discussing properties of the maximizer which guide the weight selection in the first step.

The maximization of (2.2) over a choice of S is equivalent to the minimization of the Kullback-Leibler divergence

$$\mathbb{S}(\Psi, \Phi) := \int_{-\pi}^{\pi} \Psi(e^{j\theta}) \log \frac{\Psi(e^{j\theta})}{\Phi(e^{j\theta})} d\theta,$$

between Ψ and $\Phi(e^{j\theta}) = \gamma^2 - |S(e^{j\theta})|^2$. This represents a notion of distance between a desired "shape" provided by Ψ and $\gamma^2 - |S|^2$. It turns out that it is convenient to replace S with a corresponding positive-real function

$$F = \frac{\gamma - S}{\gamma + S}. \tag{2.3}$$

This has the same McMillan degree as S and the interpolation constraints of S and F are in direct correspondence. Further, the minimizer of $\mathbb{S}(\Psi, \gamma^2 - |S|^2)$ subject to the interpolation constraints is unique and is attained at the same place as the minimizer of $\mathbb{S}(\Psi, \Re e\, F)$ over positive-real F's which are subject to the corresponding constraints (see [14, page 972]). The introduction of F has the added advantage of allowing a convenient normalization $\frac{1}{2\pi}\int_{-\pi}^{\pi} \Re e\, F(e^{j\theta})d\theta = 1$ via a conformal mapping that takes one of the interpolation conditions to the origin and scales accordingly the others. Thus, the second step amounts to minimizing

$$\mathbb{S}(\Psi(e^{j\theta}), \Re e\, F(e^{j\theta})), \tag{2.4}$$

subject to inherited constraints on F.

To compare this formalism with the classical approach of H_∞-control consider

$$f_d(z) := \operatorname{argmin}\{\|f(z)\|_\infty \ : \ f(z_i) = w_i W_d(z_i)^{-1}\},$$

where w_i's are interpolation values on the sensitivity function imposed by the stability requirement, W_d is a weighting function and $S(z) = W_d(z)f(z)$ is the resulting sensitivity function. Incorporating $W_d(z)$ in this formalism affects the degree of sensitivity function (being added to the degree of f) and thereby inflates the degree of the resulting controller accordingly[1]. In our formulation on the other hand, the degree of S is the same as that of F, which in turn can be bound by the number of interpolation constraints provided the weight is chosen within a specified class of rational functions. More specifically (see [13, 14, 16, 41]), the optimal F is such that $\Re e\, F = \Psi/\mathfrak{Q}$ with $\mathfrak{Q}$ positive and having spectral factors in $\mathcal{K}$. Thus, if Ψ is selected within

$$\mathcal{D} = \left\{|\sigma(e^{j\theta})|^2 : \ \sigma(z) \in \mathcal{K}\right\},$$

the degree of $\Re e\, F$ is at most equal to the generic degree of Ψ (since the denominators of Ψ and $\mathfrak{Q}$ cancel out). Thus, the optimal F, and therefore S as well, have degrees bounded by the number of interpolation constrains.

[1] Assuming that P and S are rational with P strictly proper, the controller $C = (1-S)/(PS)$ is proper and the following inequality relates the relevant McMillan degrees:

$$\deg C \leq \deg P + \deg S - n_z - n_p,$$

where n_z and n_p denote the numbers of unstable poles and non-minimum phase zeros of the plant, respectively (see [55] and [54]).

In view of the above, our basic plan is as follows. Starting from a function $S_d(z)$ which has the desired shape for a sensitivity function but may not necessarily satisfy the interpolation conditions, as step (i), we translate this into a desired shape for the real part of the corresponding positive-real function

$$\Phi_d(e^{j\theta}) := \Re e\, F_d(e^{j\theta}), \text{ where } F_d(z) := \frac{\gamma - S_d(z)}{\gamma + S_d(z)}, \tag{2.5}$$

and seek a pair $(\Psi, \mathfrak{Q})$ in $\mathcal{D}$ so that $\frac{\Psi}{\mathfrak{Q}}$ is "close to" Φ_d . Then in step (ii), we use this particular choice for Ψ and compute the positive-real interpolant F which minimizes (2.4), always subject to the relevant interpolation constraints. The choice of Ψ represents a compromise on the desired frequency characteristic for F, and therefore S, that permits a bound on the McMillan degree as indicated above. Next two sections tackle the problem of finding Ψ in two ways.

2.3 Weight selection via convex approximation

We begin with a (possibly) high-order $S_d(e^{j\theta})$ which has the desired shape, but it does not necessarily satisfy the interpolation conditions. The corresponding $F_d(e^{j\theta})$ and $\Phi_d(e^{j\theta})$ are constructed via (2.5). We then seek a pair $(\Psi(e^{j\theta}), \mathfrak{Q}(e^{j\theta}))$ such that $\Psi(e^{j\theta})/\mathfrak{Q}(e^{j\theta})$ approximates $\Phi_d(e^{j\theta})$. Using a slight relaxation, this approximation can be implemented as the following convex optimization problem

$$(\Psi, \mathfrak{Q}) = \underset{\Psi, \mathfrak{Q} \in \mathcal{D}}{\operatorname{argmin}} \|\Psi(e^{j\theta}) - \mathfrak{Q}(e^{j\theta})\Phi_d(e^{j\theta})\|_\infty. \tag{2.6}$$

This can be solved using semi-definite programming. In practice, reformulation of the conditions (2.1) leads to

$$S(z) = H(I - zA)^{-1}B + Q(z)V(z),$$

in which $A \in \mathbb{R}^{n\times n}, B \in \mathbb{R}^{n\times 1}$, and $H \in \mathbb{R}^{1\times n}$ are interpolation data, $Q(z)$ is any analytic function in $\mathbb{D}^c$ and

$$V(z) = \frac{\det(zI - A^*)}{\det(I - zA)}$$

is a scalar inner function (i.e., all pass). In fact, eigenvalues of A are the corresponding interpolation points. With this new formulation of the interpolation conditions, Ψ and $\mathfrak{Q}$ which belong to $\mathcal{D}$, i.e., trigonometric functions having poles at the interpolation points and their reflections, can be expressed as (cf. [37])

$$\Psi(z) = G(z)^* M_\Psi G(z), \quad \mathfrak{Q}(z) = G(z)^* M_\mathfrak{Q} G(z), \tag{2.7}$$

with

$$G(z) := (I - zA)^{-1} B, \quad M_\Psi - A M_\Psi A^* = B v_\Psi + v_\Psi^* B, \quad M_\mathfrak{Q} - A M_\mathfrak{Q} A^* = B v_\mathfrak{Q} + v_\mathfrak{Q}^* B,$$

where v_Ψ and $v_\mathfrak{Q}$ are row vectors. Using the positive real lemma and the representations in (2.7), we can readily express positivity of Ψ and $\mathfrak{Q}$ on the boundary of $\mathbb{D}^c$ as linear matrix inequalities. Minimization in (2.6) can then be treated as a semi-definite feasibility problem on the boundary of $\mathbb{D}^c$, i.e.,

$$-\epsilon < \Psi(e^{j\theta}) - \mathfrak{Q}(e^{j\theta}) \Phi_d(e^{j\theta}) < \epsilon \tag{2.8}$$

for all $\theta \in [-\pi, \pi)$, with $\epsilon > 0$, as a pre-specified tolerance level. Feasibility of the solutions in (2.8) depends on the choice of ϵ and will be revealed via solving linear matrix inequalities by applying the positive real lemma again.

The resulting F (where $\Re e\, F = \Psi/\mathfrak{Q}$) may not lead to an admissible sensitivity function via (2.3), because (2.6) does not take care of satisfying the interpolation conditions. However, the resulting Ψ is used in the second step of the algorithm, i.e., minimization of (2.4) subject to the interpolation conditions, to find the optimal F and then the desired sensitivity function via (2.3).

This section explained the first step in shaping algorithm in which we used a relaxed version of the approximation $\frac{\Psi}{\mathfrak{Q}} \sim \Phi_d$ for choosing the weight Ψ. To remove possible error which enters into the problem due to this relaxation, we will address an alternative approach in the next section, and bound the error $\|\Psi/\mathfrak{Q} - \Phi_d\|$ instead.

2.4 Weight selection via quasi-convex optimization

Similar to the previous section, we start with a $S_d(e^{j\theta})$ and construct the corresponding $F_d(e^{j\theta})$ and $\Phi_d(e^{j\theta})$ via (2.5). To approximate Φ_d with $\Psi/\mathfrak{Q}$, we consider the optimization

$$(\Psi, \mathfrak{Q}) = \underset{\Psi, \mathfrak{Q} \in \mathcal{D}}{\operatorname{argmin}} \left\| \frac{\Psi(e^{j\theta})}{\mathfrak{Q}(e^{j\theta})} - \Phi_d(e^{j\theta}) \right\|_\infty . \tag{2.9}$$

This is a non-convex problem which, interestingly, can be solved exactly by turning it into a quasi-convex one as follows. Write

$$\Psi(e^{j\theta}) = \frac{\psi(\theta)}{|\tau(e^{j\theta})|^2}, \quad \mathfrak{Q}(e^{j\theta}) = \frac{\mathfrak{q}(\theta)}{|\tau(e^{j\theta})|^2},$$

for positive trigonometric polynomials

$$\begin{aligned} \psi(\theta) &:= \beta_0 + \beta_1 \cos(\theta) + \cdots + \beta_n \cos(n\theta), \\ \mathfrak{q}(\theta) &:= 1 + \alpha_1 \cos(\theta) + \cdots + \alpha_n \cos(n\theta). \end{aligned}$$

On the other hand, Φ_d can be written as

$$\Phi_d(\theta) = \frac{c_0 + c_1 \cos(\theta) + \cdots + c_k \cos(k\theta)}{d_0 + d_1 \cos(\theta) + \cdots + d_k \cos(k\theta)},$$

where $k \gg n$ as it usually arises from a weighted H_∞-minimization problem, however, the algorithm pertains to any general choice of k. The minimization (2.9) can now be cast as the following quasi-convex optimization problem:

$$\min\{\delta : \mid \psi(\theta) - \mathfrak{q}(\theta)\Phi_d(\theta) \mid < \delta \mathfrak{q}(\theta), \quad \psi(\theta) > 0, \quad \mathfrak{q}(\theta) > 0, \quad \forall \theta \in [0, \pi]\}. \tag{2.10}$$

Quasi-convexity of (2.10) is due to the fact that the positivity of $\psi(\theta)$ and $\mathfrak{q}(\theta)$ defines intersection of infinitely many half-spaces while the first inequality in (2.10) leads to more intersection of half-spaces (cf. [67]).

Solution of (2.10) will be obtained using a localization/cutting-plane method, and in particular, the ellipsoid algorithm (see [7]). We now explain how to deal with the constraint $\psi(\theta) > 0$, and the same procedure applies almost verbatim to the other constraints. Briefly, continuity of $\psi(\theta)$ implies that it cannot be both positive and negative in $[0, \pi]$ without crossing zero at some point, i.e., $\exists\ \theta_0 \in [0, \pi] : \psi(\theta_0) = 0$.

Therefore, solutions of $\psi(\theta) = 0$ generate positivity cuts for the ellipsoid algorithm. These solutions can readily be obtained by finding roots of

$$\frac{\beta_n}{2}z^{2n} + \frac{\beta_{n-1}}{2}z^{2n-1} + \cdots + \frac{\beta_1}{2}z^{n+1} + \beta_0 z^n + \frac{\beta_1}{2}z^{n-1} + \cdots + \frac{\beta_{n-1}}{2}z + \frac{\beta_n}{2} = 0$$

with modulus one (i.e., $|z| = 1$). An alternative method to solve (2.10) is to express all constraints of the problem as linear matrix inequalities and then using a bisection on δ.

To recap, this section provides an appropriate weight, Ψ for the first step of the loop-shaping algorithm. Then, in step (ii), we use this Ψ to minimize (2.4) subject to the interpolation conditions. This finally gives rise to a low-order sensitivity function (via (2.3)) which satisfies internal stability of the closed-loop system and has the desired shape along the frequency range as well.

2.5 Case studies in sensitivity shaping

We now revisit three case studies on loop-shaping. The first one below which is from [56] deals with a simple discrete-time plant. The second one is in [30, 55] and is based on a continuous-time plant with non-minimum phase zeros. For convenience of notation, we convert this problem into the discrete-time domain. The third is in [55] and deals with mixed sensitivity reduction for a discrete-time plant. Compared to the standard H_∞-design techniques (e.g., [30]), the approach we present here, as well as Nagamune's approach in [55, 56] and [57], all give rise to controllers with lower McMillan degree.

Example 2.1 (from [56]) Consider the discrete-time plant

$$P(z) = \frac{1}{z + 1.1}.$$

with the desired specifications

$$\begin{cases} \mid S(e^{i\theta}) \mid < 0.6, & \theta \in [0, 0.3] \\ \mid S(e^{i\theta}) \mid < 2, & \theta \in [0.3, \pi] \end{cases}, \tag{2.11}$$

for the closed-loop sensitivity. In the following, we find a sensitivity function which guarantees internal stability of the closed-loop and at the same time satisfies (2.11).

This plant has a non-minimum phase zero at infinity and an unstable pole at $z = -1.1$. Hence, the sought sensitivity function should satisfy the following interpolation constraints

$$S(\infty) = 1, \ S(-1.1) = 0. \tag{2.12}$$

It has been shown in [56] that the specifications (2.11) cannot be satisfied by any interpolant of degree one. One way to address this issue is to introduce additional interpolation constraints. Following [56] we introduce an additional condition $S(1.1) = 0$ so as to taper the magnitude of the sensitivity function at low frequencies. For shaping sensitivity function along the lines of steps outlined earlier, we use a first-order transfer function

$$S_d(z) = \frac{1.3124z - 1.3124}{z - 0.3124}, \tag{2.13}$$

which satisfies the desired specification (2.11), but not necessarily the interpolation conditions (2.12). This is a Chebyshev filter with the pass-band gain of 2, i.e., norm bound constraint of the desired sensitivity. This $S_d(z)$ generates the corresponding $\Phi_d(z)$ via (2.5). Then solving convex optimization problem (2.6) provides a weighting function $\Psi(z)$ with zeros at $z = \{-0.9897, -0.2813\}$ (and at their reflections), whereas $\Psi(z)$ obtained from quasi-convex formalism (2.10) has zeros at $z = \{-0.7671, -0.4047\}$ (and at their reflections). Using these two Ψ's, separately, in the second step, we minimize (2.4) subject to the interpolation conditions. These minimizations are established via a homotopy method as in [38] and the resulting sensitivities using the convex approximation and the quasi-convex framework are

$$S_1(z) = \frac{z^2 - 1.2100}{z^2 + 0.6852z - 0.2097}, \quad S_2(z) = \frac{z^2 - 1.2100}{z^2 + 0.6739z - 0.1925}, \tag{2.14}$$

respectively. Figure 2.1 shows $|S_d(e^{j\theta})|_{dB}, |S_1(e^{j\theta})|_{dB}, |S_2(e^{j\theta})|_{dB}$ and the desired specifications which are clearly met by both S_1 and S_2. We make a comparison between the two approaches after the next example.

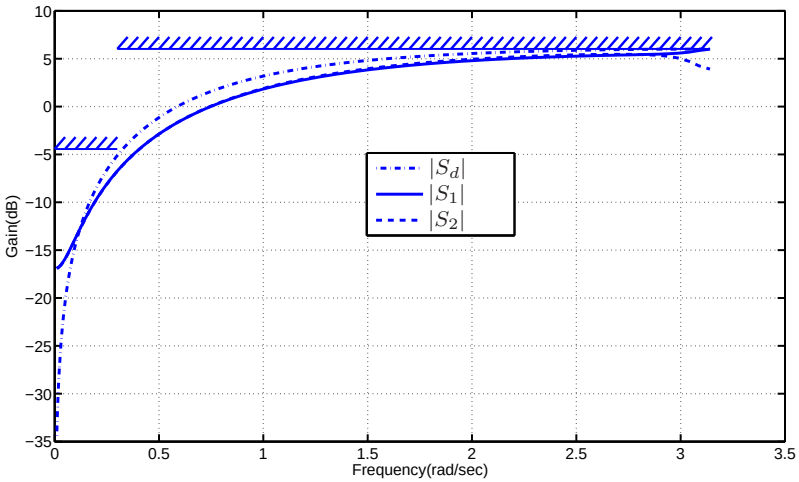

Figure 2.1: Plots of $|S_d|$ in (2.13), $|S_1|$ and $|S_2|$ in (2.14) and the desired specification corresponding to Example 2.1

Example 2.2 (from [30, 55]) Consider the continuous-time plant

$$\hat{P}(s) = \frac{(s-1)(s-2)}{(s+1)(s^2+s+1)},$$

and the following specifications

$$\begin{cases} \mid \hat{S}(j\omega) \mid \leq \ 0.1, \quad 0 \leq \omega < 0.01 \text{ (rad/s)} \\ \|\hat{S}(j\omega)\|_\infty \ < \ 1.3 \end{cases} \tag{2.15}$$

for the closed-loop sensitivity function. Since we mostly work in the z-domain, we use "$\hat{}$" to denote functions in the s-domain.

In the s-domain the system has three non-minimum phase zeros at $s = 1, 2$ and infinity. Therefore, for internal stability (see [68]) the sensitivity function must satisfy

$$\hat{S}(1) = \hat{S}(2) = \hat{S}(\infty) = 1.$$

We translate these to the z-domain using a Möbius transformation. The interpolation constraints on $S(z = \frac{1+s}{1-s}) = \hat{S}(s)$ become

$$S(\infty) = S(-3) = S(-1) = 1. \tag{2.16}$$

Accordingly, the required specifications (2.15) change to

$$\begin{cases} \mid S(e^{j\theta}) \mid \leq \ 0.1, \quad 0 \leq \theta < 0.02 \text{ (rad/s)} \\ \|S(e^{j\theta})\|_\infty \ < \ 1.3 \end{cases}. \tag{2.17}$$

Now, in order to avoid the boundary condition $S(-1) = 1$ and for ease of comparison, we follow Nagamune [55] and define $S_\varepsilon(z) := S(\frac{z}{1+\varepsilon})$, where ε is a small positive number–say, $\varepsilon = 0.005$. Then, the interpolation conditions (2.16) change to

$$S_\varepsilon(\infty) = S_\varepsilon(-3.015) = S_\varepsilon(-1.005) = 1. \tag{2.18}$$

These three conditions can be satisfied by interpolants of degree 2. However because of the tight specification at low-frequency given in (2.17) there is no sensitivity function of degree 2 which meets both (2.17) and (2.18) at the same time (see [55]). To address this issue, following [55] we introduce an extra interpolation condition $S_\varepsilon(1.002) = 0$. This condition increases the degree of interpolant by one and it also helps satisfy low-frequency requirement. In the next section we present a less-ad-hoc approach for pre-specified increase in the degree of sensitivity function.

Now, starting from

$$S_d(z) = \frac{z^4 - 0.2399z^3 - 0.7727z^2 - 0.0763z + 0.0960}{z^4 - 0.1726z^3 - 0.5342z^2}, \tag{2.19}$$

which is the resulting sensitivity function using standard H_∞-design in [30], we find the corresponding $\Phi_d(z)$ and solve (2.6) and (2.10). These give rise to two choices for $\Psi(z)$ with zeros at $z = \{-0.4457 \pm 0.2053j, 0.5811\}$ and $z = \{-0.2749 \pm 0.5607j, 0.5532\}$, respectively. Finally, using these two choices for Ψ in minimization of (2.4), subject to the stability conditions, and then transformation back to the continuous domain lead to

$$\begin{aligned} \hat{S}_1(s) &= \frac{1.0011s^3 + 3.6185s^2 + 12.0545s - 0.0120}{s^3 + 4.1454s^2 + 10.4851s + 1.0316}, \\ \hat{S}_2(s) &= \frac{1.0003s^3 + 1.5003s^2 + 4.7702s - 0.0048}{s^3 + 1.7164s^2 + 4.1254s + 0.4242}, \end{aligned} \tag{2.20}$$

corresponding to convex approximation and quasi-convex formalism, respectively. Figure 2.2 shows $|\hat{S}_d(j\omega)|_{dB}$ (continuous equivalent of $|S_d(e^{j\theta})|_{dB}$), $|\hat{S}_1(j\omega)|_{dB}, |\hat{S}_2(j\omega)|_{dB}$ and the desired specifications. This figure reveals that although both $\hat{S}_1$ and $\hat{S}_2$ match

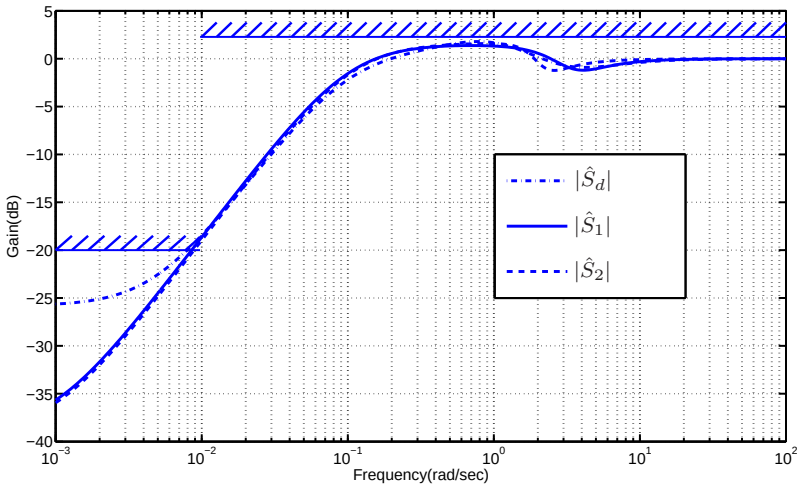

Figure 2.2: Plots of $|\hat{S}_d|$ in (2.19), $|\hat{S}_1|$ and $|\hat{S}_2|$ in (2.20) and the desired specification corresponding to Example 2.2

$\hat{S}_d$ very well, none of them quite satisfy the constraint (2.15) around the frequency 0.01 (rad/s). The reason is that even $\hat{S}_d$ (obtained from standard H_∞-design in [30]), whose shape was the "target" in this design problem violates the required specification around the frequency 0.01 (rad/s). To avoid this problem we let the desired input function be the following simple but more conservative first-order Chebyshev discrete filter that satisfies (2.17) and has a pass-band gain of 1.3 (i.e., norm bound constraint of the desired sensitivity)

$$S_d(z) = \frac{1.0171z - 1.0171}{z - 0.5648}. \tag{2.21}$$

This $S_d(z)$ generates the corresponding $\Phi_d(z)$ via (2.5). Then solving (2.6) and (2.10) provides weighting functions $\Psi(z)$'s with two sets of spectral-zeros at $z = \{0.3950, -0.5717, -0.3838\}$ and $z = \{-0.4692, 0.1114 \pm 0.4011j\}$, respectively. Using these Ψ's in the second step, we minimize (2.4) subject to the corresponding interpolation conditions. The optimal F's then result in the sensitivity functions (after transformation back to the s-domain)

$$\begin{aligned} \hat{S}_1(s) &= \frac{1.0026s^3 + 4.1922s^2 + 21.6182s - 0.0216}{s^3 + 5.3527s^2 + 18.1637s + 2.2750}, \\ \hat{S}_2(s) &= \frac{1.0013s^3 + 3.0464s^2 + 10.3143s - 0.0103}{s^3 + 3.6586s^2 + 8.4911s + 1.2020}, \end{aligned} \tag{2.22}$$

for convex and quasi-convex frameworks, respectively. The corresponding controllers are

$$\hat{C}_1(s) = \frac{1.1605s^3 + 2.3210s^2 + 2.3210s + 1.1605}{s^3 + 4.1922s^2 + 21.6182s - 0.0216},$$
$$\hat{C}_2(s) = \frac{0.6122s^3 + 1.2244s^2 + 1.2244s + 0.6122}{s^3 + 3.0464s^2 + 10.3143s - 0.0103},$$

respectively. Figure 2.3 shows $|\hat{S}_d(j\omega)|_{dB}$ (equivalent of (2.21) in the s-domain), $|\hat{S}_1(j\omega)|_{dB}, |\hat{S}_2(j\omega)|_{dB}$, and horizontal lines marking the desired specifications. It is

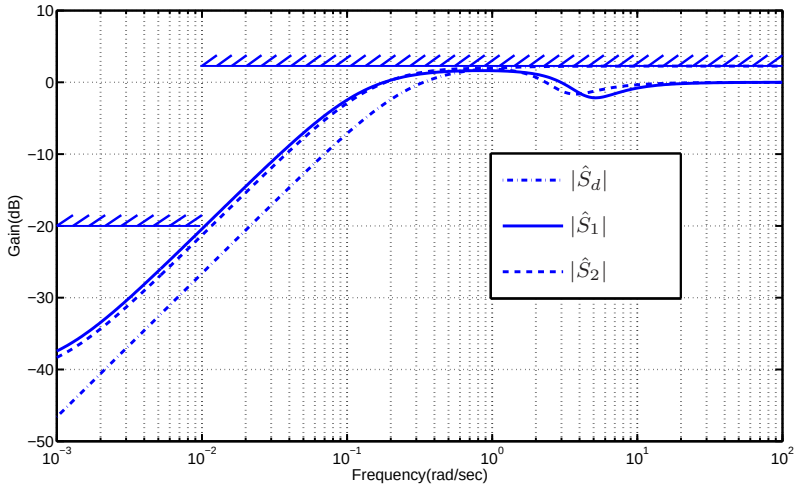

Figure 2.3: Plots of $|\hat{S}_d|$ in (2.21), $|\hat{S}_1|$ and $|\hat{S}_2|$ in (2.22) and the desired specification corresponding to Example 2.2

evident that the obtained sensitivities both satisfy all the requirements and have McMillan degree equal to 3, whereas the resulting sensitivity in [30] which is based on standard H_∞-design is of degree 4 and does not quite meet the specifications at low frequencies.

Remark 2.1 Comparison of the results for two different formalisms proposed in this chapter shows that there is no significant difference between them. In fact, for a given Φ_d, these two methods seek to minimize the errors $\|\Psi(e^{j\theta}) - \mathfrak{Q}(e^{j\theta})\Phi_d(e^{j\theta})\|$ and $\|\Psi(e^{j\theta})/\mathfrak{Q}(e^{j\theta}) - \Phi_d(e^{j\theta})\|$, respectively. If there exists an exact pair of $(\Psi, \mathfrak{Q})$ in $\mathcal{D}$ which makes both errors small, then both alternatives will have similar performances. But, in cases where these errors cannot be made small the latter seems superior.

To clarify this point, we consider the high-order sensitivity

$$\hat{S}_d(s) = \frac{s^4 + 6.1447s^3 + 12.5910s^2 + 5.1273s + 0.0238}{s^4 + 6.7561s^3 + 10.9777s^2 + 5.6874s + 0.4656} \tag{2.23}$$

from [30] and we try to approximate it with a second-order transfer function. Fitting the corresponding Ψ via convex approximation and quasi-convex approach leads to sensitivity functions

$$\begin{aligned} \hat{S}_1(s) &= \frac{1.0015s^2 + 2.8431s + 2.2622}{s^2 + 3.8081s + 1.7467}, \\ \hat{S}_2(s) &= \frac{0.9337s^2 + 1.4503s + 0.0071}{s^2 + 1.2530s + 0.1449}, \end{aligned} \tag{2.24}$$

respectively. Superiority of the latter formalism is clear from Figure 2.4. Note that the two "sensitivity functions" $\hat{S}_1$ and $\hat{S}_2$ are <u>not</u> required to satisfy the interpolation conditions. They are just "second-order approximants" of $\hat{S}_d(s)$ obtained via the two optimization methods, without consideration of interpolation, for the sole purpose of demonstrating that quasi-convex formalism is more direct as it pertains to "fitting".

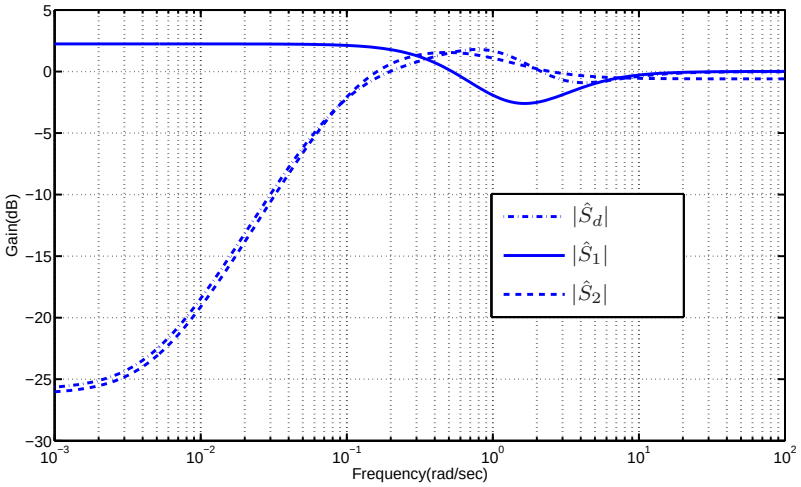

Figure 2.4: Plots of $|\hat{S}_d|$ in (2.23), and $|\hat{S}_1|$, $|\hat{S}_2|$ in (2.24)

Example 2.3 (from [55]) Consider the discrete-time plant

$$P(z) = \frac{1}{z - 1.05},$$

and let $T := \frac{PC}{1+PC}$ denote the closed-loop complementary sensitivity function. The goal is to design a sensitivity function which gives rise to a stable closed-loop system and satisfies the following constraints

$$\begin{cases} |S(e^{j\theta})| < 0.1 (= -20\text{dB}), & \text{for } \theta \in [0, 0.3] \text{ rad/s}, \\ |T(e^{j\theta})| = |1 - S(e^{j\theta})| < 0.5 \ (\approx -6.02 \text{ dB}), & \text{for } \theta \in [2.5, \pi] \text{ rad/s}, \\ |S(e^{j\theta})| < 2 \ (\approx 6.02 \text{ dB}), & \text{for } \theta \in [0 \ , \ \pi] \text{ rad/s}. \end{cases} \tag{2.25}$$

This plant has one unstable pole at $z = 1.05$ and one non-minimum phase zero at infinity. Thus, internal stability of the closed-loop system requires that

$$S(1.05) = 0, \ S(\infty) = 1, \tag{2.26}$$

and of course that S is analytic in $\mathbb{D}^c$. Furthermore, we can represent all the nominal performance conditions in (2.25) in terms of only S or T. Since according to [55] no sensitivity function of degree 1 can satisfy the conditions (2.25) and (2.26) at the same time, again following [55], we augment the interpolation conditions by imposing

$$S(-1.01) = 1, \ S(1.01e^{\pm 0.3j}) = 0.$$

so as to allow interpolants of a suitably high degree that can meet the performance objectives.

We continue with the choice

$$S_d(z) = \frac{0.3664z^4 - 1.4656z^3 + 2.1984z^2 - 1.4656z + 0.3664}{z^4 - 1.8408z^3 + 1.7064z^2 - 0.7234z + 0.2109},$$

which satisfies the frequency requirements, but not the interpolation conditions. This S_d has been constructed via Matlab filter design command (cheb1ord) simply on the basis of the performance bounds. We use the corresponding $\Phi_d(e^{j\theta})$ in the optimization problem (2.10) to obtain $\Psi = \psi/|\tau|^2$. This has roots at $\{0.6980 \pm 0.6025j, 0.1880 \pm 0.4894j\}$. Using this choice of Ψ we minimize (2.4) subject to the relevant interpola-

tion conditions to obtain $F(z)$. This minimizer, via (2.3), gives

$$S(z) = \frac{z^4 - 2.3426z^3 + 1.1478z^2 + 0.8699z - 0.6825}{z^4 - 1.5613z^3 + 0.6973z^2 + 0.1770z - 0.1166}.$$

This is a fourth-order sensitivity function and corresponds to the third-order controller

$$C(z) = \frac{0.7813z^3 - 0.4506z^2 - 0.6929z + 0.5658}{z^3 - 1.2926z^2 - 0.2094z + 0.6500}.$$

Figure 2.5 shows that the resulting sensitivity and complementary sensitivity functions satisfy all design requirements.

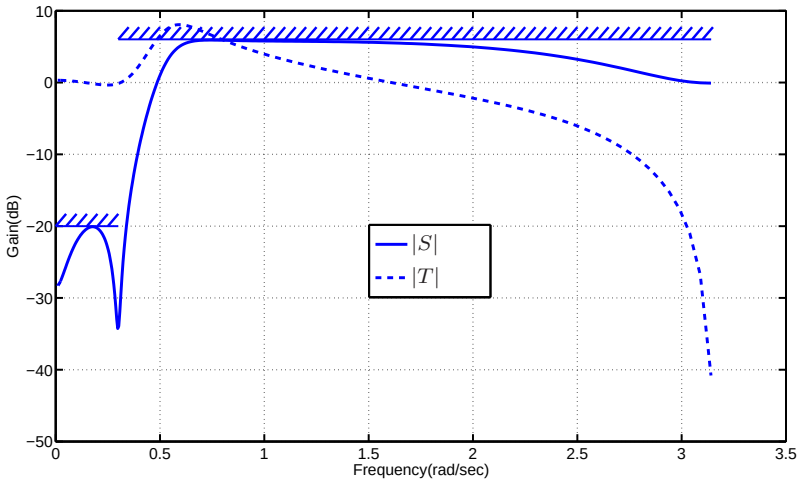

Figure 2.5: Plots of the resulting $|S|$, $|T|$ and the desired specification in Example 2.3

Using a more classical H_∞-design technique for this example one could seek

$$\inf_C \left\| \begin{bmatrix} W_1 S \\ W_2 T \end{bmatrix} \right\|_\infty$$

subject to the internal stability conditions, where W_1 and W_2 are appropriate weights. This formalism which has been used in [55] does not lead to a satisfactory result.

2.6 Double weighted entropy functional

Following [42] we now explore a more versatile functional which again allows a bound on the degree of interpolants obtained via optimization. An added weight W can be introduced in (2.2) as follows

$$\underset{S}{\operatorname{argmax}} \int_{-\pi}^{\pi} \Psi(e^{j\theta}) \log(\gamma^2 - |W(e^{j\theta})S(e^{j\theta})|^2) d\theta, \tag{2.27}$$

and the optimization carried out subject to the usual interpolation constraints. Both weights Ψ and W in (2.27) play the role of "tuning parameters" for control design (see [42]). Incorporating the extra weight $W(z)$ leads to an increase in the order of $S(z)$. In cases where the constraints in the sensitivity shaping problem are too stringent, the resulting increase in the degree of $S(z)$ may be necessary, and W provides a convenient tuning parameter. We demonstrate the efficacy of this formalism by reworking Example 2.2.

Example 2.2 (Continued) The number of interpolation conditions for internal stability of the closed-loop system is $n = 3$. Hence, the natural generic degree of interpolants is $n - 1 = 2$, which is not sufficient as indicated earlier for meeting the performance objectives. Here, instead of following [55] in imposing added ad-hoc interpolation constraints, we explore the flexibility afforded by a choice of a (stably invertible) weighting function W in (2.27). More specifically, we choose

$$W(z) = \frac{1.2z - 0.75}{z - 0.99}. \tag{2.28}$$

This is a first-order low-pass filter, consistent with the high-pass characteristic of the desired sensitivity function. Incorporating this $W(z)$, dictates that $W(s)S_\varepsilon(s)$ satisfies (2.18) change to

$$W(\infty)S_\varepsilon(\infty) = 1.2, W(-3.015)S_\varepsilon(-3.015) = 1.1281, W(-1.005)S_\varepsilon(-1.005) = 1.0556.$$

We now repeat the procedure of the previous section starting with $S_d(z)$ in (2.21). At the end, the minimizer needs to be scaled by $W^{-1}(z)$. The final result in the s-domain is

$$\hat{S}(s) = \frac{1.0029s^3 + 2.2394s^2 + 22.2859s + 0.1119}{s^3 + 3.4884s^2 + 18.5675s + 2.5842}, \tag{2.29}$$

for the sensitivity function and

$$\hat{C}(s) = \frac{1.2490s^3 + 2.4980s^2 + 2.4980s + 1.2490}{s^3 + 2.2394s^2 + 22.2859s + 0.1119}$$

for the corresponding controller. Figure 2.6 shows the modulus of $\hat{S}_d(j\omega), \hat{W}(j\omega)$ (continuous equivalent of $W(z)$), as well as the modulus of $\hat{S}(j\omega)$ in dB over frequency. It is seen that all desired requirements are met. Furthermore, comparison of the plots in Figures 2.3 and 2.6 reveals the role of weighting function $W(z)$ in sensitivity shaping. In the latter case the modulus of the resulting sensitivity is closer to the original step-like specification.

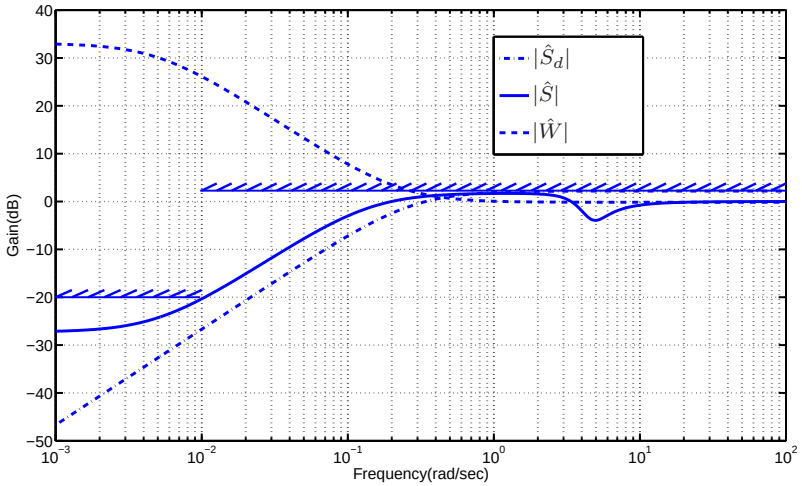

Figure 2.6: Plots of $|\hat{S}_d|$ in (2.21), $|\hat{S}|$ in (2.29), $|\hat{W}|$ in (2.28), and the desired specification corresponding to Example 2.2

2.7 Concluding remarks

In this chapter, we considered issues of weight selection for control synthesis via an approach which is based on minimization of weighted entropy-like functionals. The approach originated in [13] (see also [14, 41, 42]) and was introduced to handle the McMillan degree of analytic interpolants — as these interpolants represent closed-loop operators in control synthesis problems. For additional exposition of the approach and comparison with an alternative viewpoint due to Gahinet, Apkarian, Skelton, Grigoriades, and Iwasaki we refer to [42] (see also [31]).

In the present chapter we focused on the viewpoint in the work by Nagamune, Blomqvist, and others (see [8, 48, 54–57]) and cast weight selection for control synthesis as an optimization problem. This is a non-convex optimization which we dealt with it in two different ways: (i) turning it into a convex problem via a suitable relaxation and (ii) finding the exact solution in a quasi-convex framework.

Chapter 3

Multivariable analytic interpolation with a degree constraint

We consider a Nehari problem for matrix-valued, positive-real functions, and characterize the class of (generically) minimal-degree solutions. Analytic interpolation problems (such as the one studied herein) for positive-real functions arise in time-series modeling and system identification. The degree of positive-real interpolants relates to the dimension of models and to the degree of matricial power-spectra of vector-valued time-series. The main result of this chapter generalizes earlier results in scalar analytic interpolation with a degree constraint, studied in the previous chapter, where the class of (generically) minimal-degree solutions is characterized by an arbitrary choice of "spectral-zeros". Naturally, in the current multivariable setting, there is freedom in assigning the zero structure of the power spectrum, i.e., the spectral-zeros as well as their respective invariant subspaces. The characterization utilizes Rosenbrock's theorem on assignability of dynamics via linear state feedback.

3.1 Introduction

Analytic interpolation arises in a variety of applications such as model-matching in control theory (e.g., [6, 24, 30, 72]), maximum power transfer in circuit theory (see [2,19,70,71]), and spectral estimation in signal processing (see e.g., [33,34,36,37]). A complete parametrization of bounded-degree solutions for scalar analytic interpolation problems has been obtained in terms of the zeros of certain corresponding spectral factors [13–15, 33, 35]. These are referred to as the spectral-zeros. For scalar problems the dynamics of the inverse spectral factors are completely determined by the spectral-zeros. However, in the case of multivariable interpolation problems nontrivial (i.e., noncyclic) Jordan structures are possible. The purpose of this chapter is to study the freedom in specifying the invariant factors for the inverse spectrum. We utilize Rosenbrock's theorem on assignability of dynamics via linear state feedback to characterize interpolants and their zero dynamics.

In this chapter, we consider analytic interpolation with $m \times m$ *matrix-valued, positive-real functions*. Very much as in H_∞-control the dimension of the interpolants relates to the complexity of a model, a filter, or a controller. The complexity of the interpolation is characterized by the number of interpolation conditions, n. In the multivariable case where the interpolation conditions are constraints along different directions, n *is the rank of a corresponding Pick matrix* (see [37]), or equivalently of a Hankel operator. While the standard approach [30], based on linear fractional transformations, describes the complete solution set as a function-ball around a central interpolant, it gives no insight as to possible minimal-degree solutions.

Historically, over the last few decades there has been effort to describe minimal-degree solutions for analytic interpolation problems (see e.g., [33, 35, 47, 71]), with significant developments over the past 10 years [13, 15, 17, 41]. These studies led to a complete parametrization of bounded-degree interpolants for the most general Sarason-type analytic interpolation in the scalar case [14]. Although attention to analogous results in matrix-valued interpolation with bounded McMillan degree has already been drawn more than 20 years ago in [33], progress has been slow. We mention some recent nice work by Blomqvist et al. [9].

The main contribution of the current chapter is to characterize a family of solutions to multivariable analytic interpolation with degree constraints. This generalizes scalar results where a parametrization of interpolants is given in terms of admissible spectral-

zeros. This is no longer the case in multivariable problems where the spectral-zero dynamics relate to noncyclic Jordan structures, in general. Thus, a variety of solutions may have zero-dynamics that relate to the same Jordan form. The generically minimal degree of solutions for multivariable problems is $n - m$ (n being the rank of a Pick matrix and $m \times m$ the size of interpolants). We utilize a formalism based on a multivariable moment problem in [39] that describes a class of solutions of degree $n - m$ in a convenient factored form; the real part of interpolants gives rise to a matrix-valued spectral density function that solves the moment problem. We then utilize Rosenbrock's theorem on pole assignability by state feedback to specify all Jordan structures that are possible for the inverse of corresponding spectral factors. We will discuss a number of questions that pertain to the complete parametrization of solutions that remain open.

The structure of this chapter is as follows. In Section 3.2, we introduce analytic interpolation and its connection to moment problem. We also review earlier results in the multivariable setting. In Section 3.3 and 3.4 we identify classes of spectral-zero dynamics that correspond to solutions of the analytic interpolation problem with McMillan degree $n - m$. The parametrization of all solutions in the multivariable setting cannot be based on eigenvalues and Jordan structure of the spectral-zero dynamics only, unlike the scalar case, as highlighted in Section 3.5. In Section 3.6 we present examples from spectral analysis and from circuit synthesis that motivated the theory, and which illustrate the applicability and relevance of the results.

3.2 Notation and preliminaries

Throughout this chapter, we denote by $\mathcal{C}$ the set of square matrix-valued functions which are analytic in $\mathbb{D}$, the open unit disk of the complex plane, and have positive Hermitian-part (Carathéodory class). There is a natural correspondence between elements in $\mathcal{C}$ and the class of finite Hermitian positive matrix-valued measures on $(-\pi, \pi]$ denoted by $\mathcal{M}$. In fact, analytic interpolation constraints on functions in $\mathcal{C}$ can be cast as moment constraints on corresponding measures in $\mathcal{M}$ [3, 49]. We now make the connection between the two as our results in this chapter draw heavily on recent developments in the multivariable moment problem [39].

3.2.1 Analytic interpolation

We consider the problem of parameterizing all functions $F \in \mathcal{C}$ of size $m \times m$ which satisfy

$$F(z) = F_{\mathrm{o}}(z) + Q(z)V(z), \quad \text{for } z \in \mathbb{D}, \tag{3.1a}$$

with known $F_{\mathrm{o}}(z), V(z)$, and the parameter $Q(z)$ all being square matrix-functions. Equation (3.1a) represents an interpolation condition. Indeed, along directions where $V(z)$ vanishes $F(z) - F_{\mathrm{o}}(z)$ vanishes as well, and thus, $F(z)$ interpolates $F_{\mathrm{o}}(z)$. The matrix-function $Q(z)$ is required to be analytic in $\mathbb{D}$, and thereby, without loss of generality, we can always assume $V(z)$ is inner (all-pass), i.e.,

$$V(z)^*V(z) = V(z)V(z)^* = I, \quad \text{for all } |z| = 1, \tag{3.1b}$$

where "*" denotes "conjugate-transpose". In cases where $V(z)$ is a scalar multiple of the identity, $F(z)$ possesses the same value as $F_{\mathrm{o}}(z)$ at the roots of $V(z)$, whereas in general with an arbitrary inner $V(z)$, constraint (3.1a) is in the category of tangential interpolation (see [3]).

We are interested in finite dimensional interpolation problems where $V(z)$ is a rational function of McMillan degree n. Therefore, we write

$$F_{\mathrm{o}}(z) = H(I - zA)^{-1}B, \quad \text{and} \tag{3.1c}$$

$$V(z) = D + Cz(I - zA)^{-1}B, \tag{3.1d}$$

where $A \in \mathbb{R}^{n\times n}$, B full column rank in $\mathbb{R}^{n\times m}$, $H \in \mathbb{R}^{m\times n}$, (A, B) is a reachable pair, and the eigenvalues of A lie in $\mathbb{D}$. Moreover, $C \in \mathbb{R}^{m\times n}$ and $D \in \mathbb{R}^{m\times m}$ are suitably chosen so that (C, A) is an observable pair and $V(z)$ satisfies (3.1b). The completion of (A, B) into an inner matrix-valued function $V(z)$ is well known and is part of the bounded real lemma, cf. [2].

Equations (3.1a-d), which are standing assumptions throughout, form the standard Nehari-type problem with the triplet of matrices (A, B, H) as the interpolation data. It turns out that a positive Hermitian-part solution of (3.1a-d) exists if and only if the Lyapunov equation

$$R - ARA^* = BH + H^*B^* \tag{3.2}$$

has a positive semi-definite solution for R, which is thought of as the corresponding

Pick matrix (see e.g., [37, 40]). In cases where R is strictly positive definite there exist infinitely many solutions. Our interest in this chapter is to identify the family of interpolants, $F(z)$'s, which satisfy (3.1a-d) and have low McMillan degree. We now outline the correspondence between interpolation problem (3.1a-d) and a related moment problem.

3.2.2 Connection with moment problem

Consider the linear discrete-time dynamical system

$$x_k = Ax_{k-1} + Bu_k, \quad \text{for } k \in \mathbb{Z}, \tag{3.3}$$

where $x_k \in \mathbb{R}^n$, and $u_k \in \mathbb{R}^m$ are the state and the input vectors, respectively. The input-to-state transfer function of this system is

$$G(z) := (I - zA)^{-1}B,$$

where "z" stands for the transform of the delay operator, and thus, "stability" of $G(z)$ corresponds to "analyticity in $\mathbb{D}$". Let the input u_k be a stationary zero-mean random process with the matrix-valued density function $\Phi_{uu}(\theta),\ \theta \in (-\pi, \pi]$, where $\Phi_{uu}(\theta)d\theta \in \mathcal{M}$. Then, the state covariance matrix of (3.3) can be obtained via the following integral [51]

$$E\{x_k x_k^*\} = \frac{1}{2\pi}\int_{-\pi}^{\pi} G(e^{j\theta})\Phi_{uu}(\theta)G(e^{j\theta})^* d\theta.$$

The classical moment problem amounts to the (inverse) problem of finding an input spectral density function $\Phi_{uu}(\theta)$ which is consistent with a given state covariance matrix $E\{x_k x_k^*\}$. It turns out that a non-negative definite matrix R admits such a representation, i.e.,

$$R = \frac{1}{2\pi}\int_{-\pi}^{\pi} G(e^{j\theta})\Phi_{uu}(\theta)G(e^{j\theta})^* d\theta, \tag{3.4}$$

and hence qualifies as a state covariance of (3.3), if and only if the following equivalent

conditions hold (see [37, 40]):

$$\operatorname{rank}\begin{bmatrix} R - ARA^* & B \\ B^* & 0 \end{bmatrix} = 2m, \tag{3.5a}$$

$$R \text{ satisfies (3.2) for a choice of } H. \tag{3.5b}$$

Further, consistent spectral densities, Φ_{uu}'s, for the moment problem (3.4) are in a bijective correspondence with solutions to the interpolation problem (3.1a-d). More precisely, corresponding to any positive-real matrix-function $F(z)$ which satisfies (3.1a-d) for a given triplet of (A, B, H), there exists a solution to the moment problem (3.4) with the triplet of data (A, B, R) such that

$$F(z) = \frac{1}{2\pi}\int_{-\pi}^{\pi}\left(\frac{1+ze^{j\theta}}{1-ze^{j\theta}}\right)\Phi_{uu}(\theta)d\theta + jc, \tag{3.6}$$

where jc is an arbitrary skew-Hermitian constant. This is the content of Riesz-Herglotz's theorem [21]. Conversely, any density function of more general measure that satisfies (3.4) originates as the boundary limit of the real part of a positive-real solution to (3.1a-d), i.e.,

$$\Phi_{uu}(\theta) = \lim_{\rho \nearrow 1} \Re e\, F(\rho e^{j\theta}).$$

We wish to emphasize two points: first, H (interpolation data) and R (moment data) relate to each other via (3.2). Second, a change of coordinates in (3.3), i.e.,

$$(A, B) \mapsto (T^{-1}AT, T^{-1}B),$$

transforms the state covariance matrix as follows

$$R \mapsto T^{-1}R(T^{-1})^*,$$

accordingly. In the sequel, we select a coordinate system so that the controllability grammian

$$L_{\mathrm{c}} := \frac{1}{2\pi}\int_{-\pi}^{\pi} G(e^{j\theta})G(e^{j\theta})^* d\theta$$

equals the identity matrix (i.e., if $L_{\mathrm{c}} \neq I$, choose T equal to the Hermitian square

root of L_c). Thus, in this coordinate system

$$AA^* + BB^* = I.$$

This particular normalization simplifies the interpolation condition (3.1a) which now becomes

$$\frac{1}{2\pi}\int_{-\pi}^{\pi} F(e^{j\theta})G(e^{j\theta})^* d\theta = H.$$

3.2.3 Solutions to the general moment problem

Reference [39], building on earlier works, e.g., [13–15], characterized all positive solutions to the moment problem (3.4) as minimizers of suitably weighted relative entropy functionals. More specifically, let $\Psi(\theta)d\theta$ and $\Phi(\theta)d\theta$ belong to $\mathcal{M}$ and define the relative entropy functional

$$\mathbf{S}(\Psi\|\Phi) := \frac{1}{2\pi}\int_{-\pi}^{\pi} \operatorname{trace}(\Psi\log\Psi - \Psi\log\Phi)d\theta. \tag{3.7}$$

Then, for a given admissible (A, B, R), i.e., such that (3.5a-b) hold, all positive solutions to the moment problem (3.4) can be obtained as minimizers of $\mathbf{S}(\Psi\|\Phi_{uu})$ for a choice of Ψ, i.e., they are of the form

$$\underset{\Phi_{uu}}{\operatorname{argmin}} \left\{ \mathbf{S}(\Psi\|\Phi_{uu}) : \quad R = \frac{1}{2\pi}\int_{-\pi}^{\pi} G(e^{j\theta})\Phi_{uu}(\theta)G(e^{j\theta})^* d\theta \right\}, \tag{3.8}$$

with Ψ being a free parameter. Minimizers of this optimization problem are shown to be in the form of

$$\Phi_{uu}(\theta) = \sigma(e^{j\theta})\left(G(e^{j\theta})^*\lambda G(e^{j\theta})\right)^{-1}\sigma(e^{j\theta})^*,$$

with λ, a Hermitian matrix of Lagrange multipliers, and σ, a matrix-valued spectral factor of Ψ, i.e., $\sigma\sigma^* := \Psi$. Given σ, the value of λ can be obtained numerically via a continuation method (see [39]).

For the special choice of $\sigma(e^{j\theta}) = I + Ke^{j\theta}G(e^{j\theta})$, selected so that $A - BK$ is Hurwitz,

we obtain a solution of the form

$$\Phi_{uu}(\theta) = \left(G_{\rm o}(e^{j\theta})^* \lambda G_{\rm o}(e^{j\theta})\right)^{-1}, \quad \text{with} \tag{3.9a}$$

$$G_{\rm o}(e^{j\theta}) = \left(I - e^{j\theta}(A - BK)\right)^{-1} B, \tag{3.9b}$$

where $\Phi_{uu}(\theta)$ in (3.9a-b) is a rational spectral density function of degree at most $2n$, and thereby, corresponds (via (3.6)) to a positive-real $F(e^{j\theta})$ of McMillan degree at most n. This F is, indeed, the solution of the corresponding interpolation problem (3.1a-d) for the triplet of data (A, B, H). In this chapter, we identify and characterize a subclass of an even lower McMillan degree. In fact, the minimal McMillan degree which is generically feasible is $n - m$, and we show that for a choice of K we can generate a family of solutions of degree $n - m$.

3.3 Jordan structure of spectral-zero dynamics

In this section, we use Rosenbrock's theorem [66] to describe the flexibility in assigning the invariant factors of the inverse dynamics of interpolants in the multivariable setting. Earlier results for the scalar case (see e.g., [13, 15, 35]) suggest that the spectral-zeros can be arbitrarily assigned. However, the associated Jordan structure of these spectral-zeros is always cyclic. In the matricial interpolation this is not the case and the spectral-zero dynamics relate to nontrivial (i.e., noncyclic) Jordan structures as well.

3.3.1 Rosenbrock's theorem on assignability of dynamics via linear state feedback

We first recall the notion of invariant polynomials. Let $\Pi_t(z)$ for $t = 1, 2, \ldots, r$ denote the greatest common divisor of all the minors of order t of $zI - A$. Then each polynomial in the series

$$\Pi_r(z), \Pi_{r-1}(z), \ldots, \Pi_1(z), \Pi_0(z) \equiv 1$$

is divisible by the succeeding one and the quotients

$$p_1(z) = \frac{\Pi_r(z)}{\Pi_{r-1}(z)}, p_2(z) = \frac{\Pi_{r-1}(z)}{\Pi_{r-2}(z)}, \ldots, p_r(z) = \frac{\Pi_1(z)}{\Pi_0(z)}$$

are the *invariant polynomials* of A (see e.g., [32, 43]).

Next, we need the notion of controllability indices. Let (A, B) be a controllable pair, assume that B has full column rank, and consider the ordered set of vectors

$$b_1, \ldots, b_m, Ab_1, \ldots, Ab_m, A^2b_1, \ldots, A^2b_m, \ldots,$$

where b_i is the ith column of B. Following Popov ([65]), $A^k b_j$ is an "antecedent" of $A^\mu b_\nu$ if it is listed earlier in the above ordered list (i.e., if $km + j < \mu m + \nu$). We denote by κ_i the smallest positive integer for which $A^{\kappa_i} b_i$ is a linear combination of its antecedents. Then, κ_i's for $i \in \{1, 2, \ldots, m\}$ are the *controllability indices* of the pair (A, B).

The controllability indices are also known as *Kronecker invariants* and their sum is equal to n, the dimension of the system. They are invariant under state feedback, similarity transformation, and invertible linear transformation on the columns of B. Intuitively, each of these indices can be thought of as an integer value which quantifies how deep one can get into the state space using the corresponding input channel.

Rosenbrock's theorem on pole assignment: Consider the controllable pair (A, B) (as before) with controllability indices κ_i's in decreasing order for $i = 1, 2, \ldots, m$. Let $\{p_i(z);\ i = 1, 2, \ldots, m\}$ be any set of polynomials which satisfy

$$p_i(z) \mid p_{i-1}(z),$$

i.e., p_i divides p_{i-1}, and $\sum_{i=1}^{m} \deg p_i(z) = n$. Then the conditions

$$\sum_{i=1}^{j} \deg\ p_i(z) \geq \sum_{i=1}^{j} \kappa_i$$

for $j = 1, 2, \ldots, m$ are necessary and sufficient for the existence of linear map $K : \mathbb{R}^n \mapsto \mathbb{R}^m$ such that $\{p_i(z)\}$ is the set of invariant polynomials of $A - BK$.

This theorem was proven in [66, page 190] (see also [23] and [46], and an elegant constructive proof based on a geometric argument by Flamm in [29]).

3.3.2 Spectral-zero dynamics assignability in multivariable interpolation

The (generically) minimal-degree solutions for scalar interpolation have been fully parameterized (see e.g., [13–15,35]) by an arbitrary choice of "spectral-zeros". These spectral-zeros are in fact the zeros of a meromorphic extension of the real part of the interpolating function. Naturally, in the matricial case, there are more degrees of freedom. Herein, we use the notion of "spectral-zero dynamics" which helps draw analogous results in multivariable interpolation. For any $F(z) \in \mathcal{C}$, denote by $W_{\rm o}$ the outer spectral factor of the inverse of the real part of F, i.e.,

$$\left(\Re e\, F(e^{j\theta})\right)^{-1} = W_{\rm o}(e^{j\theta})^* W_{\rm o}(e^{j\theta}), \tag{3.10}$$

with $W_{\rm o}(z) =: D_{\rm o} + C_{\rm o} z\,(I - zA_{\rm z})^{-1} B_{\rm o}$, a minimal realization of $W_{\rm o}(z)$. We call $A_{\rm z}$ the spectral-zero dynamics of $F(z)$ as it determines the pole-structure of $\left(\Re e\, F(e^{j\theta})\right)^{-1}$. Theorem 3.1, below, characterizes a family of minimal-degree solutions to multivariable interpolation that correspond to choices of spectral-zero dynamics.

Theorem 3.1 Consider data (A, B, H) for multivariable interpolation problem defined by (3.1a-d) and assume that (3.2) admits a positive definite solution R, i.e., that the problem is solvable. Let κ_i's for $i = 1, 2, \ldots, m$ denote the controllability indices of (A, B) in decreasing order. Then, corresponding to any Hurwitz $A_{\rm z} \in \mathbb{R}^{(n-m)\times(n-m)}$ whose invariant polynomials $\{p_i(z);\ i = 1, 2, \ldots, m\}$ satisfy

$$\sum_{i=1}^{j} \deg\ p_i(z) + j \geq \sum_{i=1}^{j} \kappa_i, \quad \text{for } j = 1, \ldots, m, \tag{3.11}$$

there exists an interpolant $F(z)$ of McMillan degree at most $n - m$ whose spectral-zero dynamics has the same Jordan structure as $A_{\rm z}$.

Corollary 3.1 Consider the interpolation problem (3.1a-d) with a corresponding $R \succ 0$ and let $A_{\rm z}$ be a Hurwitx matrix. If any of the following conditions holds:

1. $A_{\rm z}$ is cyclic,
2. m divides n and all the controllability indices of (A, B) are equal, i.e., $\kappa_1 = \ldots = \kappa_m = \frac{n}{m}$,

3. m does not divide n and the controllability indices of (A, B) are as follows

$$\kappa_j = \begin{cases} \lfloor \frac{n}{m} \rfloor + 1 & \text{for } j = 1, \ldots, \mathsf{mod}(n, m) \\ \lfloor \frac{n}{m} \rfloor & \text{for } j = \mathsf{mod}(n, m) + 1, \ldots, m \end{cases},$$

where $\lfloor \frac{n}{m} \rfloor$ stands for "the integer part of $\frac{n}{m}$", and "$\mathsf{mod}(n, m)$" gives the remainder of division n/m,

there exists an interpolant $F(z)$ of McMillan degree at most $n - m$ whose spectral-zero dynamics has the Jordan structure as A_z.

The first condition implies that deg $p_1(z) = n - m$, while $p_2 = \ldots = p_m = 1$ and thus Theorem 3.1 applies. The other two can be argued in a similar way. An example where the second condition holds is that of the trigonometric moment problem in which

$$A = \begin{bmatrix} O & O & \cdots & O & O \\ I & O & \cdots & O & O \\ & \ddots & \ddots & \vdots & \vdots \\ & & & & \\ O & O & & I & O \end{bmatrix}, \quad B = \begin{bmatrix} I \\ O \\ \vdots \\ \\ O \end{bmatrix}, \tag{3.12}$$

with I and O the identity and the zero matrices of size $m \times m$, A an $(l+1) \times (l+1)$ and B an $(l+1) \times 1$ block matrices, respectively. The size of each block is $m \times m$, and hence, the actual size of A, B are $n \times n$ and $n \times m$, with $n = (l+1)m$. These correspond to a block-Topeltiz matrix

$$R = \begin{bmatrix} R_0 & R_1 & \cdots & R_l \\ R_{-1} & R_0 & \cdots & R_{l-1} \\ \vdots & \vdots & \ddots & \vdots \\ R_{-l} & R_{-l+1} & \cdots & R_0 \end{bmatrix}, \tag{3.13}$$

where the size of each R_i is $m \times m$ and

$$F(z) = \frac{1}{2} R_0 + R_1 z + \cdots + R_l z^l + o(z^l).$$

For this case of (A, B) all the controllability indices are equal to $\frac{n}{m} = l + 1$. Section 3.5 discusses further the trigonometric moment problem.

It should be noted that in general there may not exist solutions $F(z)$ of degree less than $n - m$. In fact, very much as in the scalar case where $m = 1$, both the data set of admissible triplets (A, B, R) for which a solution of degree less than $n - m$ is possible, as well as the complement where $n - m$ is the minimal degree, have a nonempty interior, i.e., they are both generic conditions (see e.g., [33, pages 50 & 80–83]). This is due to the semi-algebraic nature of the underlying problem.

Note also that the set of conditions (3.11) are only sufficient for the existence of degree $n - m$ solutions corresponding to the Jordan structure of a given A_z. This will be taken up in the next section. The proof of Theorem 3.1 requires a couple of preceding steps, given as two separate lemmas.

Lemma 3.1 Let $F(z)$ be a rational function of McMillan degree $n-m$, which is strictly positive-real with $\Re e\, F(z)$ uniformly bounded in $\mathbb{D}$. Then, there exists $\hat{F}(z)$ which is also strictly positive-real and of McMillan degree $n-m$ such that $\Re e\, \hat{F}(e^{j\theta}) = \big(\Re e\, F(e^{j\theta})\big)^{-1}$.

Proof: The function $\hat{F}$ in the lemma is the analytic part of $(\Re e\, F)^{-1}$. Briefly, explicit construction of left and right spectral factorizations of the real part of $F(e^{j\theta})$

$$\Re e\, F(e^{j\theta}) = W_{\mathfrak{L}}(e^{j\theta}) W_{\mathfrak{L}}^*(e^{j\theta}) = W_{\mathfrak{R}}^*(e^{j\theta}) W_{\mathfrak{R}}(e^{j\theta}) \tag{3.14}$$

is always possible. These are rational matrix-valued functions of the same degree as $F(z)$. Conversely, starting from spectral factors $W_{\mathfrak{L}}(z)$ and $W_{\mathfrak{R}}(z)$ it is easy (and standard how) to obtain $F(z)$ by isolating the analytic part of products in (3.14) with suitable coordinate transformation in state-space. The inverse of left spectral factors of $F(z)$ can now serve as right spectral factors of the sought $\hat{F}(z)$. Clearly, there is no possibility of degree inflation and the proof of the lemma follows. □

The above fact sets a bijection $F \leftrightarrow \hat{F}$ between functions in this class.

Lemma 3.2 Let $A, B, G_{\rm o}(z)$ Let $A, B, G_{\rm o}(z)$ be as in (3.9b), let $\Delta(K,\lambda) := G_{\rm o}^*\lambda G_{\rm o}$ for $\lambda \in \mathbb{R}^{n\times n}$, and let K satisfy:

(i) $A - BK$ is Hurwitz,

(ii) $\mathsf{rank}(A - BK) = n - m$.

Then, there exists a rational matrix-valued function $\hat{F}(z)$ of degree $n - m$ such that $\Delta(K,\lambda) = \Re e\, \hat{F}$.

Proof: We write $\Delta(K,\lambda)$ as the two-sided series:

$$\begin{aligned} B^*\left(I - z^{-1}(A-BK)^*\right)^{-1}\lambda\left(I - z(A-BK)\right)^{-1}B = \\ \cdots + z^{-2}B^*A_{\rm o}^{*2}\Lambda B + z^{-1}B^*A_{\rm o}^*\Lambda B + B^*\Lambda B + \\ zB^*\Lambda A_{\rm o}B + z^2B^*\Lambda A_{\rm o}^2B + \cdots, \end{aligned} \tag{3.15}$$

with $A_{\rm o} := A - BK$ and Λ the solution of the Lyapunov equation

$$\Lambda - A_{\rm o}^*\Lambda A_{\rm o} = \lambda. \tag{3.16}$$

It readily follows from equation (3.15) that $\Delta(K,\lambda) = \Re e\, \hat{F}$ for

$$\hat{F}(z) = \frac{1}{2}B^*\Lambda B + B^*\Lambda A_{\rm o}z(I - zA_{\rm o})^{-1}B. \tag{3.17}$$

On the other hand, since $\mathrm{rank}(A_{\rm o}) = n - m$, the rank of the observability matrix of $\hat{F}(z)$

$$\mathcal{O}_{\hat{F}} := \begin{bmatrix} B^*\Lambda \\ B^*\Lambda A_{\rm o} \\ \vdots \\ B^*\Lambda A_{\rm o}^{n-1} \end{bmatrix} A_{\rm o} \tag{3.18}$$

cannot exceed $n - m$, hence neither can the McMillan degree of $\hat{F}(z)$. □

Remark 3.1 The two lemmas establish a mapping $(K, \lambda) \mapsto \hat{F} \mapsto F$. Therefore, the construction of interpolants begins with a choice of K that satisfies the conditions in Lemma 3.2. We then solve the optimization problem (3.8) which gives rise to the desired λ, and hence Λ. This Λ via (3.17) generates the matrix-valued function $\hat{F}$. Finally, the interpolant F is the analytic part of $(\Re e\, \hat{F})^{-1}$.

Proof of Theorem 3.1: For any spectral-zero dynamics $A_{\rm z}$ with invariant polynomials $\{p_i(z);\ i = 1, 2, \ldots, m\}$ that satisfy (3.11), the sequence of polynomials $z^i p_i(z)$ satisfies the condition of Rosenbrock's theorem for the pair (A, B). Thus there exists a K such that $A - BK$ has $\{z^i p_i(z);\ i = 1, 2, \ldots, m\}$ as its invariant polynomials, and hence

$$A - BK \overset{\text{similar}}{\sim} \begin{bmatrix} A_{\rm z} & 0 \\ Y & 0 \end{bmatrix}, \tag{3.19}$$

with Y as a matrix of compatible size. This choice of K gives rise to a matricial power spectral density $\Phi_{uu}(\theta)$ as in (3.9a-b). Then, from Lemma 3.2 we conclude that there exists a rational function $\hat{F}(z)$ of McMillan degree $n - m$ such that $\Phi_{uu}(\theta)^{-1} = \Re e\, \hat{F}(e^{j\theta})$. Positivity of its Hermitian part on the circle ensures that $\hat{F}(z)$ is a positive-real function. Finally, application of Lemma 3.1 implies that there exists a positive-real function $F(z)$ of McMillan degree $n - m$ such that $\Phi_{uu}(\theta) = \Re e\, F(e^{j\theta})$. Indeed, this $F(z)$ is a solution to multivariable interpolation (3.1a-d) and this proves the claim of the theorem. □

3.4 Alternative solutions of McMillan degree $n - m$

In this part, we show that for a given triplet of data (A, B, H) in the multivariable interpolation where $m > 1$, there may exist interpolants of McMillan degree $n - m$ with spectral-zero dynamics which do not satisfy inequalities (3.11). Indeed, the condition $\text{rank}(A - BK) = n - m$ that played a central role in the earlier section is only sufficient and not necessary in order to obtain solutions of McMillan degree $n - m$. In other words, such a rank condition, and hence the drop of the degree, originate from the rank deficiency of observability matrix $\mathcal{O}_{\hat{F}}$ in (3.18). In cases where $\text{rank}(\mathcal{O}_{\hat{F}}) = n - m$ and $\text{rank}(A - BK) > n - m$, there may be more degrees of freedom in assigning spectral-zero dynamics of the interpolants so that instead of

(3.19) we have

$$A - BK \overset{\text{similar}}{\sim} \begin{bmatrix} A_z & 0 \\ Y_1 & Y_2 \end{bmatrix}. \tag{3.20}$$

Here, Y_1 and Y_2 are matrices of compatible size, Y_2 is unobservable dynamics, and A_z, whose invariant polynomials do not need to satisfy (3.11), is the only block that contributes in spectral-zero dynamics of the solution. The following example is to illustrate this point.

Example 3.1 Consider the interpolation data

$$A = \begin{bmatrix} \frac{1}{2} & 1 & 0 & 0 \\ 0 & \frac{1}{2} & 1 & 0 \\ 0 & 0 & \frac{1}{2} & 0 \\ 0 & 0 & 0 & \frac{1}{2} \end{bmatrix}, \; B = \begin{bmatrix} 0 & 0 \\ 0 & 0 \\ 1 & 0 \\ 0 & 1 \end{bmatrix}, \; H = \begin{bmatrix} 0.0012 & -0.3351 & 0.2507 & 0 \\ 0 & 0 & 0 & 0.2507 \end{bmatrix}, \tag{3.21}$$

where $n = 4, m = 2$. It is shown that for this triplet of (A, B, H) there exists a solution $F(z)$ of McMillan degree $n - m = 2$ corresponding to a spectral-zero dynamics which does not fall in the class specified by Theorem 3.1 (i.e., does not satisfy (3.11)).

We solve the problem by following the path described in Remark 3.1. In particular, we take $K = 0$ and this choice results in

$$\lambda \approx \begin{bmatrix} 0.2258 & -0.4163 & 0.1771 & 0.0000 \\ -0.4163 & 0.6275 & -0.0283 & 0.0000 \\ 0.1771 & -0.0283 & 0.7348 & 0.0000 \\ 0.0000 & 0.0000 & 0.0000 & 1.4996 \end{bmatrix}$$

via continuation method (see [39]). We then find the corresponding Λ from (3.16) and this results in a positive-real $F(z)$ of McMillan degree 2. To see that $F(z)$ is of degree 2 it suffices to consider the degree of the corresponding positive-real $\hat{F}(z)$. These degrees coincide. In fact, we will be working mostly with $\hat{F}(z)$ instead of $F(z)$. From (3.17)

$$\begin{aligned} \hat{F}(z) &= \frac{1}{2} B^* \Lambda B + B^* \Lambda A z (I - zA)^{-1} B \\ &= \begin{bmatrix} 1 & 0 \\ 0 & 1 \end{bmatrix} + \begin{bmatrix} \frac{z}{1-\frac{1}{2}z} & 0 \\ 0 & \frac{z}{1-\frac{1}{2}z} \end{bmatrix}. \end{aligned}$$

The observability matrix

$$\mathcal{O}_{\hat{F}} = \begin{bmatrix} B^*\Lambda A \\ B^*\Lambda A^2 \\ B^*\Lambda A^3 \\ B^*\Lambda A^4 \end{bmatrix} = \begin{bmatrix} 0\ 0 & 1 & 0 \\ 0\ 0 & 0 & 1 \\ 0\ 0 & 0.5 & 0 \\ 0\ 0 & 0 & 0.5 \\ 0\ 0 & 0.25 & 0 \\ 0\ 0 & 0 & 0.25 \\ 0\ 0 & 0.125 & 0 \\ 0\ 0 & 0 & 0.125 \end{bmatrix},$$

is of rank 2 and the realization

$$A_{\hat{F}} = \begin{bmatrix} \frac{1}{2} & 0 \\ 0 & \frac{1}{2} \end{bmatrix}, \quad B_{\hat{F}} = C_{\hat{F}} = D_{\hat{F}} = I_2 \tag{3.22}$$

is minimal. Hence, $\hat{F}(z)$ as well as $F(z)$ are both of McMillan degree 2. We emphasize that in this example $F(z)$ of degree $n-m$ corresponds to a choice of matrix $A-BK$ whose rank is greater than $n-m$; in fact, $A-BK$ is full-rank (remember $K=0$).

We now show that the resulting $A_{\hat{F}}$ does not satisfy the set of inequalities (3.11) in Theorem 3.1. Note that the invariant polynomials of the desired spectral-zero dynamics, $A_{\hat{F}}$ in (3.22), are $p_1 = p_2 = z - \frac{1}{2}$. On the other hand, controllability indices of the given (A, B) are easily obtained as $\kappa_1 = 3$ and $\kappa_2 = 1$. Clearly, this set of $\{p_1, p_2, \kappa_1, \kappa_2\}$ violates the inequalities in (3.11). In fact, application of Rosenbrock's theorem (in which the set of conditions is both necessary and sufficient) implies that there is no value for K such that similarity in (3.19) holds for any choice of Y. Therefore, given the set of interpolation data (3.21), interpolants with spectral-zero dynamics similar to $A_{\hat{F}}$ in (3.22) cannot be obtained via Theorem 3.1. This completes the proof of this example. □

We will present an alternative approach to this example in the next chapter. This second approach (given in Section 4.2) provides more insight into the problem and also contains interesting details that prove our claim without using Rosenbrock's theorem.

To sum up, the first conclusion to be drawn in multivariable interpolation is that corresponding to any spectral-zero dynamics whose invariant polynomials satisfy (3.11),

there exists a solution of McMillan degree $n-m$. Remark 3.1 summarizes the construction of this class of interpolants. Further, there may exist solutions of degree $n-m$ whose spectral-zero dynamics do not satisfy the set of inequalities in (3.11). The existence of such solutions depends on a particular H in interpolation data (e.g., as in Example 3.1). Therefore in general, there is no systematic way to find solutions whose spectral-zero dynamics do not fall in the class specified by Theorem 3.1. Finally, because of the basic limitations on linear state feedback, described by Rosenbrock's theorem, the proposed framework of this chapter cannot assign a certain class of Jordan structures as the spectral-zero dynamics of solutions for any choice of H in interpolation data. The following corollary addresses this fact.

Corollary 3.2 Consider data (A, B, H) for multivariable interpolation problem defined by (3.1a-d) and assume that the problem is solvable. Let κ_i's for $i = 1, 2, \ldots, m$ be the controllability indices of (A, B) in decreasing order and $A_z \in \mathbb{R}^{(n-m)\times(n-m)}$ be a Hurwitz matrix with invariant polynomials $\{p_i(z);\ i = 1, 2, \ldots, m\}$. Then, in order to assign the Jordan structure of A_z as the spectral-zero dynamics of a solution F, the analytic part of Φ_{uu} in (3.9a), the following inequalities must hold:

$$\sum_{i=1}^{j} \deg\ p_i(z) + m \geq \sum_{i=1}^{j} \kappa_i, \quad \text{for } j = 1, \ldots, m. \tag{3.23}$$

The proof is immediate by Rosenbrock's theorem. Briefly, adding m distinct eigenvalues $\{z_1, \ldots, z_m\}$ to A_z changes its first invariant polynomial to $\hat{p}_1(z) = p_1(z)(z - z_1)\cdots(z - z_m)$. Then, the sequence of polynomials $\hat{p}_1, p_2, \ldots, p_m$ satisfies the condition of Rosenbrock's theorem for the pair (A, B). Further, the augmentation of p_1 to the above $\hat{p}_1$ gives the maximum degrees of freedom in assigning the spectral-zero dynamics of Φ_{uu} in (3.9a) and the proof follows.

If we compare the set of conditions (3.11) in Theorem 3.1 with (3.23) in Corollary 3.2, inequalities in the former case guarantee the existence of interpolants with McMillan degree $n-m$ (assuming that the problem has nonempty solution set), whereas in the latter case, the existence of such solutions depends on the particular H in interpolation data as well. This comparison in Example 3.1, with the given (A, B, H) in (3.21), shows that although the choice of $A_z = A_{\hat{F}} = \begin{bmatrix} \frac{1}{2} & 0 \\ 0 & \frac{1}{2} \end{bmatrix}$ violates the conditions (3.11)

in Theorem 3.1, it satisfies (3.23). Thereby, because of the specific interpolation data we could find a solution of degree $n - m$ in that case.

We finish this section with a simple example that illustrates Corollary 3.2. Consider the interpolation data

$$A = \begin{bmatrix} \frac{1}{2} & 1 & 0 & 0 & 0 & 0 \\ 0 & \frac{1}{2} & 1 & 0 & 0 & 0 \\ 0 & 0 & \frac{1}{2} & 1 & 0 & 0 \\ 0 & 0 & 0 & \frac{1}{2} & 1 & 0 \\ 0 & 0 & 0 & 0 & \frac{1}{2} & 0 \\ 0 & 0 & 0 & 0 & 0 & \frac{1}{2} \end{bmatrix}, \quad B = \begin{bmatrix} 0 & 0 \\ 0 & 0 \\ 0 & 0 \\ 0 & 0 \\ 1 & 0 \\ 0 & 1 \end{bmatrix},$$

with a corresponding H such that the problem has nonempty solution set. With this set of data where $n = 6$, $m = 2$, $\kappa_1 = 5$ and $\kappa_2 = 1$, neither Theorem 3.1 nor Corollary 3.2 leads to an interpolant of degree $n - m = 4$ with spectral-zero dynamics

$$A_{\mathrm{z}} = \begin{bmatrix} \frac{1}{3} & 1 & 0 & 0 \\ 0 & \frac{1}{3} & 0 & 0 \\ 0 & 0 & \frac{1}{3} & 1 \\ 0 & 0 & 0 & \frac{1}{3} \end{bmatrix}.$$

The reason is that both invariant polynomials of A_{z} in this case are of degree 2 and this violates not only (3.11) but also the inequalities in (3.23).

3.5 Correspondence between Jordan structures and solutions

Contrary to the scalar case [13,14], the Jordan structure of the spectral-zero dynamics in multivariable interpolation is not sufficient to specify an interpolant uniquely. This is to be expected since the same zero dynamics may be contributed by different channels. However, if the interpolation is sought in a fractional form as in [33], then the choice of the "numerator" of the spectral factor in a likewise factorized form may be sufficient to ensure uniqueness (modulo multiplication by a unitary matrix). The next example demonstrates the first point, followed by a discussion of uniqueness in the context of the trigonometric moment problem in the spirit of [33].

Example 3.2 Consider

$$A = \begin{bmatrix} 0\ 0\ 0\ 0 \\ 0\ 0\ 0\ 0 \\ 1\ 0\ 0\ 0 \\ 0\ 1\ 0\ 0 \end{bmatrix},\ B = \begin{bmatrix} 1\ 0 \\ 0\ 1 \\ 0\ 0 \\ 0\ 0 \end{bmatrix}, H = \begin{bmatrix} 2\ 0\ 2\ 0 \\ 0\ 2\ 0\ 2 \end{bmatrix},$$

and let the desired Jordan structure for spectral-zero dynamics of solutions be

$$A_{\mathrm{z}} = \begin{bmatrix} -1/2 & 0 \\ 0 & -1/3 \end{bmatrix}, \tag{3.24}$$

which falls in the class specified by Corollary 3.1. It can be shown that there exist more than one K that give rise to interpolants with Jordan structure (3.24) as their spectral-zero dynamics. To see this, we follow the construction in Remark 3.1 with two choices of K as

$$K_1 = \begin{bmatrix} 1/2 & 0 & 0\ 0 \\ 0 & 1/3 & 0\ 0 \end{bmatrix}, K_2 = \begin{bmatrix} 1/3 & 0 & 0\ 0 \\ 0 & 1/2 & 0\ 0 \end{bmatrix}.$$

These lead to $\hat{F}_1$ and $\hat{F}_2$ with minimal realizations

$$\hat{F}_1 : \left\{ \begin{bmatrix} -\frac{1}{2} & 0 \\ 0 & -\frac{1}{3} \end{bmatrix}, \begin{bmatrix} 1\ 0 \\ 0\ 1 \end{bmatrix}, \begin{bmatrix} -0.34 & 0 \\ 0 & -0.25 \end{bmatrix}, \begin{bmatrix} 0.28 & 0 \\ 0 & 0.24 \end{bmatrix} \right\},$$
$$\hat{F}_2 : \left\{ \begin{bmatrix} -\frac{1}{3} & 0 \\ 0 & -\frac{1}{2} \end{bmatrix}, \begin{bmatrix} 1\ 0 \\ 0\ 1 \end{bmatrix}, \begin{bmatrix} -0.25 & 0 \\ 0 & -0.34 \end{bmatrix}, \begin{bmatrix} 0.24 & 0 \\ 0 & 0.28 \end{bmatrix} \right\},$$

respectively. Therefore, the spectral-zero dynamics of the corresponding interpolants F_1 and F_2 share the same Jordan structure. □

Theorem 3.1 provides a rather clear picture of the solutions of degree $n - m$ for the special case of interpolation of trigonometric matrix functions. Corollary 3.3, in the following, gives the full parametrization of degree $n - m$ solutions to this class of problems.

Corollary 3.3 Consider the trigonometric moment problem with data (A, B, R) as in (3.12) and (3.13) and $R \succ 0$. Then, *every* interpolant F of McMillan degree $n - m$ can be obtained (as described in Remark 3.1) for a *unique* choice of K which satisfies

(i) $A - BK$ is Hurwitz,

(ii) $\mathsf{rank}(A - BK) = n - m$,

and determines the spectral-zero dynamics of $F(z)$.

Proof: This proof consists of two parts. We first show that each $n - m$ degree interpolant can be obtained by a choice of K as described in Remark 3.1. The uniqueness of the corresponding K for every interpolant is the second part of the proof.

First part: We begin with a solution F of McMillan degree $n - m$ and write the minimal realization of the corresponding $\hat{F}$ (see Lemma 3.1) as

$$\hat{F} =: D_{\hat{F}} + C_{\hat{F}} z (I - z A_{\hat{F}})^{-1} B_{\hat{F}}, \tag{3.25}$$

where $\Re e\, \hat{F} = (\Re e\, F)^{-1}$, $A_{\hat{F}} \in \mathbb{R}^{(n-m)\times(n-m)}$, $B_{\hat{F}} \in \mathbb{R}^{(n-m)\times m}$ and $C_{\hat{F}}, D_{\hat{F}}$ are matrices of compatible size. For simplicity and without loss of generality we assume

$$A_{\hat{F}} =: \begin{bmatrix} \alpha_{11} & \alpha_{12} & \cdots & \alpha_{1l} \\ \alpha_{21} & \alpha_{22} & \cdots & \alpha_{2l} \\ \vdots & \vdots & & \vdots \\ \\ \alpha_{l1} & \alpha_{l2} & \cdots & \alpha_{ll} \end{bmatrix}, \quad \text{and} \quad B_{\hat{F}} = \begin{bmatrix} I \\ O \\ \vdots \\ \\ O \end{bmatrix}, \tag{3.26}$$

with each block of size $m \times m$ (remember $n = (l + 1)m$). However in the sequel, we do not work with individual blocks of $A_{\hat{F}}$. We show that there always exists a matrix K of dimension $m \times n$ such that

$$\hat{F} = \frac{1}{2} B^* \Lambda B + B^* \Lambda (A - BK) z \left(I - z(A - BK)\right)^{-1} B, \tag{3.27}$$

where $\Lambda \in \mathbb{R}^{n\times n}$ comes from the solution of the corresponding moment problem.

As seen in Lemma 3.2, (3.27) is not a minimal realization of $\hat{F}$ because of the Condition (ii) that leads to rank deficiency of the observability matrix in this realization. We now show that there always exists an invertible $T \in \mathbb{R}^{(n-m)\times(n-m)}$ that relates the minimal part of (3.27) to (3.25) via similarity transformation. In order to proceed with the proof we need to partition K, Λ, and T into $m \times m$ blocks as well:

$$K =: \begin{bmatrix} K_1 & K_2 & \cdots & K_l & O \end{bmatrix},$$

$$\Lambda =: \begin{bmatrix} \Lambda_{11} & \Lambda_{12} & \cdots & \Lambda_{1(l+1)} \\ \Lambda_{21} & \Lambda_{22} & \cdots & \Lambda_{2(l+1)} \\ \vdots & \vdots & & \vdots \\ \Lambda_{(l+1)1} & \Lambda_{(l+1)2} & \cdots & \Lambda_{(l+1)(l+1)} \end{bmatrix}, \quad T =: \begin{bmatrix} T_{11} & T_{12} & \cdots & T_{1l} \\ T_{21} & T_{22} & \cdots & T_{2l} \\ \vdots & \vdots & & \vdots \\ T_{l1} & T_{l2} & \cdots & T_{ll} \end{bmatrix}. \tag{3.28}$$

The last block of K becomes zero because of the Condition (ii).

From the above discussion and using the introduced notations, we now solve the following sets of equations to find the desired K and T.

$$A_{\hat{F}}T = T \begin{bmatrix} -K_1 & -K_2 & \cdots & -K_l \\ I & O & \cdots & O \\ & \ddots & \ddots & \vdots \\ O & O & I & O \end{bmatrix}_{(n-m)\times(n-m)}, \tag{3.29a}$$

$$B_{\hat{F}} = T \begin{bmatrix} I \\ O \\ \vdots \\ O \end{bmatrix}_{(n-m)\times m}, \tag{3.29b}$$

$$C_{\hat{F}} = \begin{bmatrix} \Lambda_{11}K_1 + \Lambda_{12} & \Lambda_{11}K_2 + \Lambda_{13} & \cdots & \Lambda_{11}K_l + \Lambda_{1(l+1)} \end{bmatrix} T^{-1}, \tag{3.29c}$$

$$D_{\hat{F}} = \frac{1}{2}B^*\Lambda B = \frac{1}{2}\Lambda_{11}. \tag{3.29d}$$

It is straightforward to see that $l+1$ blocks $\Lambda_{11}, \Lambda_{12}, \cdots, \Lambda_{1(l+1)}$ give enough degrees of freedom to satisfy (3.29c-d). In other words, considering $\Lambda_{11} = 2D_{\hat{F}}$ it is always possible for $\Lambda_{12}, \cdots, \Lambda_{1(l+1)}$ to satisfy (3.29c), regardless of the values of K and T.

On the other hand, (3.29b) implies

$$\begin{bmatrix} T_{11} \\ T_{21} \\ \vdots \\ T_{l1} \end{bmatrix} = \begin{bmatrix} I \\ O \\ \vdots \\ O \end{bmatrix}, \tag{3.30}$$

and (3.29a) always has a solution for K and an invertible T. To see this, we proceed with (3.29a), using (3.30),

$$\begin{aligned}
A_{\hat{F}} \begin{bmatrix} T_{11} \\ T_{21} \\ \vdots \\ T_{l1} \end{bmatrix} &= \begin{bmatrix} -K_1 \\ O \\ \vdots \\ O \end{bmatrix} + \begin{bmatrix} T_{12} \\ T_{22} \\ \vdots \\ T_{l2} \end{bmatrix}, \\
A_{\hat{F}} \begin{bmatrix} T_{12} \\ T_{22} \\ \vdots \\ T_{l2} \end{bmatrix} &= \begin{bmatrix} -K_2 \\ O \\ \vdots \\ O \end{bmatrix} + \begin{bmatrix} T_{13} \\ T_{23} \\ \vdots \\ T_{l3} \end{bmatrix}, \\
&\vdots \\
&\vdots \\
&\vdots \\
A_{\hat{F}} \begin{bmatrix} T_{1(l-1)} \\ T_{2(l-1)} \\ \vdots \\ T_{l(l-1)} \end{bmatrix} &= \begin{bmatrix} -K_{l-1} \\ O \\ \vdots \\ O \end{bmatrix} + \begin{bmatrix} T_{1l} \\ T_{2l} \\ \vdots \\ T_{ll} \end{bmatrix}, \\
A_{\hat{F}} \begin{bmatrix} T_{1l} \\ T_{2l} \\ \vdots \\ T_{ll} \end{bmatrix} &= \begin{bmatrix} -K_l \\ O \\ \vdots \\ O \end{bmatrix}.
\end{aligned} \tag{3.31}$$

The above set includes l^2 blocks of equation and l^2 blocks of unknown. By following these equations and using the fact that the first column of T is equal to $B_{\hat{F}}$ we arrive

at

$$
\begin{aligned}
\begin{bmatrix} T_{12} \\ T_{22} \\ \vdots \\ T_{l2} \end{bmatrix} &= A_{\hat{F}} B_{\hat{F}} + \begin{bmatrix} K_1 \\ O \\ \vdots \\ O \end{bmatrix}, \\
\begin{bmatrix} T_{13} \\ T_{23} \\ \vdots \\ T_{l3} \end{bmatrix} &= A_{\hat{F}}^2 B_{\hat{F}} + A_{\hat{F}} \begin{bmatrix} K_1 \\ O \\ \vdots \\ O \end{bmatrix} + \begin{bmatrix} K_2 \\ O \\ \vdots \\ O \end{bmatrix}, \\
&\vdots \\
&\vdots \\
&\vdots \\
\begin{bmatrix} T_{1l} \\ T_{2l} \\ \vdots \\ T_{ll} \end{bmatrix} &= A_{\hat{F}}^{l-1} B_{\hat{F}} + A_{\hat{F}}^{l-2} \begin{bmatrix} K_1 \\ O \\ \vdots \\ O \end{bmatrix} + \cdots + \begin{bmatrix} K_{l-1} \\ O \\ \vdots \\ O \end{bmatrix}, \\
\begin{bmatrix} O \\ O \\ \vdots \\ O \end{bmatrix} &= A_{\hat{F}}^{l} B_{\hat{F}} + A_{\hat{F}}^{l-1} \begin{bmatrix} K_1 \\ O \\ \vdots \\ O \end{bmatrix} + \cdots + A_{\hat{F}} \begin{bmatrix} K_{l-1} \\ O \\ \vdots \\ O \end{bmatrix} + \begin{bmatrix} K_l \\ O \\ \vdots \\ O \end{bmatrix}.
\end{aligned}
$$

This set of equations gives rise to the matrices T and K that satisfy (3.29a). Moreover, considering controllability of the pair $(A_{\hat{F}}, B_{\hat{F}})$ and the structure of $B_{\hat{F}}$ in (3.26) it is obvious that all the columns of T are independent of each other. Therefore, T is invertible and this completes the first part of the proof. □

Second part: Let F_1 and F_2 be two $n-m$ degree solutions to the trigonometric moment problem, obtained via Remark 3.1 and corresponding to K_{F_1}, K_{F_2}. Without loss of generality we can assume $K_{F_2} = 0$. We show that if $F_1 = F_2$, then $K_{F_1} = 0$ as well.

If $F_1 = F_2$, and hence $\hat{F}_1 = \hat{F}_2$, then the minimal realizations of $\hat{F}_1$ and $\hat{F}_2$ are identical modulo a similarity transformation, i.e., there exists an invertible $T \in \mathbb{R}^{(n-m)\times(n-m)}$ such that

$$\begin{cases} A_{\hat{F}_1} = T A_{\hat{F}_2} T^{-1} \\ B_{\hat{F}_1} = T B_{\hat{F}_2} \\ C_{\hat{F}_1} = C_{\hat{F}_2} T^{-1} \\ D_{\hat{F}_1} = D_{\hat{F}_2} \end{cases}, \tag{3.32}$$

where $\{A_{\hat{F}_i}, B_{\hat{F}_i}, C_{\hat{F}_i}, D_{\hat{F}_i}\}$ for $i = 1, 2$ are the corresponding minimal realizations. On the other hand, K_{F_1} can be partitioned as

$$K_{F_1} = [K_{1j}]_{j=1,\dots,l+1},$$

where each K_{1j} is a block matrix of size $m \times m$. Then the rank condition on $A - BK_{F_1}$ implies that $K_{1(l+1)} = 0$ and from the realizations of $\hat{F}_1$, $\hat{F}_2$ as in (3.17) we have

$$A_{\hat{F}_1} = \begin{bmatrix} -K_{11} & -K_{12} & \cdots & -K_{1l} \\ I & O & \cdots & O \\ & \ddots & \ddots & \vdots \\ O & O & I & O \end{bmatrix}, \quad B_{\hat{F}_1} = \begin{bmatrix} I \\ O \\ \vdots \\ O \end{bmatrix},$$

$$A_{\hat{F}_2} = \begin{bmatrix} O & O & \cdots & O \\ I & O & \cdots & O \\ & \ddots & \ddots & \vdots \\ O & O & I & O \end{bmatrix}, \quad B_{\hat{F}_2} = \begin{bmatrix} I \\ O \\ \vdots \\ O \end{bmatrix}.$$

We only focus on the first two equations in (3.32) and prove the uniqueness, i.e., that $K_{F_1} = 0$. By using the same notation as in (3.28) for T and substituting the related

values in the first two equations of (3.32) it follows

$$\begin{bmatrix} -K_{11} & -K_{12} & \cdots & -K_{1l} \\ I & O & \cdots & O \\ & \ddots & \ddots & \vdots \\ & & & \\ O & O & I & O \end{bmatrix} \begin{bmatrix} T_{11} & T_{12} & \cdots & T_{1l} \\ T_{21} & T_{22} & \cdots & T_{2l} \\ \vdots & \vdots & & \vdots \\ & & & \\ T_{l1} & T_{l2} & \cdots & T_{ll} \end{bmatrix}$$
$$= \begin{bmatrix} T_{11} & T_{12} & \cdots & T_{1l} \\ T_{21} & T_{22} & \cdots & T_{2l} \\ \vdots & \vdots & & \vdots \\ & & & \\ T_{l1} & T_{l2} & \cdots & T_{ll} \end{bmatrix} \begin{bmatrix} O & O & \cdots & O & O \\ I & O & \cdots & O & O \\ & \ddots & \ddots & \vdots & \vdots \\ & & & & \\ O & O & & I & O \end{bmatrix} \tag{3.33}$$

and

$$\begin{bmatrix} I \\ O \\ \vdots \\ \\ O \end{bmatrix} = \begin{bmatrix} T_{11} & T_{12} & \cdots & T_{1l} \\ T_{21} & T_{22} & \cdots & T_{2l} \\ \vdots & \vdots & & \vdots \\ & & & \\ T_{l1} & T_{l2} & \cdots & T_{ll} \end{bmatrix} \begin{bmatrix} I \\ O \\ \vdots \\ \\ O \end{bmatrix}. \tag{3.34}$$

Finally, performing the multiplications in (3.33) and (3.34) reveals that T has to be identity, i.e., $T = I_{n-m}$. Thereby $K_{F_1} = 0$ and the uniqueness follows. □

3.6 Applications

This section highlights the pertinence of the main results of this chapter to practical use in multivariable spectral analysis and circuit theory. The application in spectral analysis relates to reconstruction of a matricial power spectral density from second-order statistics. The example in circuit theory deals with the inverse problem of finding a family of impedance matrices consistent with a given set of data for a two-port passive network.

3.6.1 Spectral estimation

In this part, we consider the dynamical system (3.3) and work out two examples in which matrices A and B are as in (3.12) with $n = 6, m = 2$, and $\kappa_1 = \kappa_2 = 3$. The state equations of the system, effectively, keep track of the past two values of a 2-dimensional vectorial input process. The inputs in both examples are assumed to be wide-sense stationary, and hence, the state-covariances are block-Toeplitz matrices. The problem we consider is to reconstruct the power spectral density from state-covariance statistics. In the first example, the statistics originate from an input process with the two channels strongly coupled. In the second example, the matricial power spectral density of the vectorial input process is essentially diagonal, and hence, the two input channels are not coupled. The examples explore the resolving properties of power spectral densities of the family in Theorem 3.1.

More specifically, earlier works (see e.g., [13, 37]) in high resolution spectral analysis of scalar time-series highlighted the role of spectral-zeros in spectral matching based on second-order statistics. In particular, it was shown in [33] that the spectral-zeros cannot be determined on the basis of a finite collection of second order statistics, and proceeded to characterize families of spectra which are consistent with statistics and have (generically) minimal complexity/degree. For each choice of spectral-zeros a power spectral density can be constructed which is consistent with the statistics. The choice of spectral-zeros affects resolution and can only be dictated by "prior" information on what features of the power spectral density need to be identified. In fact, it was shown in subsequent work [12] that proximity of the spectral-zeros to a particular arc of the unit circle increases resolution over a corresponding range of frequencies. The examples below underscore that the same is true in the multivariable setting as well. However, the selection of filter dynamics (A, B) and Jordan structure of the spectral-zeros, i.e., A_z, is more complex for the spectral analysis of multivariable time-series and yet, there exist open questions regarding fundamental tradeoffs between resolution and robustness, cf. [59].

Example 3.3 We assume that $u = \begin{bmatrix} u_1 & u_2 \end{bmatrix}^T$ is such that

$$u_1(n) = \sqrt{2}\cos(\frac{\pi}{3}n + \phi) + \omega_1(n), \quad \text{and}$$
$$u_2(n) = \sqrt{2}\cos(\frac{\pi}{3}n + \phi + \frac{\pi}{6}) + \omega_2(n),$$

where "^{T}" stands for the transpose operator, ω_1 and ω_2 are independent zero mean white noise processes with the same variance 0.5, and ϕ is a random variable uniformly distributed on $(-\pi, \pi]$, independent of ω_1 and ω_2. Then, the corresponding state-covariance is

$$R = \begin{bmatrix} \frac{3}{2} & \frac{\sqrt{3}}{2} & \frac{1}{2} & 0 & -\frac{1}{2} & -\frac{\sqrt{3}}{2} \\ \frac{\sqrt{3}}{2} & \frac{3}{2} & \frac{\sqrt{3}}{2} & \frac{1}{2} & 0 & -\frac{1}{2} \\ \frac{1}{2} & \frac{\sqrt{3}}{2} & \frac{3}{2} & \frac{\sqrt{3}}{2} & \frac{1}{2} & 0 \\ 0 & \frac{1}{2} & \frac{\sqrt{3}}{2} & \frac{3}{2} & \frac{\sqrt{3}}{2} & \frac{1}{2} \\ -\frac{1}{2} & 0 & \frac{1}{2} & \frac{\sqrt{3}}{2} & \frac{3}{2} & \frac{\sqrt{3}}{2} \\ -\frac{\sqrt{3}}{2} & -\frac{1}{2} & 0 & \frac{1}{2} & \frac{\sqrt{3}}{2} & \frac{3}{2} \end{bmatrix}.$$

Considering the fact that the corresponding interpolation problem has solutions of McMillan degree $n - m = 4$, we seek interpolants with spectral-zero dynamics $A_z \in \mathbb{R}^{4\times 4}$. This implies that K (discussed in Lemma 3.2) is chosen so that $\text{rank}(A-BK) = 4$, i.e., two eigenvalues of $A - BK$ are located at the origin. We then study the effect of spectral-zero dynamics in the form

$$A_z = \begin{bmatrix} A_{z_{11}} & 0 \\ 0 & A_{z_{11}} \end{bmatrix},$$

with five alternative choices for $A_{z_{11}} \in \mathbb{R}^{2\times 2}$ as follows

$$\text{(i)} : A_{z_{11}} = \begin{bmatrix} 0.4000 & -0.6928 \\ 0.6928 & 0.4000 \end{bmatrix}, \quad \text{(ii)} : A_{z_{11}} = \begin{bmatrix} 0.3500 & -0.6062 \\ 0.6062 & 0.3500 \end{bmatrix}, \quad \text{(iii)} : A_{z_{11}} = \begin{bmatrix} 0 & 1 \\ 0 & 0 \end{bmatrix},$$
$$\text{(iv)} : A_{z_{11}} = \begin{bmatrix} -0.3500 & 0.6062 \\ -0.6062 & -0.3500 \end{bmatrix}, \quad \text{(v)} : A_{z_{11}} = \begin{bmatrix} -0.4500 & 0.7794 \\ -0.7794 & -0.4500 \end{bmatrix}. \qquad (3.35)$$

The corresponding invariant polynomials of A_z are

$$\text{(i)} : p_1 = p_2 = z^2 - 0.8z + 0.64, \quad \text{(ii)} : p_1 = p_2 = z^2 - 0.7z + 0.49, \quad \text{(iii)} : p_1 = p_2 = z^2,$$
$$\text{(iv)} : p_1 = p_2 = z^2 + 0.7z + 0.49, \quad \text{(v)} : p_1 = p_2 = z^2 + 0.9z + 0.81,$$

respectively, and all satisfy the inequalities (3.11) in Theorem 3.1. In fact, the spectral-zeros in all the cases are selected with multiplicity two and in conjugate pairs. Figure 5.1 shows their location for the five alternative choices we consider, (i) at $0.8\exp(\pm j\frac{\pi}{3})$, (ii) at $0.7\exp(\pm j\frac{\pi}{3})$, (iii) all eigenvalues at the origin, (iv) with multiplicity two again at $-0.7\exp(\pm j\frac{\pi}{3})$, and (iv) at $-0.9\exp(\pm j\frac{\pi}{3})$. Figure 3.2 super-

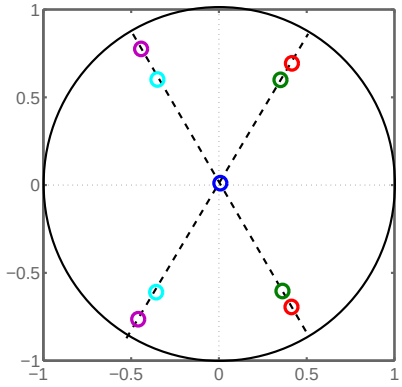

Figure 3.1: Five alternatives for spectral-zeros

imposes the corresponding matricial spectral density functions $\Re e\, F(e^{j\theta})$ with $F(z)$ of McMillan degree $n - m = 4$, and specified to belong to the family in Theorem 3.1.

Example 3.4 Similar to the previous example, suppose $u = \begin{bmatrix} u_1 & u_2 \end{bmatrix}^T$, but this time with

$$u_1(n) = \sqrt{2}\cos(\frac{\pi}{3}n + \phi) + \omega_1(n), \quad \text{and}$$
$$u_2(n) = \sqrt{2}\cos(\frac{\pi}{3}n + \psi) + \omega_2(n),$$

where ω_1 and ω_2 are the same as in Example 3.3, and both ϕ and ψ are uniformly distributed on $(-\pi, \pi]$, independent of each other and of ω_1 and ω_2. Then the state-covariance becomes

$$R = \begin{bmatrix} \frac{3}{2} & 0 & \frac{1}{2} & 0 & -\frac{1}{2} & 0 \\ 0 & \frac{3}{2} & 0 & \frac{1}{2} & 0 & -\frac{1}{2} \\ \frac{1}{2} & 0 & \frac{3}{2} & 0 & \frac{1}{2} & 0 \\ 0 & \frac{1}{2} & 0 & \frac{3}{2} & 0 & \frac{1}{2} \\ -\frac{1}{2} & 0 & \frac{1}{2} & 0 & \frac{3}{2} & 0 \\ 0 & -\frac{1}{2} & 0 & \frac{1}{2} & 0 & \frac{3}{2} \end{bmatrix}.$$

In this example there is no coupling between the two input channels. Figure 3.3 shows the matricial spectral measures for this selection of R which are again constructed with the choices of spectral-zero dynamics as in the previous example. Once again, the resulting matricial densities correspond to positive-real functions of degree 4.

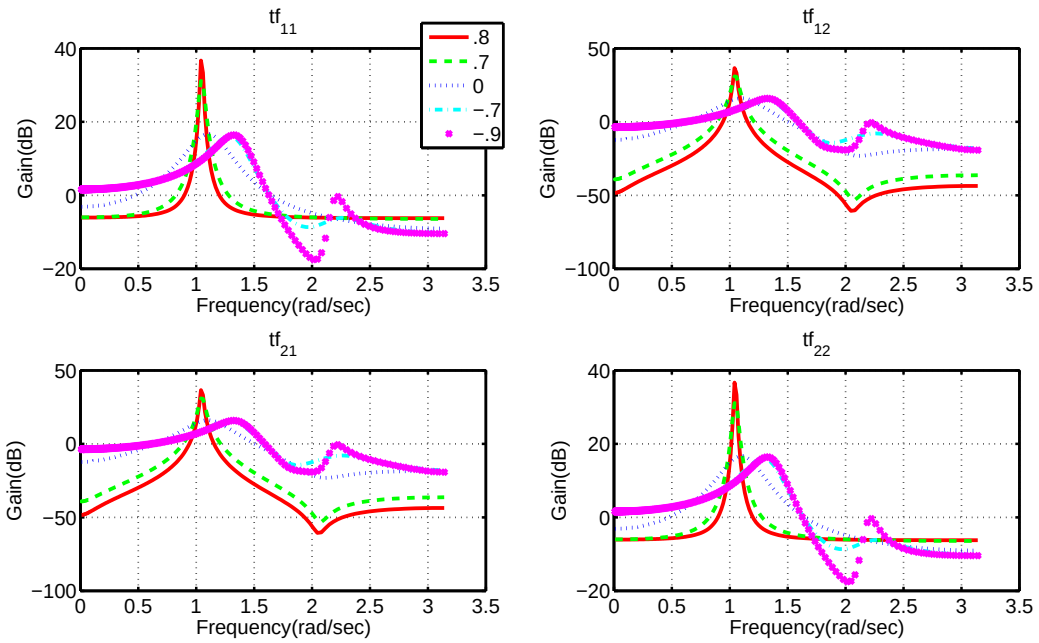

Figure 3.2: Matricial density functions corresponding to Example 3.3

Comparison between Examples 3.3 and 3.4: The actual input $u(n)$ in both cases has atomic measures at $e^{\pm j\frac{\pi}{3}}$, along with a white noise component. A selection of spectral-zero dynamics in the vicinity of $e^{\pm j\frac{\pi}{3}}$ leads to spectral density functions which are close to those actual ones. This can be seen by inspecting Figures 3.2 and 3.3. Thus, prior information as to what part of the spectrum we wish to resolve, can be used in the same way as in the scalar case [12]. It should be noted that in Figure 3.3 the off-diagonal terms of the spectral densities are almost zero (-200dB), which is consistent with the fact that the two input channels are independent.

In multivariable spectral analysis, even when we restrict our attention to generically minimal-degree power spectral densities which agree with our data (as specified by Theorem 3.1), there is still a plethora of consistent solutions. For each choice of A_z as in Theorem 3.1 we obtain a legitimate answer. Guidelines as to how to incorporate prior information for the multivariable case, analogous to those established in the scalar case (cf. [59]), need to be worked out. The point of the above examples was to highlight the effect of the available choices.

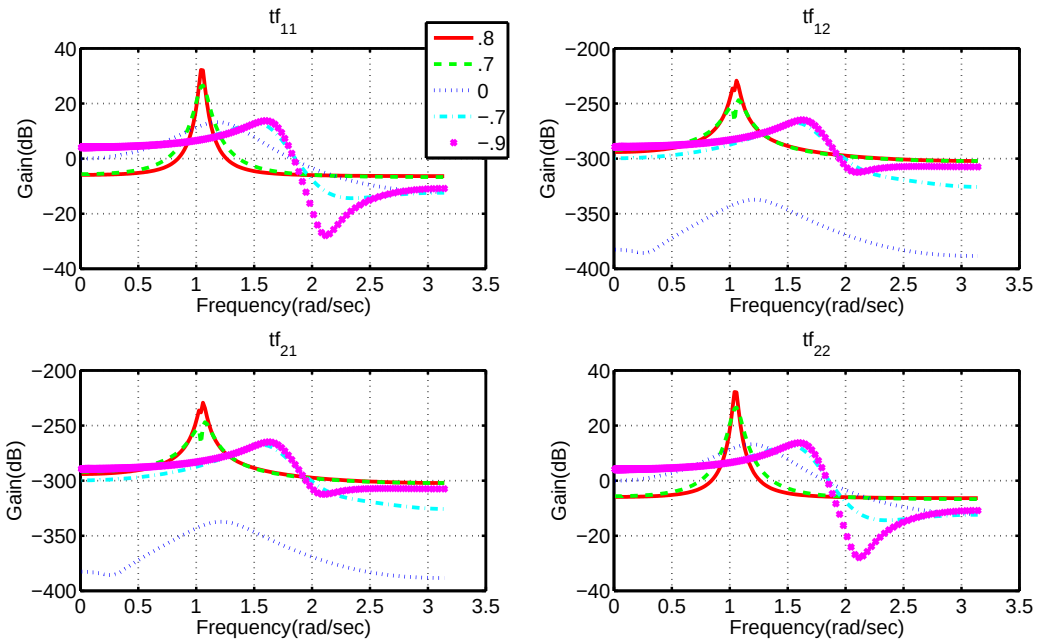

Figure 3.3: Matricial density functions corresponding to Example 3.4

3.6.2 Circuit theory

One of the basic problems in passive circuit theory is the synthesis of transfer functions/matrices with desirable properties [2]. For example, broadband matching (see e.g., [19, 27, 70]) amounts to synthesizing a coupling network to match a transmitter output with an antenna. This problem can be cast as a norm-bounded or positive-real interpolation. The former appears when the scattering parameters of the circuit are involved, whereas the latter deals with impedance or admittance matrices. We now analyze a simple example in circuit theory that illustrates the practical potential of the developed theory in this chapter.

Consider a two-port network N as a linear, time-invariant electrical circuit with passive components and assume that N matches the passive load Z_L with the output of a power generator V_g having internal resistance R_g. Figure 3.4 shows a "black box" description of such a network with $\mathbf{I}_1$, $\mathbf{I}_2$ as the currents, and $\mathbf{V}_1$, $\mathbf{V}_2$ as the voltages at the two ports of N. If we denote by $\mathbf{I} := \begin{bmatrix} \mathbf{I}_1 & \mathbf{I}_2 \end{bmatrix}^T$ and $\mathbf{V} := \begin{bmatrix} \mathbf{V}_1 & \mathbf{V}_2 \end{bmatrix}^T$ the input current and output voltage vectors, respectively, then

$$\mathbf{V}(z) = F(z)\mathbf{I}(z),$$

where the positive-real function $F(z) \in \mathcal{C}$ is the impedance matrix of N in discrete domain.

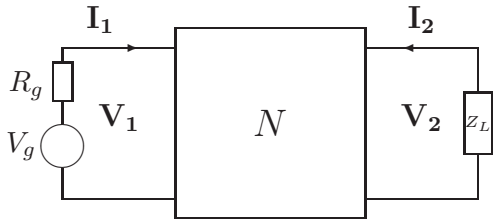

Figure 3.4: Two-port passive network as a coupling circuit

Now, suppose we excite the circuit in Figure 3.4 at frequency $z = z_{\rm o}$, and measure the current and voltage amplitudes $\mathbf{I}$ and $\mathbf{V}$ at the same frequency. The problem of finding a family of $F(z)$'s, consistent with a given set of data, is a typical impedance matching problem. Here, we wish to generate the class of low McMillan degree $F(z)$'s which leads to economical circuit design as it helps achieve the desired frequency response using lesser number of components. Further, associated with every $F(z)$ there exists a scattering matrix

$$S(z) = (F(z) - I)(F(z) + I)^{-1},$$

which is a norm-bounded quantity and relates to the more commonly adopted parameters

$$\begin{aligned} \text{incident wave:} \quad & \mathbf{V}^i := \tfrac{1}{2}(\mathbf{V} + \mathbf{I}) \ , \text{ and} \\ \text{reflected wave:} \quad & \mathbf{V}^r := \tfrac{1}{2}(\mathbf{V} - \mathbf{I}) \end{aligned}$$

in the following way

$$\mathbf{V}^r(z) = S(z)\mathbf{V}^i(z).$$

The matrix $S(z)$ is sometimes referred to as the normalized scattering parameter, because the augmented resistances are of unit value. This parameter is closely connected to the transducer power gain in broadband matching problem. In the following, we investigate a family of such scattering parameters as well as the corresponding impedance matrices for a two-port network N consistent with a given set of data.

Example 3.5 Consider the experimental set up in Figure 3.4, explained above, with the following collection of data (based on an example in [19])

$$
\begin{aligned}
(1): &\quad z_{\mathrm{o}} = 0, \quad \mathbf{I} = \begin{bmatrix} 1 & 0 \end{bmatrix}^T, \quad \mathbf{V} = \begin{bmatrix} 0.212 & -0.015 \end{bmatrix}^T, \\
(2): &\quad z_{\mathrm{o}} = 0, \quad \mathbf{I} = \begin{bmatrix} 0 & 1 \end{bmatrix}^T, \quad \mathbf{V} = \begin{bmatrix} -0.015 & 0.576 \end{bmatrix}^T, \\
(3): &\quad z_{\mathrm{o}} = \frac{1}{2}, \quad \mathbf{I} = \begin{bmatrix} 1 & 0 \end{bmatrix}^T, \quad \mathbf{V} = \begin{bmatrix} 0.201 & -0.051 \end{bmatrix}^T, \\
(4): &\quad z_{\mathrm{o}} = \frac{1}{2}, \quad \mathbf{I} = \begin{bmatrix} 0 & 1 \end{bmatrix}^T, \quad \mathbf{V} = \begin{bmatrix} -0.051 & 0.430 \end{bmatrix}^T, \\
(5): &\quad z_{\mathrm{o}} = \frac{1}{3}, \quad \mathbf{I} = \begin{bmatrix} 1 & 0 \end{bmatrix}^T, \quad \mathbf{V} = \begin{bmatrix} 0.204 & -0.037 \end{bmatrix}^T, \\
(6): &\quad z_{\mathrm{o}} = \frac{1}{3}, \quad \mathbf{I} = \begin{bmatrix} 0 & 1 \end{bmatrix}^T, \quad \mathbf{V} = \begin{bmatrix} -0.037 & 0.481 \end{bmatrix}^T.
\end{aligned}
$$

The problem of characterizing consistent impedance matrices can simply be cast as the interpolation problem (3.1a-d) with the triplet of data

$$
A = \begin{bmatrix} 0 & & & & & \\ & 0 & & & & \\ & & \frac{1}{2} & & & \\ & & & \frac{1}{2} & & \\ & & & & \frac{1}{3} & \\ & & & & & \frac{1}{3} \end{bmatrix}, B = \begin{bmatrix} 1 & 0 \\ 0 & 1 \\ 1 & 0 \\ 0 & 1 \\ 1 & 0 \\ 0 & 1 \end{bmatrix}, H = \begin{bmatrix} 0.212 & -0.015 & 0.201 & -0.051 & 0.204 & -0.037 \\ -0.015 & 0.576 & -0.051 & 0.430 & -0.037 & 0.481 \end{bmatrix},
$$

where all the off-diagonal elements of A are zero. In this example $n = 6$, $m = 2$, and for convenience of notation we choose the same spectral-zero dynamics as in Example 3.3 and 3.4. Therefore, the resulting interpolants are of McMillan degree $n - m = 4$ and represent a family of consistent $F(z)$'s corresponding to choices of A_{z} in (3.35). These impedance matrices are given in Appendix A. Figure 3.5, on the other hand, shows the magnitudes of the corresponding scattering parameters (in dB) with different frequency specifications.

Scattering parameters play an important role in the theory of broadband matching. This subject, which is also referred to as maximum power transfer problem, involves the design of a coupling network to maximize the transfer of power from a known source (or transmitter) to a given load (or antenna) over a specified frequency band of interest. In the design process, the preassigned transducer power gain is what determines the desired scattering matrix (e.g., via Darlington synthesis [22, and references therein]). In this example, we dealt with broadband matching from an analysis point

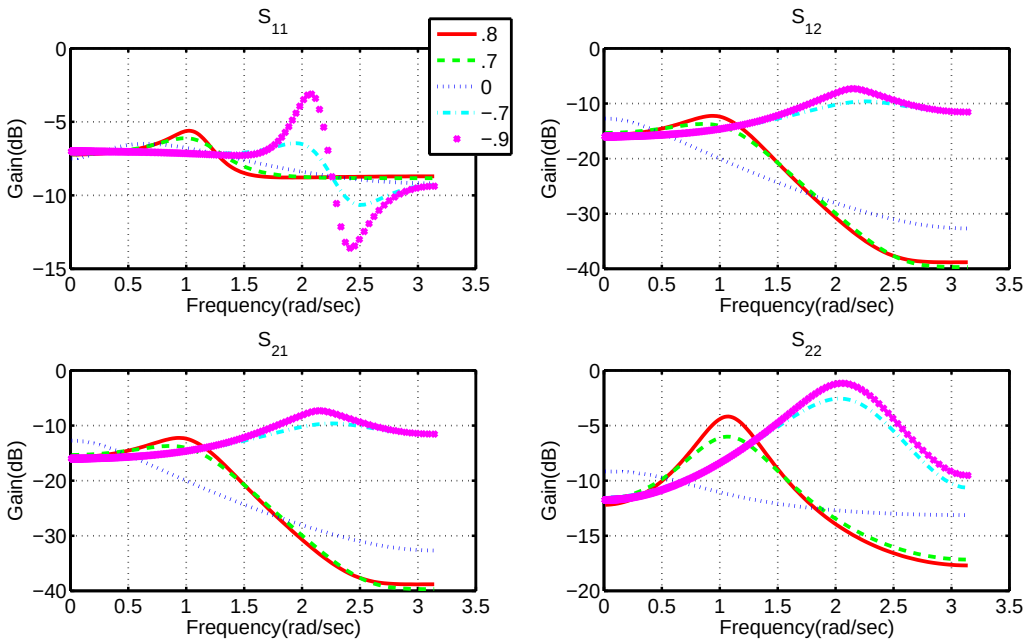

Figure 3.5: Magnitudes of the scattering parameters corresponding to the two-port N in Example 3.5

of view by solving the corresponding interpolation problem and generating a family of low degree scattering (and impedance) matrices. This example demonstrates the effect of spectral-zeros (which characterize low degree solutions) on the frequency response of the scattering matrix (shown in Figure 3.5).

3.7 Concluding remarks

Analytic interpolation with degree constraint is motivated by control and signal processing applications. Earlier studies for scalar interpolation (e.g. [13, 14, 33]) led to a parametrization of solutions in terms of the so-called spectral zeros. Our contribution in this chapter is to study the spectral-zero dynamics for analytic interpolation with $m \times m$ matrix-valued functions and to characterize corresponding invariant subspaces and Jordan structures that are permissible for (generically minimal) McMillan degree $n - m$ interpolants (n being the size and rank of the corresponding Pick matrix). While interpolants of McMillan degree lower than $n - m$ may be possible, depending on the data, the class of solutions of McMillan degree $n - m$ is always non-empty and represents a natural generic family of interpolants of low complexity. An obstruction in assigning invariant subspaces for the spectral zero dynamics is related to the type of obstruction in assigning poles via state feedback, as characterized by the celebrated Rosenbrock's theorem. Finally, we worked out two types of illustrating examples on multivariable spectral analysis and passive circuit theory.

Chapter 4

General discussions on analytic interpolation

This chapter is a follow up to Chapter 3. We reprove Lemma 3.1 and 3.2 with a different approach in the case of scalar interpolation. We also demonstrate (without using Rosenbrock's theorem) the limitations of Theorem 3.1 for general matricial interpolation problems. The analytic interpolation comes in two different forms depending on whether the interpolants required to be positive-real or norm-bounded. The two are equivalent, though the correspondence of solutions to matricial interpolation in these two classes is anything but trivial. Here, we presents guidelines as starting points to tackle the problem of norm-bounded interpolation.

4.1 Alternative proof for scalar interpolation

As mentioned in the previous chapter, references [13–15,35] parameterized the (generically) minimal-degree solutions to scalar interpolation by an arbitrary choice of spectral-zeros. In this part, we present yet another approach to full characterization of scalar interpolants based on canonical representation of the underlying system (3.3). Indeed, we follow a similar line of thought as in the previous chapter– namely, solving the optimization problem (3.8) which gives rise to the solution of the form (3.9a-b). Theorem 4.1 below is in the same spirit of Theorem 3.1 and focuses on scalar interpolation.

Theorem 4.1 Consider data (A, B, H) for scalar interpolation problem (i.e., $m = 1$) defined by (3.1a-d) and assume that the problem is solvable. Then corresponding to any $K \in \mathbb{R}^{1\times n}$ which satisfies:

(i) $A - BK$ is Hurwitz,

(ii) $\mathsf{rank}(A - BK) = n - 1$,

there exists a unique solution $F(z)$ of degree $n - 1$ to interpolation problem. The choice of K determines the corresponding spectral-zeros and gives a full characterization of solutions.

The following lemmas play the same role as Lemma 3.1 and 3.2 for the scalar case with alternative proofs.

Lemma 4.1 Let $F(z)$ be a scalar rational function of degree $n - 1$, which is strictly positive-real with $\Re e\, F(z)$ uniformly bounded in $\mathbb{D}$. Then, there exists $\hat{F}(z)$ with similar properties such that $\Re e\, \hat{F}(e^{j\theta}) = \left(\Re e\, F(e^{j\theta})\right)^{-1}$.

Proof: Let (A_F, B_F, C_F, D_F) be a minimal state space realization for F, i.e., $A_F \in \mathbb{R}^{(n-1)\times(n-1)}$, $B_F \in \mathbb{R}^{(n-1)\times 1}$, and so on. We write the (right) spectral factorization of the real part of F as follows

$$\Re e\, F = W_{\mathfrak{R}}^* W_{\mathfrak{R}},$$

with

$$W_{\mathfrak{R}}(z) = N + Lz(I - zA_F)^{-1}B_F, \tag{4.1}$$

where N, L are obtained via the positive real lemma and N is nonzero. Note that if we take N equal to zero then

$$\Re e\, F(z) = B_F^*(I - z^{-1}A_F^*)^{-1}L^*L(I - zA_F)^{-1}B_F$$

that implies we can take the right spectral factor of F as

$$W_{\mathfrak{R}_o}(z) = L(I - zA_F)^{-1}B_F = LB_F + LA_Fz(I - zA_F)^{-1}B_F.$$

Therefore, N in (4.1) is nonzero. Provided that N is invertible we have

$$W_{\mathfrak{R}}(z)^{-1} = N^{-1} - N^{-1}Lz\left(I - z(A_F - B_F N^{-1}L)\right)^{-1} B_F N^{-1}, \tag{4.2}$$

which is of degree $n-1$. This implies

$$(\Re e\, F)^{-1} = W_{\mathfrak{R}}^{-1}(W_{\mathfrak{R}}^*)^{-1} =: \Re e\, \hat{F}, \tag{4.3}$$

where $\hat{F}$ is a strictly positive-real function of degree $n-1$. □

Lemma 4.2 Let (A, B) denote a controllable pair with $B \in \mathbb{R}^{n\times 1}$. Then

1. Corresponding to any pair of $\lambda \in \mathbb{R}^{n\times n}$ and $K \in \mathbb{R}^{1\times n}$ that satisfies:

   (i) $A - BK$ is Hurwitz,

   (ii) $\mathsf{rank}(A - BK) = n - 1$,

   there exists a rational function $\hat{F}(z)$ of degree $n-1$ such that

   $$\Re e\, \hat{F} = G_{\mathrm{o}}^* \lambda G_{\mathrm{o}},$$

   with

   $$G_{\mathrm{o}}(z) = (I - z(A - BK))^{-1} B. \tag{4.4}$$

2. Corresponding to any rational function $\hat{F}(z)$ of degree $n-1$, $\exists \lambda \in \mathbb{R}^{n\times n}$ and $\exists! K \in \mathbb{R}^{1\times n}$ such that

   $$G_{\mathrm{o}}^* \lambda G_{\mathrm{o}} = \Re e\, \hat{F}$$

   with G_{o} as in (4.4).

Proof:

1. Verbatim to the proof of Lemma 3.2 we can write (see 3.15)

   $$G_{\mathrm{o}}^* \lambda G_{\mathrm{o}} = \Re e\, \hat{F}, \quad \text{where} \quad \hat{F}(z) = \frac{1}{2} B^* \Lambda B + B^* \Lambda A_{\mathrm{o}} z (I - z A_{\mathrm{o}})^{-1} B, \tag{4.5}$$

   with

   $$A_{\mathrm{o}} = A - BK, \quad \text{and} \quad \Lambda - A_{\mathrm{o}}^* \Lambda A_{\mathrm{o}} = \lambda.$$

Without loss of generality we assume (A, B) is in the controller canonical form which implies

$$A =: \begin{bmatrix} -a_1 & -a_2 & \cdots & \cdots & -a_n \\ 1 & 0 & \cdots & \cdots & 0 \\ 0 & 1 & 0 & \cdots & \vdots \\ \vdots & \ddots & \ddots & \ddots & \vdots \\ 0 & \cdots & 0 & 1 & 0 \end{bmatrix}, \quad B = \begin{bmatrix} 1 \\ 0 \\ \vdots \\ \vdots \\ 0 \end{bmatrix}, \tag{4.6}$$

and $A_{\rm o}$ is in the form of

$$A_{\rm o} =: \begin{bmatrix} -\alpha_1 & -\alpha_2 & \cdots & -\alpha_{n-1} & 0 \\ 1 & 0 & \cdots & \cdots & \vdots \\ 0 & 1 & 0 & \cdots & \vdots \\ \vdots & \ddots & \ddots & \ddots & \vdots \\ 0 & \cdots & 0 & 1 & 0 \end{bmatrix}_{n\times n}.$$

The last component of the first row in matrix $A_{\rm o}$ is zero because of the condition $\text{rank}(A - BK) = n - 1$. On the other hand, since the last column of $A_{\rm o}$ is a zero vector, the last component of $B^*\Lambda A_{\rm o}$ in (4.5) is always zero, i.e.,

$$B^*\Lambda A_{\rm o} =: \begin{bmatrix} c_1 & c_2 & \cdots & c_{n-1} & 0 \end{bmatrix}_{1\times n}. \tag{4.7}$$

By simple derivation and using the structure of $A_{\rm o}$ and B

$$(I - zA_{\rm o})^{-1}B = \frac{\begin{bmatrix} 1 \\ z \\ z^2 \\ \vdots \\ z^{n-1} \end{bmatrix}}{\det(I - zA_{\hat{F}})}, \tag{4.8}$$

where

$$A_{\hat{F}} = \begin{bmatrix} -\alpha_1 & -\alpha_2 & \cdots & \cdots & -\alpha_{n-1} \\ 1 & 0 & \cdots & \cdots & 0 \\ 0 & 1 & 0 & \cdots & \vdots \\ \vdots & \ddots & \ddots & \ddots & \vdots \\ 0 & \cdots & 0 & 1 & 0 \end{bmatrix}_{n-1\times n-1}.$$

Now by replacing (4.7) and (4.8) in (4.5) it follows

$$\hat{F}(z) = \frac{1}{2}B^*\Lambda B + C_{\hat{F}}z(I - zA_{\hat{F}})^{-1}B_{\hat{F}},$$

with

$$B_{\hat{F}} = \begin{bmatrix} 1 \\ 0 \\ \vdots \\ \vdots \\ 0 \end{bmatrix}_{n-1\times 1}, C_{\hat{F}} := \begin{bmatrix} c_1 & c_2 & \cdots & c_{n-1} \end{bmatrix}_{1\times n-1}.$$

This reveals that $\hat{F}$ is a rational function of degree $n-1$. □

2. Without loss of generality we again assume (A, B) is in the controller canonical from as in (4.6) and $(A_{\hat{F}}, B_{\hat{F}}, C_{\hat{F}}, D_{\hat{F}})$ is a minimal controller canonical representation for $\hat{F}$, e.g.,

$$A_{\hat{F}} =: \begin{bmatrix} -\alpha_1 & -\alpha_2 & \cdots & \cdots & -\alpha_{n-1} \\ 1 & 0 & \cdots & \cdots & 0 \\ 0 & 1 & 0 & \cdots & \vdots \\ \vdots & \ddots & \ddots & \ddots & \vdots \\ 0 & \cdots & 0 & 1 & 0 \end{bmatrix}_{n-1\times n-1}, \quad B_{\hat{F}} = \begin{bmatrix} 1 \\ 0 \\ \vdots \\ \vdots \\ 0 \end{bmatrix}_{n-1\times 1}.$$

We now show that there exist a $\lambda \in \mathbb{R}^{n\times n}$ and a unique $K \in \mathbb{R}^{1\times n}$ such that

$$\Re e\, \hat{F} = G_{\mathrm{o}}^*\lambda G_{\mathrm{o}}.$$

The following is a constructive way to find such a λ and K.

We define

$$A_{\mathrm{o}} := \begin{bmatrix} -\alpha_1 & -\alpha_2 & \cdots & -\alpha_{n-1} & 0 \\ 1 & 0 & \cdots & \cdots & \vdots \\ 0 & 1 & 0 & \cdots & \vdots \\ \vdots & \ddots & \ddots & \ddots & \vdots \\ 0 & \cdots & 0 & 1 & 0 \end{bmatrix}_{n\times n},$$

and seek a K that satisfies

$$A - BK = A_{\mathrm{o}}. \tag{4.9}$$

It is easy to see that

$$K = \begin{bmatrix} \alpha_1 - a_1 & \alpha_2 - a_2 & \cdots & \alpha_{n-1} - a_{n-1} & -a_n \end{bmatrix}$$

is the unique solution of (4.9) and that $\hat{F}$ can be written as

$$\hat{F}(z) = D_{\hat{F}} + \begin{bmatrix} C_{\hat{F}} & 0 \end{bmatrix} z \left(I - z(A - BK)\right)^{-1} B.$$

The expansion of the real part of $\hat{F}$ results in

$$\begin{aligned} \Re e\, \hat{F}(z) = \cdots + z^{-2} B^*(A - BK)^{*2}\Lambda B + z^{-1} B^*(A - BK)^*\Lambda B + \\ B^*\Lambda B + zB^*\Lambda(A - BK)B + z^2 B^*\Lambda(A - BK)^2 B + \cdots, \end{aligned}$$

where

$$B^*\Lambda B = D^*_{\hat{F}} + D_{\hat{F}}, \quad \text{and} \quad B^*\Lambda(A - BK) = \begin{bmatrix} C_{\hat{F}} & 0 \end{bmatrix}.$$

If we denote by $\begin{bmatrix} \Lambda_{11} & \Lambda_{12} & \cdots & \Lambda_{1n-1} & \Lambda_{1n} \end{bmatrix}$ the first row of Λ, then considering the structure of A, B and K it follows

$$\Lambda_{11} = D^*_{\hat{F}} + D_{\hat{F}}, \quad \text{and}$$

$$\begin{bmatrix} \Lambda_{11} & \Lambda_{12} & \cdots & \Lambda_{1n-1} & \Lambda_{1n} \end{bmatrix} \begin{bmatrix} -\alpha_1 & -\alpha_2 & \cdots & -\alpha_{n-1} & 0 \\ 1 & 0 & \cdots & \cdots & \vdots \\ 0 & 1 & 0 & \cdots & \vdots \\ \vdots & \ddots & \ddots & \ddots & \vdots \\ 0 & \cdots & 0 & 1 & 0 \end{bmatrix} = \begin{bmatrix} C_{\hat{F}} & 0 \end{bmatrix}.$$

Finally, any Hermitian matrix Λ with $\begin{bmatrix} \Lambda_{11} & \Lambda_{12} & \cdots & \Lambda_{1n-1} & \Lambda_{1n} \end{bmatrix}$ as its first row gives rise to the function

$$\hat{F}(z) = \frac{1}{2} B^* \Lambda B + B^* \Lambda (A - BK) z \left(I - z(A - BK)\right)^{-1} B,$$

and the real-part of $\hat{F}$ is obtained as

$$\Re e\, \hat{F}(z) = B^* (I - z^{-1} (A - BK)^*)^{-1} \lambda \left(I - z(A - BK)\right)^{-1} B,$$

where $\lambda = \Lambda - (A - BK)^* \Lambda (A - BK)$. □

Remark 4.1 Although different Λ's with the same first row in part 2 of Lemma 4.2 generate different λ's via Lyapunov equation, all these λ's lead to the same $G_{\mathrm{o}}^* \lambda G_{\mathrm{o}}$ (because of the canonical structure of A, B).

Proof of Theorem 4.1: Briefly, the first part of Lemma 4.2 implies that for any choice of K which satisfies the conditions in Theorem, there exists a rational function $\hat{F}$ of degree $n - 1$ such that

$$B^* (I - z^{-1} (A - BK)^*)^{-1} \lambda \left(I - z(A - BK)\right)^{-1} B = \Re e\, \hat{F}(z).$$

Positivity of its Hermitian part on the circle ensures that $\hat{F}(z)$ is a positive-real function. This $\hat{F}$ via Lemma 4.1 gives rise to a positive-real solution of degree $n-1$ to the interpolation problem. We emphasize that the choice of λ (that relates to H through the solution of the corresponding moment problem) takes care of interpolation conditions. The second part of Lemma 4.2 along with Lemma 4.1 guarantees the full characterization of degree $n - 1$ interpolants. □

4.2 Restrictions on zero dynamics of solutions imposed by the rank condition in Lemma 3.2

Theorem 3.1 builds on the rank condition in Lemma 3.2 to obtain interpolants of McMillan degree $n-m$. This condition implies that $A-BK$ must have rank deficiency of m. On the other hand, the Jordan structure of $A-BK$ includes the desired spectral-zero dynamics of the particular solution. Therefore, there must exist an invertible

matrix T such that

$$(A - BK)T = T \begin{bmatrix} A_z & 0 \\ Y & 0 \end{bmatrix}, \tag{4.10}$$

with Y as a matrix of compatible size. The transformation matrix T can be partitioned as

$$T =: \begin{bmatrix} T_1 & T_2 \end{bmatrix},$$

where the columns of T_2 form a basis for $\mathcal{N}(A - BK)$, the null space of $A - BK$, and the columns of T_1 form a basis for the complementary subspace. We will use the following lemma which is of independent interest.

Lemma 4.3 Let (A, B) denote a controllable pair with $B \in \mathbb{R}^{n \times m}$ a full column rank matrix, and K be a matrix of compatible size. Then,

(i) $\mathsf{rank}(A - BK) \geq n - m$, for any choice of K.

(ii) If $\mathsf{rank}(A - BK) = n - m$, then $\mathcal{N}(A - BK)$ is independent of K.

Proof: (i) For simplicity and without loss of generality we assume that A and B are in the form

$$A =: \begin{bmatrix} A_1 & A_2 \\ A_3 & A_4 \end{bmatrix}, \quad B = \begin{bmatrix} 0 \\ I \end{bmatrix}, \tag{4.11}$$

where I denotes the identity matrix of dimension m, $A_1 \in \mathbb{R}^{(n-m)\times(n-m)}$, and A_2 to A_4 are matrices of compatible size. Since (A, B) is controllable,

$$\begin{aligned} n &= \operatorname{rank} \begin{bmatrix} zI - A & B \end{bmatrix} \\ &= \operatorname{rank} \begin{bmatrix} zI - A_1 & -A_2 & 0 \\ -A_3 & zI - A_4 & I \end{bmatrix} \end{aligned}$$

for all $z \in \mathbb{C}$. Therefore $\operatorname{rank} \begin{bmatrix} A_1 & A_2 \end{bmatrix} = n - m$ and

$$\operatorname{rank}(A - BK) = \operatorname{rank} \begin{bmatrix} A_1 & A_2 \\ A_3 - K_1 & A_4 - K_2 \end{bmatrix} \geq n - m,$$

for any $K =: \begin{bmatrix} K_1 & K_2 \end{bmatrix}$.

(ii) If $\text{rank}(A-BK) = n-m$, the analysis in (i) implies that the rows of $\begin{bmatrix} A_3 - K_1 & A_4 - K_2 \end{bmatrix}$ are linear combinations of the rows of $\begin{bmatrix} A_1 & A_2 \end{bmatrix}$. Therefore,

$$A - BK = \begin{bmatrix} I \\ X \end{bmatrix} \begin{bmatrix} A_1 & A_2 \end{bmatrix} = \begin{bmatrix} A_1 & A_2 \\ XA_1 & XA_2 \end{bmatrix},$$

for some X, and

$$\mathcal{N}(A - BK) = \left\{ \begin{bmatrix} x \\ y \end{bmatrix} : \quad A_1 x + A_2 y = 0 \right\}$$

is independent of K. □

Assuming the partitioning and notation in (4.11) and (A, B, K) as in the lemma, it is clear that

$$\mathcal{N}(A - BK) = \mathcal{N}\left(\begin{bmatrix} A_1 & A_2 \end{bmatrix} \right),$$

and hence, we choose $T_1 = \begin{bmatrix} A_1 & A_2 \end{bmatrix}^T$. Then, from (4.10)

$$\begin{aligned} (A - BK) \left[\begin{bmatrix} A_1^T \\ A_2^T \end{bmatrix} T_2 \right] = \\ \left[\begin{bmatrix} A_1^T \\ A_2^T \end{bmatrix} T_2 \right] \begin{bmatrix} A_z & 0 \\ Y & 0 \end{bmatrix}. \end{aligned} \tag{4.12}$$

We multiply (4.12) from the left by $\begin{bmatrix} A_1 & A_2 \end{bmatrix}$ to obtain

$$\begin{aligned} \begin{bmatrix} A_1 & A_2 \end{bmatrix} \begin{bmatrix} I \\ X \end{bmatrix} \left(A_1 A_1^T + A_2 A_2^T \right) = \\ \left(A_1 A_1^T + A_2 A_2^T \right) A_z, \end{aligned} \tag{4.13}$$

using the fact that $\begin{bmatrix} A_1 & A_2 \end{bmatrix} T_2 = 0$. From (4.13) we conclude that A_z is similar to $A_1 + A_2 X$.

By substituting the value of A from Example 3.1 we have

$$A_1 = \begin{bmatrix} \frac{1}{2} & 1 \\ 0 & \frac{1}{2} \end{bmatrix}, \; A_2 = \begin{bmatrix} 0 & 0 \\ 1 & 0 \end{bmatrix},$$
$$A_3 = \begin{bmatrix} 0 & 0 \\ 0 & 0 \end{bmatrix}, \; A_4 = \begin{bmatrix} \frac{1}{2} & 0 \\ 0 & \frac{1}{2} \end{bmatrix}.$$

From the above discussion it follows that if K is chosen so as to satisfy $\text{rank}(A - BK) = 2$, then

$$\text{spestral-zero dynamics} \overset{\text{similar}}{\sim} A_1 + A_2X = \begin{bmatrix} \frac{1}{2} & 1 \\ x_{11} & \frac{1}{2} + x_{12} \end{bmatrix},$$

for $X =: \begin{bmatrix} x_{11} & x_{12} \\ x_{21} & x_{22} \end{bmatrix}$. But, there is no choice of X for which $A_1 + A_2X$ can be made similar to $A_{\hat{F}}$ given in (3.22) that is a multiple of the identity. Therefore in Example 3.1, it is impossible both to satisfy $\text{rank}(A - BK) = 2$ and, at the same time, to have $A_{\hat{F}}$ as the Jordan structure of the spectral-zero dynamics. This completes the proof of our claim. □

4.3 Future direction: the counterpart problem of multivariable interpolation with norm-bounded interpolants

So far, we have considered the analytic interpolation defined by (3.1a-d) for positive-real functions (Carathéodory problem). In this section, instead, we focus on norm-bounded interpolants. We denote by $\mathcal{S}$ the set of square matrix-valued functions which are analytic in $\mathbb{D}$ and bounded in norm. This class of functions (known as Schur class) is more common in formulations of robust control problems (see e.g., [30]). In the scalar case, the (generically) minimal-degree solutions to norm-bounded interpolation have been fully parameterized (see [14]), whereas in the multivariable setting it is still an open problem. Here we study two ways to tackle this problem. In both cases, we present specific guidelines as to how to proceed with this problem. The complete solution, however, requires more work to be done and is part of the future research.

4.3.1 Representing constraints on norm-bounded interpolants as moment conditions

We consider the interpolation problem (3.1a-d) and assume that F belongs to $\mathcal{S}$ (and not to $\mathcal{C}$). All the other assumptions hold exactly the same as in Chapter 3. Using the normalization introduced at the end of Section 3.2.2 the interpolation condition (3.1a) can be written as follows

$$\frac{1}{2\pi}\int_{-\pi}^{\pi} F(e^{j\theta})G(e^{j\theta})^* d\theta = H. \tag{4.14}$$

We can represent (4.14) as the following moment constraint

$$R := \begin{bmatrix} I & \Sigma^* \\ \Sigma & I \end{bmatrix} = \frac{1}{2\pi}\int_{-\pi}^{\pi} \begin{bmatrix} 0 & G \\ G & 0 \end{bmatrix} \underbrace{\begin{bmatrix} I & F \\ F^* & I \end{bmatrix}}_{\Phi} \begin{bmatrix} 0 & G^* \\ G^* & 0 \end{bmatrix} d\theta. \tag{4.15}$$

where Σ is the solution of Lyapunov equation

$$\Sigma - A\Sigma A^* = BH,$$

and $\Phi(\theta)d\theta \in \mathcal{M}$ is the unknown positive measure. We can also write (4.15) as

$$R = \frac{1}{2\pi}\int_{-\pi}^{\pi} \Gamma(e^{j\theta})\Phi(\theta)\Gamma(e^{j\theta})^* d\theta \tag{4.16}$$

with

$$\Gamma(e^{j\theta}) := \begin{bmatrix} 0 & G(e^{j\theta}) \\ G(e^{j\theta}) & 0 \end{bmatrix} = (I - e^{j\theta}\mathcal{A})^{-1}\mathcal{B}, \quad \mathcal{A} := \begin{bmatrix} A & 0 \\ 0 & A \end{bmatrix}, \quad \mathcal{B} := \begin{bmatrix} 0 & B \\ B & 0 \end{bmatrix}.$$

From Chapter 3 we know how to find minimal-degree solutions to (4.16). The remaining task is to extract those solutions that are in the form of $\Phi = \begin{bmatrix} I & F \\ F^* & I \end{bmatrix}$ with an analytic F. This last effort has not been established in the course of this thesis and is part of the future developments.

We emphasize that there exists a duplicated dynamic in the resulting Φ because of the special structure of Γ, i.e., the generically minimal-degree of Φ in (4.16) is $4(n-m)$. This duplicated dynamic can be easily removed (e.g., via balanced truncation) and

the generically minimal McMillan degree of F would be $n-m$. In the next section we study an alternative approach to the problem of multivariable interpolation with norm-bounded interpolants.

4.3.2 Direct formulation of norm-bounded analytic interpolation

Reference [39] successfully carried out the full parametrization of positive solutions to the matricial moment problem as minimizers of a relative entropy functional (as seen in (3.8)). Here we follow the same idea to find a characterization of solutions to the interpolation problem defined by (4.14) and (3.1b-d), where F belongs to $\mathcal{S}$.

Without loss of generality we assume $\|F\|_\infty < 1$. We then formulate the problem as follows

$$\underset{F}{\operatorname{argmin}} \left\{ \mathbf{S}(\Psi \| (I - FF^*)) : H = \frac{1}{2\pi}\int_{-\pi}^{\pi} F(e^{j\theta})G(e^{j\theta})^* d\theta, \right. \\ \left. 0 = \frac{1}{2\pi}\int_{-\pi}^{\pi} F(e^{j\theta})e^{jk\theta} d\theta, \ \forall k = 1,2,3,\dots \right\}, \quad (4.17)$$

where 0 is the $m \times m$ zero matrix and the last equation originates from the analyticity constraint on F. The first step to proceed with the optimization problem (4.17) is to solve it for $\Psi = I$ that is called the central solution. Therefore, we consider the optimization

$$\underset{F}{\operatorname{argmin}} \left\{ -\frac{1}{2\pi}\int_{-\pi}^{\pi} \operatorname{trace} \log \left(I - F(e^{j\theta})F(e^{j\theta})^* \right) d\theta : \quad \mathcal{H} = \mathbf{L}(F) \right\}, \quad (4.18)$$

where $\mathbf{L}$ is the linear operator

$$\mathbf{L} : F \mapsto \mathcal{H} = \frac{1}{2\pi}\int_{-\pi}^{\pi} F(e^{j\theta})\mathcal{G}(e^{j\theta})^* d\theta$$

with

$$\mathcal{H} := \begin{bmatrix} H & 0 & 0 & \cdots \end{bmatrix}, \quad \mathcal{G}(e^{j\theta})^* := \begin{bmatrix} G(e^{j\theta})^* & e^{j\theta}I & e^{j2\theta}I & \cdots \end{bmatrix}.$$

Provided that there exists a minimizer for (4.18), stationarity condition for the entropy functional dictates the form of such a minimizer.

The Lagrangian of the problem is

$$\mathcal{L}(\lambda, F) = -\frac{1}{2\pi}\int_{-\pi}^{\pi} \operatorname{trace}\log\left(I - FF^*\right) d\theta - \Re e\,\langle \lambda, \mathcal{H} - \mathbf{L}(F)\rangle,$$

where λ is the lagrange multiplier and "$\langle .,. \rangle$" stands for the inner product. Taking the (Gateaux) derivative of $\mathcal{L}$ in the direction δ (cf. [39]) and using the expression for the differential of the matrix logarithm (see Appendix B) we arrive at

$$\begin{aligned} d\mathcal{L}(\lambda, F; \delta) = \frac{1}{2\pi}\int_{-\pi}^{\pi} \operatorname{trace}\,\left[2(I - FF^*)^{-1}\Re e\,(\delta F^*)\right] d\theta + \\ \frac{1}{2\pi}\int_{-\pi}^{\pi} \operatorname{trace}\,\left[\Re e\,\left((\mathbf{L}^*(\lambda))^*\delta\right)\right] d\theta, \end{aligned}$$

where $\mathbf{L}^* : \lambda \mapsto \lambda\mathcal{G}$ is the adjoint transformation of $\mathbf{L}$. The stationary condition $d\mathcal{L}(\lambda, F; \delta) \equiv 0$ then gives

$$\mathcal{L}(\lambda, F; \delta) = \operatorname{trace}\int_{-\pi}^{\pi} \Re e\,\left[\left(2F^*(I - FF^*)^{-1} + (\mathbf{L}^*(\lambda))^*\right)\delta\right] d\theta = 0, \quad \forall \delta.$$

If we separate the real and imaginary part of δ as $\delta =: \delta_x + j\delta_y$ it follows

$$\begin{aligned} \mathcal{L}(\lambda, F; \delta) = \operatorname{trace}\int_{-\pi}^{\pi} [\Re e\ \ (2F^*(I - FF^*)^{-1} + (\mathbf{L}^*(\lambda))^*)\ \delta_x - \\ \Im m\ \ (2F^*(I - FF^*)^{-1} + (\mathbf{L}^*(\lambda))^*)\ \delta_y]\, d\theta = 0, \quad \forall \delta_x, \delta_y. \end{aligned}$$

Therefore, the stationarity condition implies

$$2F^*(I - FF^*)^{-1} = -\left(\mathbf{L}^*(\lambda)\right)^*,$$

and hence,

$$(I - FF^*)^{-1}F = -\frac{1}{2}\lambda\mathcal{G}. \tag{4.19}$$

The next step is to extract the explicit form of minimizer by solving (4.19) for F. Using this form along with a homotopy approach to find the corresponding λ gives rise to the solution of (4.17) for a general Ψ. Finally, we should come up with a choice of Ψ that leads to pole-zero cancelations in the form of solution (very much as in Section 3.2.3, see also [39]) and hence, gives us a low McMillan degree interpolant. These steps have not been established yet and have a great chance of succeed for the future work.

4.4 Concluding remarks

We revisited scalar analytic interpolation and presented alternative proofs for Lemma 3.1 and 3.2. More precisely, building on the multivariable formalism given in [39] and using a base dependent realization in state space we restudied full parametrization of interpolants in scalar setting by a choice of spectral-zeros in a different way. We also showed how full characterization of solutions to multivariable interpolation faces some limitations because of the extra freedom in assigning invariant subspaces of the spectral-zeros.

In the rest of this chapter, we focused on norm-bounded analytic interpolation. We described two possible approaches to this problem. The first one cast the norm-bounded interpolation as a moment problem, whereas the second approach is direct. More technical details and derivations need to be covered for these two formalisms, and here, we only presented the guidelines as an starting point.

Chapter 5

Fractional models as control design elements

It is a well-known fact that set-point following, in linear control systems, requires an integrator in the feedback loop. However, such an integrator introduces phase lag which may often have a destabilizing effect. A variety of options exist for adding lead to mediate this effect. In this chapter we consider yet another option, a fractional integrator. We study possible implementations of the fractional integrator and the effect of such an element in achieving set-point following specifications. We also investigate the use of fractional elements in sinusoidal tracking.

5.1 Introduction

Fractional derivatives are useful in modeling a wide range of physical systems. In particular, they are encountered when modeling certain types of distributed parameter systems involving delay lines, electromagnetism, diffusion, turbulence, and many others (see e.g., [18, 25, 26]). While such models are infinite dimensional, their fractional representation is often quite compact. Moreover, the algebra and function theory for fractional integrators and fractional derivatives is well developed (e.g., [61, 64]). Models utilizing fractional calculus have also been considered for control applications, see e.g., [4, 20, 50, 63]. We refer to [1] for a review of the literature and an extensive list of references on this subject.

We focus on a special class of dynamical systems which in frequency domain are governed by a fractional power of the Laplace variable s. Such models are encountered in spectral analysis of different biological processes such as speech, music, and electrocardiogram (ECG) signals when the spectral characteristic varies with rates which are not integer multiples of 20 [dB/dec] (see e.g., [62]). Our interest in fractional integrator stems from the fact that, for control purposes, such elements provide enough DC gain to ensure steady-state tracking. Indeed, an integrator in the loop is not necessary—a fractional integrator suffices. Such fractional elements provide infinite DC gain while they introduce less lag than a regular integrator. Thus, the use of the fractional integrator as a design element may afford a significant improvement in phase margin for similar steady-state performance.

The transfer function of the fractional integrator in the Laplace domain is $1/s^{\alpha}$ for $0 < \alpha < 1$. For the most part we consider the case where the exponent α is equal to $1/2$. Note that $1/s^{\alpha}$ for $0 < \alpha < 1$, is a positive-real function just as $1/s$. Therefore, it is realizable with passive elements. We present and compare different implementations of $1/\sqrt{s}$, i.e., the "half-capacitor". The range of frequency for which lumped implementations display a "-10 [dB/dec] attenuation and -45^{o} phase lag" characteristic depends on the number and values of the components. These factors and the corresponding tradeoffs in the fabrication process play the major role in the efficiency of a design, and questions in this regard remain open for further investigations.

The contribution of this study consists in pointing out the significance and potential use of fractional integrators and sinusoidal fractional components as feedback design elements. Further, various implementations are discussed and compared. Options for micro-electro-mechanical systems (MEMS) and integrated circuit realizations and the use of such circuits in communications are the directions of future research.

5.2 Implementation of a half-integrator

Following standard literature on continued fractions (e.g., [11,61,69]), we study alternative implementations of fractional integrator. We consider this as a "half-capacitor" with the truncated transmission line model given in Figure 5.1, where I (current) is

the input, V (voltage) is the output and the corresponding transfer function is

$$G(s) = \frac{V(s)}{I(s)} = R_0 + \cfrac{1}{C_1 s + \cfrac{1}{R_1 + \cfrac{1}{C_2 s + \cfrac{1}{R_2 + \cfrac{1}{\ddots + \cfrac{1}{C_n s + \frac{1}{R_n}}}}}}}. \tag{5.1}$$

For suitable choices of resistors and capacitors, the truncated transmission line can approximate a half-integrator over an arbitrary frequency band. We present three different sets of R_k's and C_k's for $k = 1, \ldots, n$, which all three lead to a characteristic of a half-integrator. These sets of values are

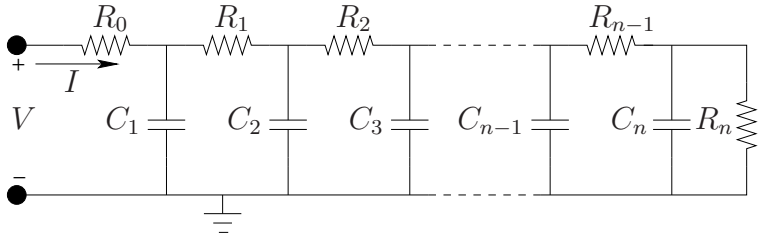

Figure 5.1: Truncated transmission line

$$\text{1-st realization: } \begin{cases} C_1 = C_2 = C_3 = \cdots = C_n = C \\ R_1 = R_2 = R_3 = \cdots = R_n = R\,, \\ R_0 = \frac{1}{2}R \end{cases} \tag{5.2}$$

$$\text{2-nd realization: } \begin{cases} C_k = k\ [\mu\text{F}],\ \text{for } k = 1, 2, \ldots, n \\ R_k = k\ [\Omega], \quad \text{for } k = 1, 2, \ldots, n\,, \\ R_0 = 0 \end{cases} \tag{5.3}$$

and the third realization which is based on the Padé approximation will be given later in this section. We discuss these three implementations separately in the following parts.

5.2.1 First realization

Consider the truncated transmission line in Figure 5.1 with the standard choice of (5.2) for the components. Figures 5.2 and 5.3 are respectively the Bode and Nyquist diagrams of this circuit for $n = 90, R = 100[\Omega]$, and $C = 100[\mu\text{F}]$.

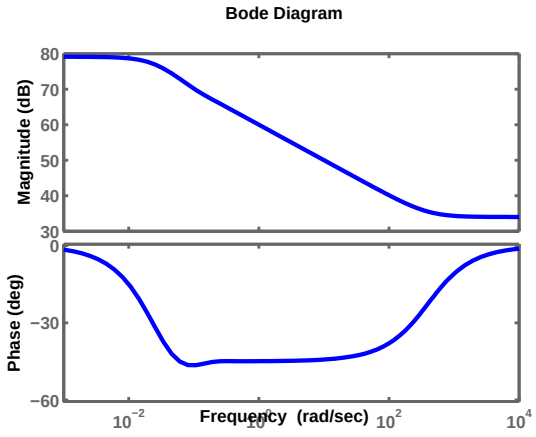

Figure 5.2: Bode plot for $n = 90, R = 100[\Omega]$ and $C = 100[\mu\text{F}]$

It is seen that this transmission line approximates pretty accurately characteristic of $1/\sqrt{s}$ over the mid-range of frequencies, between 10^{-1} and 10^{2} [rad/sec]. The attenuation is -10 [dB/dec] and the phase is -45^{o}. The poles and zeros of the impedance of such a circuit interlace as shown in Figure 5.4, for $n = 10$. These poles and zeros lie in the left half plane and they are all real because the corresponding ladder is a passive RC circuit. Also, from a pure mathematical aspect, (5.1) may be viewed as the n-th approximant (i.e., truncated after n-th level) of a "real J-fraction" (see [69]), and this follows that all poles of this fraction are real, simple, and have positive residues. Furthermore, they all lie on the negative half of the real axis, because the denominators of all the k-th approximants of (5.1), for $k = 1, \ldots, n$, are polynomials in s with positive coefficients.

We now mathematically prove that the truncated transmission line with the associated quantities given in (5.2) approximates a half-integrator. More precisely, we show that for this realization

$$G(s) \approx \sqrt{\frac{R}{C}}\frac{1}{\sqrt{s}}, \quad \text{for} \quad \frac{6}{n^2RC} \leq s \leq \frac{1}{6RC}, \tag{5.4}$$

where the frequency range is in Hertz and to compare with Figure 5.2, it should be scaled by 2π. We start the proof of (5.4) by using an "equivalence transformation" (see [69]) and rewriting (5.1) as

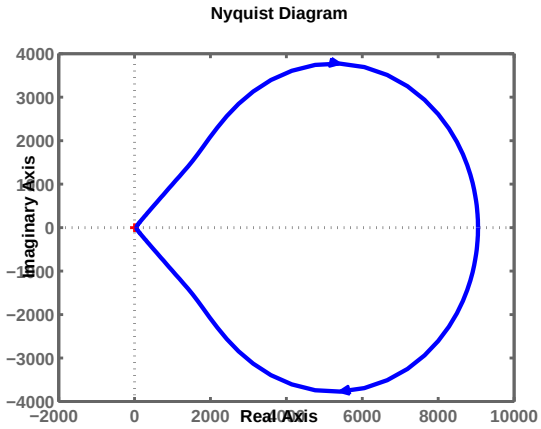

Figure 5.3: Nyquist plot for $n = 90, R = 100[\Omega]$ and $C = 100[\mu\text{F}]$

$$\frac{G(s)}{R_0} = 1 + \cfrac{\frac{1}{R_0C_1s}}{1+\cfrac{\frac{1}{R_1C_1s}}{1+\cfrac{\frac{1}{R_1C_2s}}{1+\cfrac{\frac{1}{R_2C_2s}}{\ddots+\cfrac{}{1+\frac{1}{R_nC_ns}}}}}}. \tag{5.5}$$

This is simply obtained by dividing out the leading terms. Then, by replacing R_k's and C_k's from (5.2), it follows

$$\frac{G(s)}{R_0} = 1 + \cfrac{2\gamma}{1+\cfrac{\gamma}{1+\cfrac{\gamma}{\ddots+\frac{}{1+\gamma}}}}, \tag{5.6}$$

where $\gamma := \frac{1}{RCs}$, and the number of γ's in this fraction is equal to $2n$. To establish the proof we need to take a couple of steps as the following lemmas.

Lemma 5.1 Consider

$$\mathcal{F}_1 = \cfrac{1}{1-\cfrac{\rho_1}{1+\rho_1-\cfrac{\rho_2}{1+\rho_2-\cfrac{\rho_3}{1+\rho_3-\cfrac{\rho_4}{\ddots}}}}} \tag{5.7}$$

as a continued fraction with arbitrary numbers ρ_p, for $p = 1, 2, 3, \ldots$. Then the numerator of the n-th approximant of $\mathcal{F}_1$ is equal to the sum of the first n terms of the infinite series $1 + \sum_{p=1}^{\infty} \rho_1\rho_2 \ldots \rho_p$, and the denominator of the n-th approximant is equal to one.

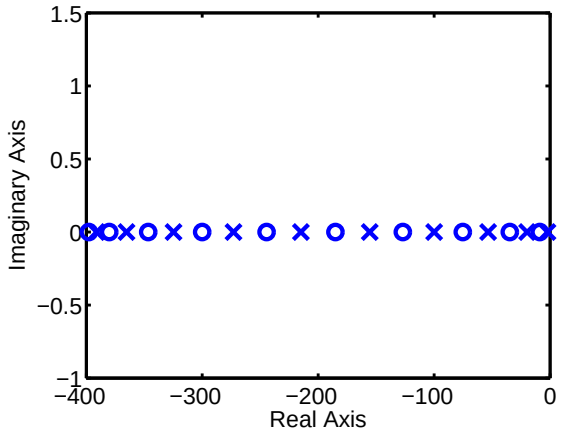

Figure 5.4: Pole-Zero Configuration

The proof which is given in [69, page 18] is straightforward and it is based on the fundamental recurrence formulas for continued fractions. Second lemma has also been stated in [69] briefly, however, here we present the proof in detail.

Lemma 5.2 The n-th approximant of the periodic continued fraction

$$\mathcal{F}_2 = b + \cfrac{a}{b + \cfrac{a}{b + \cfrac{a}{\ddots}}} \tag{5.8}$$

where $(a, b \neq 0)$, can be written in the form of

$$u + v - \cfrac{v}{\cfrac{v}{u} + \cfrac{1}{\sum\limits_{p=0}^{n-1} (\frac{v}{u})^p}},$$

with u and v respectively as the bigger and the smaller (in magnitude) roots of the equation $x^2 - bx - a = 0$.

Proof: According to the assumptions, $u + v = b$ and $uv = -a$, therefore (5.8) can be represented as

$$\mathcal{F}_2 = u + v - \cfrac{uv}{u + v - \cfrac{uv}{u + v - \cfrac{uv}{\ddots}}},$$

and using an equivalence transformation, more precisely, successive divisions by u, follows

$$\mathcal{F}_2 = u + v - v\cfrac{1}{\frac{v}{u}+1-\cfrac{v}{u+v-\cfrac{uv}{u+v-\cfrac{uv}{u+v-\cfrac{uv}{\ddots}}}}} = u + v - v\cfrac{1}{\frac{v}{u}+1-\cfrac{\frac{v}{u}}{1+\frac{v}{u}-\cfrac{\frac{v}{u}}{1+\frac{v}{u}-\cfrac{\frac{v}{u}}{\ddots}}}}.$$

The denominator of the last term in (5.9) consists of two parts:

$$\frac{v}{u} \quad \text{and} \quad 1 - \cfrac{\frac{v}{u}}{1+\frac{v}{u}-\cfrac{\frac{v}{u}}{1+\frac{v}{u}-\cfrac{\frac{v}{u}}{\ddots}}},$$

which the second one is a particular case of the inverse of $\mathcal{F}_1$ in Lemma 5.1 with the parameters

$$\rho_1 = \rho_2 = \rho_3 = \ldots = \frac{v}{u}.$$

Application of Lemma 5.1 now reveals that the n-th approximant of $\mathcal{F}_2$ can be written as

$$u + v - \cfrac{v}{\frac{v}{u}+\cfrac{1}{1+\frac{v}{u}+(\frac{v}{u})^2+\cdots+(\frac{v}{u})^{n-1}}} = u + v - \cfrac{v}{\frac{v}{u}+\cfrac{1}{\sum\limits_{p=0}^{n-1}(\frac{v}{u})^p}}$$

and this completes the proof. □

Assuming the notation introduced in Lemma 5.2, we now consider the transfer function $G(s)$ in (5.6), where

$$\frac{G(s)}{R_0} = 1 + \cfrac{2\gamma}{1+\cfrac{\gamma}{1+\cfrac{\gamma}{\ddots+\cfrac{}{1+\gamma}}}}.$$

In this particular case, u and v can be thought of as the two roots of $x^2 - x - \gamma = 0$, i.e.,

$$u = \frac{1+\sqrt{1+4\gamma}}{2}, \quad v = \frac{1-\sqrt{1+4\gamma}}{2}, \tag{5.9}$$

and clearly $u+v=1$. Application of Lemma 5.2 implies that

$$\frac{G(s)}{R_0} = 1 + 2(\frac{-v}{\frac{v}{u} + \frac{1}{\sum_{p=0}^{2n-1}(\frac{v}{u})^p}}) = 1 + 2(\frac{-v}{\frac{v}{u} + \frac{1-\frac{v}{u}}{1-(\frac{v}{u})^{2n}}}),$$

and continuing simple derivations gives rise to

$$\frac{G(s)}{R_0} = 1 + 2\left(\frac{u-v}{1-(\frac{v}{u})^{2n+1}} - u\right). \tag{5.10}$$

By replacing u and v quantities from (5.9) into (5.10) we have

$$\begin{aligned}\frac{G(s)}{R_0} &= 1 + 2\left(\frac{\sqrt{1+4\gamma}}{1+\left(\frac{-1+\sqrt{1+4\gamma}}{1+\sqrt{1+4\gamma}}\right)^{2n+1}} - \frac{1+\sqrt{1+4\gamma}}{2}\right) \\ &= 2\sqrt{1+4\gamma}\left(\frac{1}{1+\left(\frac{-1+\sqrt{1+4\gamma}}{1+\sqrt{1+4\gamma}}\right)^{2n+1}} - \frac{1}{2}\right).\end{aligned}$$

Substituting $R/2$ for R_0 and simplifying the last expression lead to

$$G(s)\sqrt{\frac{C}{R}}\sqrt{s} = \sqrt{1+\frac{1}{4\gamma}}\left(\frac{1-\left(\frac{-1+\sqrt{1+4\gamma}}{1+\sqrt{1+4\gamma}}\right)^{2n+1}}{1+\left(\frac{-1+\sqrt{1+4\gamma}}{1+\sqrt{1+4\gamma}}\right)^{2n+1}}\right). \tag{5.11}$$

The right hand side of the above equation is equal to

$$\sqrt{1+\frac{1}{4\gamma}}\tanh\left(\frac{2n+1}{2}\log(1+\frac{2}{-1+\sqrt{1+4\gamma}})\right), \tag{5.12}$$

and the first term in (5.12) is almost unity for $\gamma \geq 6$. Further, by using Taylor expansion of log-function and the fact that hyperbolic tangent is very close to unity for all arguments greater than 2.4, it is straightforward to see that the right hand side of (5.11) is almost unity for any γ between 6 and $n^2/6$. One can verify this fact by plotting (5.12) with respect to γ for different values of n. Finally, substituting $1/RCs$ for γ leads to (5.4), i.e., the fact that the truncated transmission line model with the quantities proposed in (5.2) displays the characteristic of a half-integrator over a specific frequency band.

5.2.2 Second realization

In the above, we worked out an example and established all the necessary steps which show the possibility to design a half-integrator using a RC-ladder with the simplest selection of components, as given in (5.2). The proposed truncated transmission line, discussed in the previous part, suffices to convey the main idea, however in practice, it is not an efficient design to implement a half-capacitor. In the following, we present a new RC-ladder with the same structure as in Figure 5.1, but this time with the choice of components as in (5.3). This also gives rise to a fractional integrator with exponent 1/2, i.e.,

$$G(s) = \frac{\beta}{\sqrt{s}},$$

where β is just a constant. Matlab simulation of such a transmission line with 90 pairs of (C_k, R_k) leads to an approximation whose transfer function is shown in Figures 5.5 and 5.6, as Bode and Nyquist plots, respectively. The characteristic of $1/\sqrt{s}$ in the

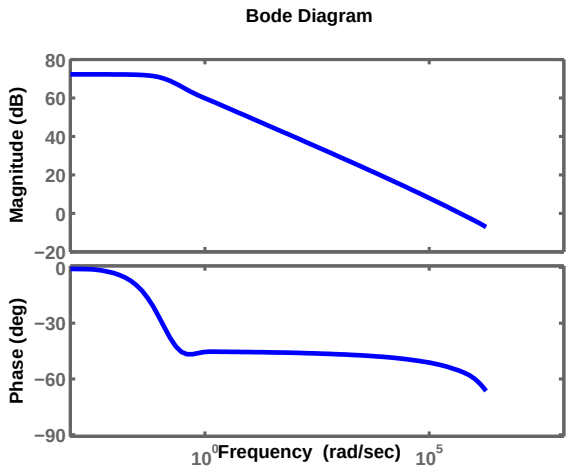

Figure 5.5: Bode plot for $n = 90, R_k = k[\Omega]$ and $C_k = k[\mu\text{F}]$

frequency range from 10^{-1} to 10^6 [rad/sec] is quite evident (notice the corresponding attenuation rate and phase). Figure 5.7 shows the bode plot when only 10 pairs of $C_k = 100k[\mu\text{F}]$ and $R_k = 100k[\Omega]$ have been used and the transmission line has been truncated after these. In this case, the range over which we observe a -10 [dB/dec] drop with phase -45^o is between 10^{-1} and 10^2 [rad/sec]. Comparing the number of components in this case with the one in Figure 5.2 reveals superiority of the latter design, though mathematical proof of the fact that the choice of components as in

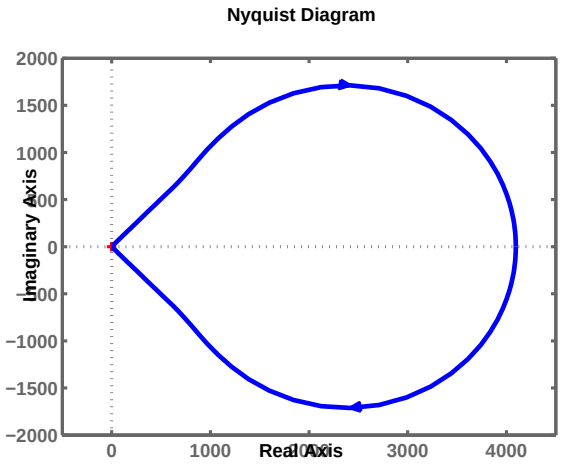

Figure 5.6: Nyquist plot for $n = 90, R_k = k[\Omega]$ and $C_k = k[\mu\text{F}]$

(5.3) for the transmission line leads to characteristic of a half-capacitor has not been worked out and still is under investigation.

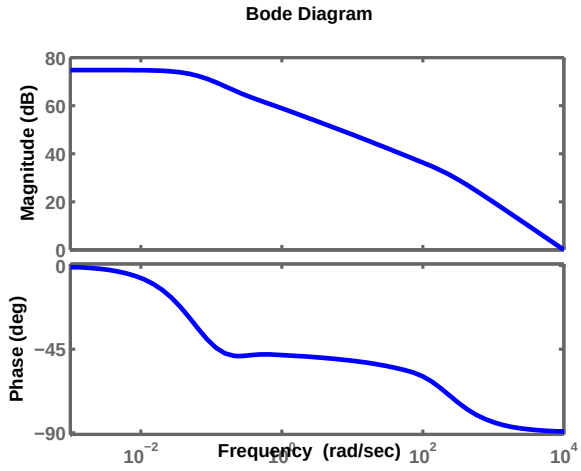

Figure 5.7: Bode plot for $n = 10, R_k = 100k[\Omega]$ and $C_k = 100k[\mu\text{F}]$

5.2.3 Third realization based on Padé approximation

We begin with the Padé approximation of $1/\sqrt{s}$ expanded about $s_0 = 1$. This is a standard procedure and in fact, once the Taylor expansion of a function $f(s)$ has been derived, the corresponding Padé approximation of an arbitrary degree is readily

available via solving linear equations. More precisely, denoting by $a_l(s)$ the numerator polynomial (of order l) and by $b_m(s)$ the denominator polynomial (of order m) for the Padé approximant of $f(s)$ (i.e, $f(s) \approx p_{l,m}(s) := a_l(s)/b_m(s)$), the coefficients of $a_l(s)$ and $b_m(s)$ are obtained by equating

$$\frac{a_l(s)}{b_m(s)} = \text{Taylor series of } f(s),$$

and neglecting higher order terms (see e.g. [5]). In the particular case where $f(s) = 1/\sqrt{s}$ and $l = m = 5$, the resulting Padé approximation is

$$p_{5,5}(s) = \frac{s^5 + 55s^4 + 330s^3 + 462s^2 + 165s + 11}{11s^5 + 165s^4 + 462s^3 + 330s^2 + 55s + 1}.$$

Following a theorem and the associated algorithm in [69, Page 170] helps obtain the RC-ladder corresponding to $p_{5,5}(s)$ as

$$G(s) = R_0 + \cfrac{1}{C_1 s + \cfrac{1}{R_1 + \cfrac{1}{C_2 s + \cfrac{1}{R_2 + \cfrac{1}{\ddots + \cfrac{1}{C_5 s + \cfrac{1}{R_5}}}}}}}, \tag{5.13}$$

with $R_0 = \frac{1}{11}$, and

$$R_1 = \tfrac{200}{429}, R_2 = \tfrac{128}{143}, R_3 = \tfrac{4096}{2805}, R_4 = \tfrac{32768}{13585}, R_5 = \tfrac{262144}{46189},$$
$$C_1 = \tfrac{11}{40}, C_2 = \tfrac{429}{640}, C_3 = \tfrac{4719}{4096}, C_4 = \tfrac{60775}{32768}, C_5 = \tfrac{877591}{262144}.$$

The Bode and Nyquist plots of this circuit are shown in Figures 5.8 and 5.9, respectively, and the characteristic of a half-integrator is seen in the frequency range from 10^{-1} to 10^{1} [rad/sec]. A scaling factor of about 10^{-6} brings the numbers back to the reasonable range of quantities for the components (R's and C's). Clearly, by increasing the number of higher order terms in the Padé approximation, and thus, the number of components, we can expand the frequency range of this half-integrator arbitrarily. This RC circuit is only for comparison purposes and not suitable for the integrated fabrication due to the varying values. For further references and background in design efficient RC-circuits see e.g., [45, 60] and [10]. We now consider the relevance of the half-integrator as a design element in a feedback loop.

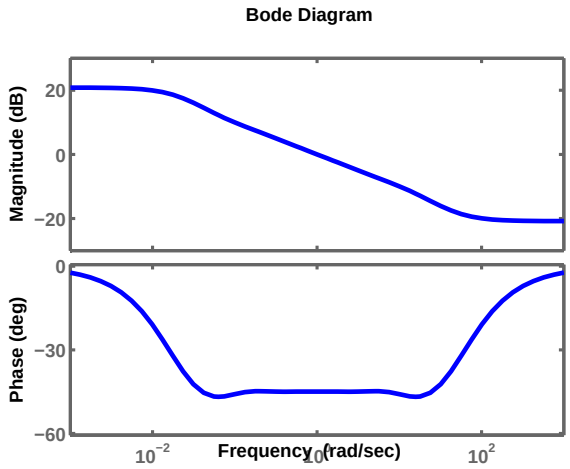

Figure 5.8: Bode plot for RC-ladder (5.13)

5.3 Half-integrator in a feedback loop

To investigate the behavior of $1/\sqrt{s}$ in a practical control design, we first consider the characteristics of a single and isolated half-integrator in the time domain. The discrepancy in low and high frequencies between the ideal half-capacitor and a truncated transmission line model, is negligible when comparing time responses. If "$\mathcal{L}$" stands for the Laplace transformation, then the impulse and step responses of $G(s) = 1/\sqrt{s}$ are

$$g(t) := \mathcal{L}^{-1}\left\{\frac{1}{\sqrt{s}}\right\} = \frac{1}{\sqrt{\pi t}}, \tag{5.14}$$
$$\text{and} \qquad \int_0^t g(\tau)d\tau = 2\sqrt{\frac{t}{\pi}},$$

respectively. They are both compared in Figures 5.10 and 5.11, with the impulse and step responses of the truncated line corresponding to Figure 5.2. In both instances the responses of the RC-ladder are perfectly matched with the responses of $G(s) = 1/\sqrt{s}$.

We now consider the simple control loop in Figure 5.12 with the unity feedback gain. The goal is to observe and study the tracking behavior of this loop for a step function r as the input command. If S and T denote the transfer functions from r to the error

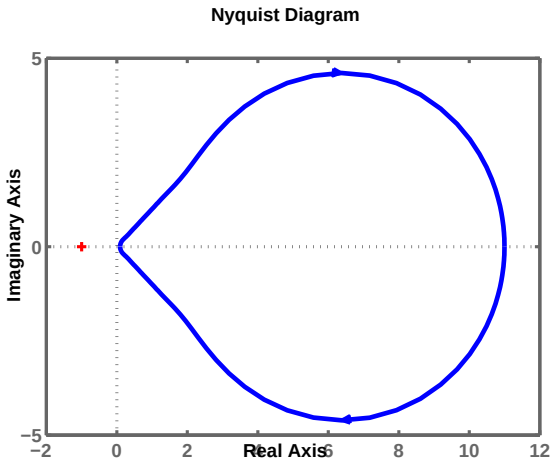

Figure 5.9: Nyquist plot for RC-ladder (5.13)

signal e and the output y respectively, it immediately follows that

$$S(s) = \frac{\sqrt{s}}{\sqrt{s}+1}, \text{ and } \quad T(s) = \frac{1}{\sqrt{s}+1}.$$

Figure 5.13 shows the step responses of the closed-loop system in the time domain which are obtained via inverse Laplace transform. These plots verify that at steady-state, the error signal converges to zero and the output y follows the step input, however, compared to a full-integrator (i.e., $1/s$), the convergence rate here is slower. In fact, the mathematical proof of this fact that e goes to zero at steady-state is quite straightforward. Let $E(s)$ denote the Laplace transform of $e(t)$, the error signal for the step input, then

$$E(s) = \frac{1}{s}S(s) = \frac{1}{\sqrt{s}(\sqrt{s}+1)} = \frac{1}{\sqrt{s}} - \frac{1}{\sqrt{s}+1}.$$

By using (5.14) and the fact that

$$\mathcal{L}^{-1}\left\{\frac{1}{\sqrt{s}+1}\right\} = \frac{1}{\sqrt{\pi t}} - \exp(t)\left(1 - \frac{2}{\sqrt{\pi}}\int_0^{\sqrt{t}} \exp(-\tau^2)d\tau\right),$$

it follows that

$$e(t) = \exp(t)\left(1 - \frac{2}{\sqrt{\pi}}\int_0^{\sqrt{t}} \exp(-\tau^2)d\tau\right).$$

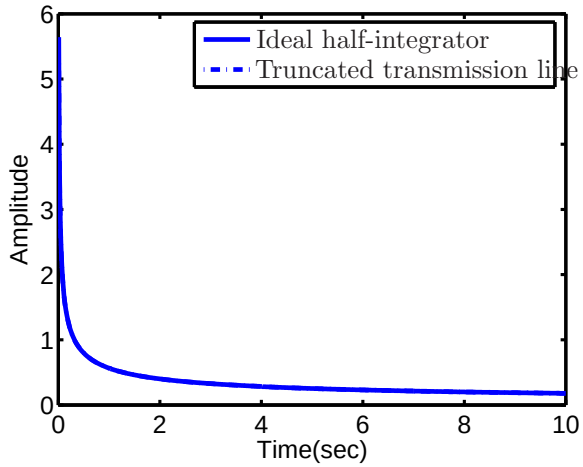

Figure 5.10: Impulse responses of $\frac{1}{\sqrt{s}}$ and a truncated transmission line

Thus, the steady-state value of error is obtained as

$$\lim_{t\to\infty} e(t) = \lim_{t\to\infty} \frac{1 - \frac{2}{\sqrt{\pi}} \int_0^{\sqrt{t}} \exp(-\tau^2) d\tau}{\exp(-t)} = \lim_{t\to\infty} \frac{\frac{1}{\sqrt{\pi t}} \exp(-t)}{\exp(-t)} = 0,$$

where in the last step L'Hospital rule has been used.

Remark 5.1 The so-called "final value theorem" in signals and systems states that the steady-state value of the error signal in Figure 5.12 is

$$\lim_{t\to\infty} e(t) = \lim_{s\to 0} sE(s). \tag{5.15}$$

For this equality to hold, $e(t)$ must have a first derivative which is bounded in $(0, \infty)$, and absolutely integrable in $[0, \infty)$. In other words, (5.15) makes sense only if $\lim e(t)$, as t tends to infinity, exists. The earlier arguments simply establish that the limit exists in our example. Then of course, knowing that the limit exits, we can also state that the steady-state error of the step response in Figure 5.12 is

$$\lim_{t\to\infty} e(t) = \lim_{s\to 0} sE(s) = \lim_{s\to 0} \frac{\sqrt{s}}{\sqrt{s}+1} = 0.$$

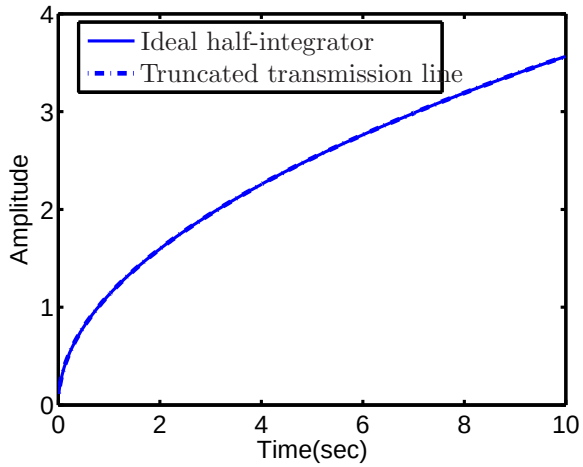

Figure 5.11: Step responses of $\frac{1}{\sqrt{s}}$ and a truncated transmission line

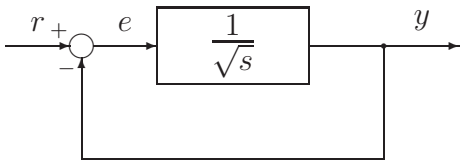

Figure 5.12: Half-integrator in a feedback loop

5.4 Sinusoidal tracking

We now study the use of element $\frac{1}{\sqrt{s^2+\omega_o^2}}$ in notch filter design. Indeed, such elements are positive-real and their presence in a feedback loop (Figure 5.14) causes the closed-loop transfer function to have a notch at ω_o, resulting in disturbance rejection or tracking at that frequency. They similarly provide infinite gain with a reduced phase lag.

The control loop in Figure 5.15 shows a fractional element for sinusoidal tracking in a unit feedback loop. The transfer function from the input to error in Laplace domain is

$$S(s) = \frac{\sqrt{s^2+1}}{\sqrt{s^2+1}+1},$$

and hence, the error signal for a sinusoidal input at frequency 1 becomes

$$E(s) = \frac{1}{s^2+1}S(s) = \frac{1}{\sqrt{s^2+1}(\sqrt{s^2+1}+1)} = \frac{1}{\sqrt{s^2+1}} - \frac{1}{\sqrt{s^2+1}+1}. \qquad (5.16)$$

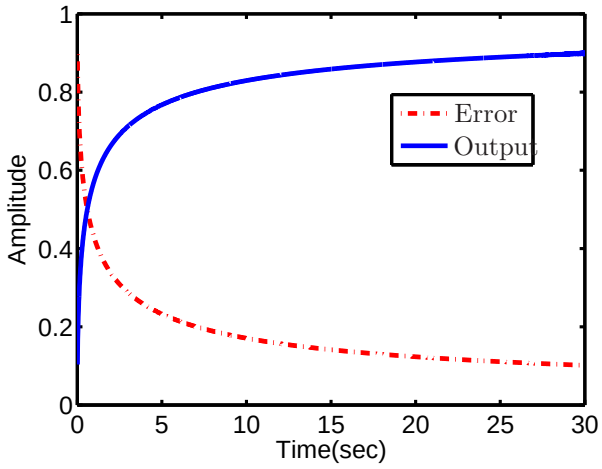

Figure 5.13: Plots of the error and output signals in Figure 5.12 for the step input

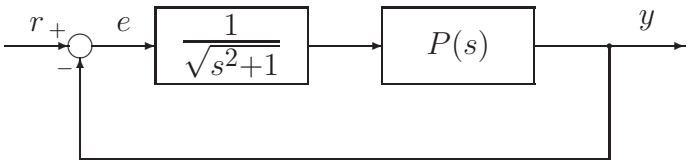

Figure 5.14: Sinusoidal tracking in a feedback loop

The first term in the right hand side of (5.16) is the Laplace transform of a causal Bessel function of the first kind and of order 0. The inverse Laplace transform of this term has a well known asymptotic expansion (cf. [52])

$$\mathcal{L}^{-1}\left\{\frac{1}{\sqrt{s^2+1}}\right\} \approx \sqrt{\frac{2}{\pi t}}\cos(t-\pi/4).$$

This implies that in time domain both terms of the error signal approach to zero at

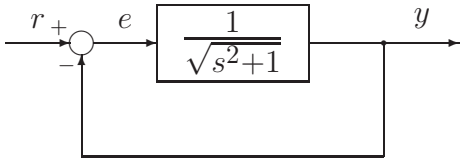

Figure 5.15: Sinusoidal tracking in a unit feedback loop

steady state, and therefore,

$$\lim_{t\to\infty} e(t) = 0.$$

Thus, the fractional element in Figure 5.15 suffices for sinusoidal tracking with the added benefit of less time-lag compared to the traditional design.

The final example in this chapter is again on sinusoidal tracking in a feedback loop with the plant

$$P(s) = \frac{1}{s+1}.$$

Figure 5.16 shows such a control loop. The sensitivity transfer function of this system

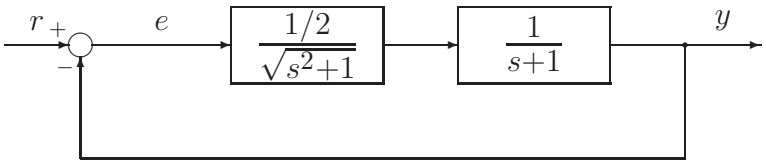

Figure 5.16: Sinusoidal tracking in a feedback loop

is

$$S(s) = \frac{\sqrt{s^2+1}(s+1)}{\sqrt{s^2+1}(s+1)+1/2}$$

and the error signal for a sinusoidal input is readily obtained as

$$E(s) = \frac{S(s)}{s^2+1} = \frac{s+1}{\sqrt{s^2+1}(\sqrt{s^2+1}(s+1)+1/2)} = \frac{2(s+1)}{\sqrt{s^2+1}} - \frac{2(s+1)^2}{\sqrt{s^2+1}(s+1)+1/2}.$$

By taking the inverse Laplace transform of the first term in $E(s)$ we arrive at the expression

$$-2J_1(t) + 2J_0(t),$$

where J_0, J_1 are Bessel functions of the first kind of order zero and one, respectively. Thereby, the first term in $E(s)$ tends to zero in time. On the other hand, the second term in $E(s)$ has all the poles in the left half side of the complex plain. Therefore, this term also decays to zero at steady state. This finally proves that the fractional element in Figure 5.16 gives us the sinusoidal tracking, and at the same time, it mediates destabilizing effects of the traditional approach.

5.5 Concluding remarks

We discussed the relevance of using a fractional integrator as a design element for set-point following in a control loop. The standard control design strategy for having zero steady-state tracking error requires an integrator in the feedback loop. The magnitude of an integrator in the frequency domain drops at a rate of 20 [dB/dec] and its phase is -90^o throughout. This may adversely affect stability and robustness of the closed-loop system as it directly affects the phase margin.

The work reported herein is based on passive circuits whose transfer functions include fractional power of s. We addressed the particular example of a half-integrator (i.e., $1/\sqrt{s}$) in detail. We showed that it allows for zero steady-state error in set-point following and at the same time introduces a smaller phase lag (compared to an integrator). A variety of RC-ladder circuits, which can realize such a half-integrating device, have been studied.

We also investigated sinusoidal tracking using a fractional element. In this thesis, we did not intend to address the possible implementations of such elements using available technologies (off-chip and on-chip) for various frequency ranges. However, this is an important subject and can be a part of a separate thesis. In addition, the potential uses of fractional models in communication circuits is yet another appealing area in this research work.

Chapter 6

Conclusions and future directions

- **Scalar interpolation with complexity constraint:** The purpose of Chapter 2 has been to explore the framework in [13,14] and [41] for feedback design with a degree constraint. This framework provided a complete parametrization of generically minimal-degree solutions to analytic interpolation problems in scalar setting. The solutions have been obtained as minimizers of suitable weighted entropy functionals by arbitrary choice of $n-1$ spectral-zeros (zeros of the weighting function), where n is the number of interpolation conditions. We focused on how to efficiently shape closed-loop transfer functions via suitable choices of the relevant weights. The weights themselves have been obtained by solving another optimization problem which took into account performance specifications. The open question in this direction is the minimum degree of interpolant that meets a given performance specification as well.

- **Multivariable interpolation with complexity constraint:** The framework reported in Chapters 3 and 4 addressed the matricial variant of a Nehari problem for positive-real functions. We generalized previous results to analytic interpolation for $m \times m$ matrix-valued functions. We showed that in the multivariable setting, the (generically) minimal McMillan degree of interpolants is $n-m$ (n being the size and rank of the corresponding Pick matrix). While interpolants of McMillan degree lower than $n-m$ may be possible, depending on the data, the class of solutions of McMillan degree $n-m$ is always non-empty and represents a natural generic family of interpolants of low complexity. In multivariable in-

terpolation, in addition to the spectral-zeros, we can also assign their invariant subspaces (spectral-zero dynamics) as well. Further, the obstruction in assigning poles via state feedback, described by Rosenbrock's theorem, imposes a set of restrictions on the family of spectral-zero dynamics.

A natural next step in this direction of research is to apply the above parametrization in multivariable control design. This is expected to be established using matrix-valued weight functions which encapsulate the desired specifications and are obtained as solutions of a well-defined optimization problem. On the other hand, in spectral analysis of multivariable stochastic processes, future research will focus on, first, how to incorporate prior information about the underlying process as a guideline for weight selection, and second, how to address the fundamental tradeoffs between resolution and robustness. Also, the direct characterization of norm-bounded interpolants in multivariable setting, discussed in Section 4.3, is another relevant topic of research.

- **Fractional models as control design elements:** The first contribution in Chapter 5 was to utilize a half-integrator as a design element for set-point following in a control loop. We showed that in order to reach zero steady state error a full integrator is not necessary—a fractional integrator suffices. Such a fractional element introduces a smaller phase lag (compared to an integrator), and hence, improves the phase margin of the control system. We also studied a variety of RC-ladder circuits which can realize a half-integrating device. Further, we investigated a fractional element for the purpose of sinusoidal tracking in a control loop.

  Although we have demonstrated the advantages of certain physically appealing elements as control design components, the possible implementations of such elements using available technologies (off-chip and on-chip) is part of the future work in this direction. Another interesting research topic on fractional models, relevant in communication circuits and transmission lines, is to develop identification techniques for MIMO distributed parameter systems.

Appendix A

Consistent impedance matrices in Example 3.5

$$F =: \begin{bmatrix} f_{11} & f_{12} \\ f_{12} & f_{22} \end{bmatrix} \Big/ d, \text{ where}$$

$$\text{(i)}: \begin{cases} f_{11} = 0.49(z^4 - 2.07z^3 + 4.17z^2 - 3.30z + 2.44), \\ f_{12} = -0.16(z^4 - 0.31z^3 + 0.81z^2 + 1.02z + 0.53), \\ f_{22} = 0.92(z^4 - 3.04z^3 + 6.04z^2 - 5.69z + 3.50), \\ d = 2(z^4 - 2.08z^3 + 4.35z^2 - 3.44z + 2.81), \end{cases}$$

$$\text{(ii)}: \begin{cases} f_{11} = 0.52(z^4 - 2.22z^3 + 5.10z^2 - 4.45z + 3.81), \\ f_{12} = -0.20(z^4 - 0.41z^3 + 1.03z^2 + 1.53z + 0.70), \\ f_{22} = 0.88(z^4 - 3.52z^3 + 8.01z^2 - 8.75z + 6.03), \\ d = 2(z^4 - 2.31z^3 + 5.48z^2 - 4.82z + 4.65), \end{cases}$$

$$\text{(iii)}: \begin{cases} f_{11} = 0.96(z^4 - 10.44z^3 + 42.10z^2 - 75.11z + 52.11), \\ f_{12} = 0.05(z^4 - 42.18z^3 + 180.85z^2 - 171.28z - 73.31), \\ f_{22} = 2.96(z^4 - 12.10z^3 + 49.36z^2 - 80.14z + 45.55), \\ d = 2(z^4 - 13.89z^3 + 69.56z^2 - 153.76z + 117.75), \end{cases}$$

$$\text{(iv)}: \begin{cases} f_{11} = 0.53(z^4 + 2.06z^3 + 4.16z^2 + 3.34z + 2.42), \\ f_{12} = -0.48(z^4 + 1.78z^3 + 2.71z^2 + 0.73z + 0.18), \\ f_{22} = 0.015(z^4 + 30.79z^3 + 155.84z^2 + 275.46z + 236.17), \\ d = 2(z^4 + 2.86z^3 + 5.57z^2 + 4.65z + 3.04), \end{cases}$$

$$\text{(v)}: \begin{cases} f_{11} = 0.47(z^4 + 1.86z^3 + 3.23z^2 + 2.27z + 1.41), \\ f_{12} = -0.41(z^4 + 1.52z^3 + 1.87z^2 + 0.49z + 0.11), \\ f_{22} = 0.04(z^4 + 15.43z^3 + 53.02z^2 + 67.37z + 47.72), \\ d = 2(z^4 + 2.30z^3 + 3.82z^2 + 2.81z + 1.58). \end{cases}$$

Appendix B

The derivative of matrix logarithm

In this section, following a number of basic formulas in matrix calculus, we take the derivative of

$$\int_{-\pi}^{\pi} \operatorname{trace} \log\left(I - FF^*\right) d\theta$$

in the direction δ. We begin with the differential

$$\begin{aligned} &\log\left(I - (F+\delta)(F^*+\delta^*)\right) - \log\left(I - FF^*\right) = \\ &\log\left(I - FF^* - F\delta^* - \delta F^* - \delta\delta^*\right) - \log\left(I - FF^*\right). \end{aligned}$$

From matrix calculus (see [28, 39, 58]),

$$\log Y - \log X = \int_0^{\infty} (X + \tau I)^{-1}(Y - X)(Y + \tau I)^{-1} d\tau$$

for matrices $X, Y \succ 0$. On the other hand,

$$(X + \tau I)^{-1} - (X + \Delta + \tau I)^{-1} = (X + \tau I)^{-1}\Delta(X + \Delta + \tau I)^{-1},$$

for a Hermitian matrix Δ. Therefore, if we take

$$\begin{aligned} X &= I - FF^* \succ 0, \\ Y &= I - FF^* - (F\delta^* + \delta F^* + \delta\delta^*) \succ 0, \\ \Delta &= -(F\delta^* + \delta F^* + \delta\delta^*), \end{aligned}$$

it follows

$$\log\left(I - FF^* - (F\delta^* + \delta F^* + \delta\delta^*)\right) - \log\left(I - FF^*\right) =$$

$$\int_0^\infty \left(I - FF^* + \tau I\right)^{-1} \left(-F\delta^* - \delta F^* - \delta\delta^*\right) \left(I - FF^* - (F\delta^* + \delta F^* + \delta\delta^*) + \tau I\right)^{-1} d\tau =$$

$$\int_0^\infty \left(I - FF^* + \tau I\right)^{-1} \left(-F\delta^* - \delta F^* - \delta\delta^*\right) \Big[\left(I - FF^* + \tau I\right)^{-1} + \left(I - FF^* + \tau I\right)^{-1}$$

$$\left(F\delta^* + \delta F^* + \delta\delta^*\right) \quad \left(I - FF^* - (F\delta^* + \delta F^* + \delta\delta^*) + \tau I\right)^{-1}\Big] d\tau.$$

By performing the multiplication in the last expression we arrive at

$$\log\left(I - FF^* - (F\delta^* + \delta F^* + \delta\delta^*)\right) - \log\left(I - FF^*\right) =$$

$$\int_0^\infty \left(I - FF^* + \tau I\right)^{-1} \left(-F\delta^* - \delta F^*\right) \left(I - FF^* + \tau I\right)^{-1} d\tau -$$

$$\int_0^\infty \left(I - FF^* + \tau I\right)^{-1} \delta\delta^* \left(I - FF^* + \tau I\right)^{-1} d\tau +$$

$$\int_0^\infty \left(I - FF^* + \tau I\right)^{-1} \left(-F\delta^* - \delta F^* - \delta\delta^*\right) \left(I - FF^* + \tau I\right)^{-1}$$

$$\left(F\delta^* + \delta F^* + \delta\delta^*\right) \left(I - FF^* + \tau I\right)^{-1} d\tau + o(\|\delta\|^2).$$

Thereby, the expression for the first derivative of $\log(I - FF^*)$ becomes

$$\int_0^\infty \left(I - FF^* + \tau I\right)^{-1} \left(-2\Re e\left(\delta F^*\right)\right) \left(I - FF^* + \tau I\right)^{-1} d\tau.$$

This finally implies

$$d\int_{-\pi}^{\pi} \operatorname{trace} \log\left(I - FF^*\right) d\theta = \operatorname{trace} \int_{-\pi}^{\pi} d\left(\log\left(I - FF^*\right)\right) d\theta =$$

$$\operatorname{trace} \int_{-\pi}^{\pi}\int_0^\infty \left(I - FF^* + \tau I\right)^{-1} \left(-2\Re e\left(\delta F^*\right)\right) \left(I - FF^* + \tau I\right)^{-1} d\tau d\theta =$$

$$-\int_{-\pi}^{\pi} \operatorname{trace}\left[2(I - FF^*)^{-1}\Re e\left(\delta F^*\right)\right] d\theta.$$

Bibliography

[1] Fractional calculus applications in automatic control and robotics. In B. M. Vinagre and Y. Chen, editors, *IEEE Proc. on Conference on Decision and Control*, Las Vegas, Dec. 2002. Tutorial Workshop - 316 pages.

[2] B. D. O. Anderson and S. Vongpanitlerd. *Network analysis and synthesis*. Prentice-Hall Inc., Englewood Cliffs, NJ, 1973.

[3] D. Z. Arov. The generalized bitangent Carathéodory-Nevanlinna-Pick problem, and (j, J_o)-inner matrix-valued functions. *Russian Acad. Sci. Izv. Math.*, 42(1):1–26, 1994.

[4] K. J. Åström. Model uncertainty and robust control. In *Lecture Notes on Iterative Identification and Control Design*, pages 63–100, Jan. 2000.

[5] G. A. Jr. Baker. *Essentials of* Padé *approximants*. Academic Press, New York, 1975.

[6] J. A. Ball, I. Gohberg, and L. Rodman. *Interpolation of rational matrix functions*, volume 45 of *Operator Theory: Advances and Applications*. Birkhäuser Verlag, Basel, 1990.

[7] D. Bertsimas and J. N. Tsitikilis. *Introduction to linear optimization*. Athena Scientific, 1997.

[8] A. Blomqvist. *A convex optimization approach to complexity constrained analytic interpolation with applications to ARMA estimation and robust control*. PhD thesis, Royal Institute of Technology, Stockholm, Sweden, TRITA-MAT-05-OS-01 2005.

[9] A. Blomqvist, A. Lindquist, and Ryozo Nagamune. Matrix-valued Nevalina-Pick interpolation with complexity constraint: an optimization approach. *IEEE Trans. on Automatic Control*, 48(12):2172–2190, Dec. 2003.

[10] G. W. Bohannan. Analog realization of a fractional control element - revisited. Available on the web from http://mechatronics.ece.usu.edu/foc/cdc02tw/cdrom/aditional/FOC_Proposal_Bohannan.pdf, Oct. 2002. Wavelength Electronics Inc.

[11] C. Brezinski. *History of continued fractions and Padé approximations*, volume 12 of *Computational Mathematics*. Springer-Verlag, New York, 1991.

[12] C. I. Byrnes, T. T. Georgiou, and A. Lindquist. A new approach to spectral estimation: A tunable high-resolution spectral estimator. *IEEE Trans. on Signal Processing*, 48(11):3189–3205, Nov. 2000.

[13] C. I. Byrnes, T. T. Georgiou, and A. Lindquist. A generalized entropy criterion for Nevanlinna-Pick interpolation: A convex optimization approach to certain problems in systems and control. *IEEE Trans. on Automatic Control*, 45(6):822–839, Jun. 2001.

[14] C. I. Byrnes, T. T. Georgiou, A. Lindquist, and A. Megretski. Generalized interpolation in H^∞ with a complexity constraint. *Trans. of the American Mathematical Society*, 358(3):965–987, 2004.

[15] C. I. Byrnes, S. V. Gusev, and A. Lindquist. A convex optimization approach to the rational covariance extension problem. *SIAM J. on Control and Optimization*, 37(1):211–229, 1999.

[16] C. I. Byrnes and A. Lindquist. A convex optimization approach to generalized moment problems. *Control and Modeling of Complex Systems: Cybernetics in the 21st Century: Festschrift in Honor of Hidenori Kimura on the Occasion of his 60th Birthday*, pages 3–21, 2003. K. Hashimoto, Y. Oishi and Y. Yamamoto, Editors, Birkhäuser.

[17] C. I. Byrnes, A. Lindquist, S. V. Gusev, and A. S. Matveev. A complete parametrization of all positive rational extensions of a covariance sequence. *IEEE Trans. on Automatic Control*, 40(11):1841–1857, Nov. 1995.

[18] W. Chen. Fractional and fractal derivatives modeling of turbulence. *eprint arXiv:nlin/0511066*, 2005.

[19] W-K. Chen. *Theory and design of broadband matching networks*. Pergamon Press, New York, 1976.

[20] Y. Chen. Ubiquitous fractional order controllers? In *The Second IFAC Symposium on Fractional Derivatives and Applications*, Portugal, Jul. 2006. 12 pages Plenary Talk Paper.

[21] P. Delsarte, Y. Genin, and Y. Kamp. Orthogonal polynomial matrices on the unit circle. *IEEE Trans. on Circuits and Systems*, CAS-25(3):149–160, Mar. 1978.

[22] P. Dewilde. Generalized Darlington synthesis. *IEEE Trans. on Circuits and Systems–I*, 45(1):41–58, Jan. 1999.

[23] B. W. Dickinson. On the fundamental theorem of linear state variable feedback. *IEEE Trans. on Automatic Control*, 19(5):577–579, Oct. 1974.

[24] J. C. Doyle, B. A. Francis, and A. Tannenbaum. *Feedback control theory*. McMillan Publishing Co., 1990.

[25] D. G. Duffy. *Transform methods for solving partial differential equations*. CRC Press, Boca Raton, FL, 1994.

[26] N. Engheta. On fractional calculus and fractional multipoles in electromagnetism. *IEEE Trans. on Antennas and Propagation*, 44(4):554–566, Apr. 1996.

[27] R. M. Fano. Theoretical limitations on the broadband matching of arbitrary impedances. Technical Report 41, Massachusetts Institute of Technology, Jan. 1948.

[28] R. P. Feynman. An operator calculus having applications in quantum electrodynamics. *Physical Review*, 84(1):108–128, 1951.

[29] D. S. Flamm. A new proof of Rosenbrock's theorem on pole assignment. *IEEE Trans. on Automatic Control*, 25(6):1128–1133, Dec. 1980.

[30] B. A. Francis. *A course in H_∞-control theory*, volume 88 of *Lecture Notes in Control and Information Sciences*. Springer-Verlag, 1987.

[31] P. Gahinet and P. Apkarian. A linear matrix inequality approach to H_∞ control. *International Journal of Robust and Nonlinear control*, 4:421–448, 1994.

[32] F. R. Gantmacher. *The theory of matrices*, volume I. Chelsea Publishing Company, New York, NY, 1959.

[33] T. T. Georgiou. *Partial realization of covariance sequences.* PhD thesis, Department of Electrical Engineering, Center for Mathematical Systems Theory, University of Florida, 1983. http://www.ece.umn.edu/users/georgiou/files/reports.html.

[34] T. T. Georgiou. Realization of power spectra from partial covariance sequences. *IEEE Trans. on Acoustic, Speech, and Signal Processing*, ASSP-35(4):438–449, Apr. 1987.

[35] T. T. Georgiou. A topological approach to Nevanlinna-Pick interpolation. *SIAM J. on Mathematical Analysis*, 18(5):1248–1260, Sept. 1987.

[36] T. T. Georgiou. Spectral analysis based on the state covariance: the maximum entropy spectrum and linear fractional parametrization. *IEEE Trans. on Automatic Control*, 47(11):1811–1823, Nov. 2002.

[37] T. T. Georgiou. The structure of state covariances and its relation to the power spectrum of the input. *IEEE Trans. on Automatic Control*, 47(7):1056–1066, Jul. 2002.

[38] T. T. Georgiou. Solution of the general moment problem via a one-parameter imbedding. *IEEE Trans. on Automatic Control*, 50(6):811–826, Jun. 2005.

[39] T. T. Georgiou. Relative entropy and the multivariable multidimensional moment problem. *IEEE Trans. on Information Theory*, 52(3):1052–1066, Mar. 2006.

[40] T. T. Georgiou. The Carathéodory-Fejér-Pisarenko decomposition and its multivariable counterpart. *IEEE Trans. on Automatic Control*, 52(2):212–228, Feb. 2007.

[41] T. T. Georgiou and A. Lindquist. Kullback-Leibler approximation of spectral density functions. *IEEE Trans. on Information Theory*, 49(11):2910–2917, Nov. 2003.

[42] T. T. Georgiou and A. Lindquist. Remarks on control design with degree constraint. *IEEE Trans. on Automatic Control*, 51(7):1150–1156, Jul. 2006.

[43] I. Gohberg, P. Lancaster, and L. Rodman. *Matrix polynomials*. Computer Sience and Applied Mathematics. Academic Press, New York, NY, 1982.

[44] J. W. Helton. Orbit structure of the möbius transformation semigroup acting on H^∞ (broadband matching). In *Topics in Functional Analysis*, volume 3 of *Advances in Mathematics Supplementary Studies*, pages 129–157. Academic Press, Inc., 1978.

[45] M. Ichise, Y. Nagayanami, and T. Kojima. An analog simulation of non-linear order transfer functions for analysis of electrode processes. *Journal of Electroanalytical Chemistry and Interfacial Electrochemistry*, 33:253–265, 1971.

[46] R. E. Kalman. Kronecker invariants and feedback. In L. Weiss, editor, *Proc. on Ordinary Differential Equations*, pages 459–471, New York, 1972. Academic Press.

[47] R. E. Kalman. Realization of covariance sequences. In *Proc. Toeplitz Memorial conference*, Tel Aviv, Israel, 1981.

[48] J. Karlsson, T. T. Georgiou, and A. Lindquist. The inverse problem of analytic interpolation with degree constraint. In *IEEE Proc. on Conference on Decision and Control*, pages 559–564, San Diego, Dec. 2006.

[49] M. G. Krein and A. A. Nudel'man. *The Markov moment problem and extermal problems*, volume 50 of *Translations of Mathematical Monographs*. American Mathematical Society, Providence, RI, 1977.

[50] J. A. T. Machado. Discrete-time fractional-order controllers. *Journal of Fractional Calculus & Applied Analysis*, 4(1):47–66, 2001.

[51] P. Masani. Recent trends in multivariable prediction theory. In P. R. Krishnaiah, editor, *Multivariate analysis*, pages 351–382. Academic Press, 1966.

[52] D. Matignon. Stability properties for generalized fractional differential systems. In *Fractional Differential Systems: Models, Method and Applications*, volume 5, pages 145–158. ESAIM, 1998.

[53] D. C. McFarlane and K. Glover. *Robust controller design using normalized coprime factor plant descriptions*, volume 138 of *Lecture Notes in Control and Information Sciences*. Springer-Verlag, Berlin, 1990.

[54] R. Nagamune. *Robust control with complexity constraint: A Nevanlinna-Pick interpolation approach*. PhD thesis, Royal Institute of Technology, Stockholm, Sweden, TRITA-MAT-02-OS-10 2002.

[55] R. Nagamune. Closed-loop shaping based on Nevalinna-Pick interpolation with a degree bound. *IEEE Trans. on Automatic Control*, 49:300–305, Feb. 2004.

[56] R. Nagamune. A shaping limitation of rational sensitivity functions with a degree constraint. *IEEE Trans. on Automatic Control*, 49:269–300, Feb. 2004.

[57] R. Nagamune and A. Blomqvist. Sensitivity shaping with degree constraint by nonlinear least-squares optimization. *Automatica*, 41(7):1219–1227, 2005.

[58] I. Najfeld and T. F. Havel. Derivations of the matrix exponential and their computation. *Advances in Applied Mathematics*, 16(3):321–375, Sept. 1995.

[59] A. Nasiri-Amini and Tryphon. T. Georgiou. Tunable line spectral estimators based on state-covariance subspace analysis. *IEEE Trans. on Signal Processing*, 54(7):2662–2671, Jul. 2006.

[60] K. B. Oldham. Semiintegral electroanalysis: Analog implementation. *Analytical Chemistry*, 45(1):39–47, Jan. 1973.

[61] K. B. Oldham and J. Spanier. *The fractional calculus*, volume 111 of *Mathematics in Science and Engineering*. Academic Press, New York, 1974.

[62] M. D. Ortigueira and J. A. T. Machado. Editorial. *Signal Processing, Fractional calculus applications in signals and systems*, 86(10):2503–2504, Oct. 2006. Elsevier North-Holland, Inc.

[63] A. Oustaloup, P. Melchior, P. Lanusse O. Cois, and F. Dancla. The CRONE toolbox for MATLAB. In *Proc. of the 2000 International Symposium on Computer-Aided Control System Design*, Alaska, Sept. 2000.

[64] I. Podlubny. *Fractional differential equations*, volume 198 of *Mathematics in Science and Engineering*. Academic Press, San Diego, 1999.

[65] V. M. Popov. Invariant description of linear time-invariant controllable systems. *SIAM J. on Control*, 10(2):252–264, May 1972.

[66] H. H. Rosenbrock. *state-space and multivariable theory*. John Wiley & Sons, Inc., 1970.

[67] K. C. Sou, A. Megretski, and L. Daniel. A quasi-convex optimization approach to parameterized model order reduction. In *IEEE Proc. on Design Automation Conference*, pages 933–938, California, Jun. 2005.

[68] A. R. Tannenbaum. Feedback stabilization of linear dynamical plants with uncertainty in the gain factor. *International Journal of Control*, 32(1):1–16, 1980.

[69] H. S. Wall. *Analytic theory of continued fractions*. D. Van Nostrand Company, Inc., New York, 1948.

[70] D. C. Youla. A new theory of broad-band matching. *IEEE Trans. on Circuit Theory*, CT-11(1):30–50, 1964.

[71] D. C. Youla and M. Saito. Interpolation with positive-real functions. *Franklin Institute*, 284(2):77–108, 1967.

[72] G. Zames. Feedback and optimal sensitivity: Model reference transformations, multiplicative seminorms, and approximate inverses. *IEEE Trans. on Automatic Control*, AC-26:301–320, 1981.